Winter 12-15-2015

Measurement, Modeling, and Mitigation of Lead Impacts from General Aviation

Stephen Neil Feinberg
Washington University in St. Louis

WASHINGTON UNIVERSITY IN ST. LOUIS

School of Engineering and Applied Science

Department of Energy, Environmental and Chemical Engineering

Dissertation Examination Committee:
Jay Turner, Chair
Richard Axelbaum
Pratim Biswas
Rex Couture
Zorimar Rivera-Núñez
Brent Williams

Measurement, Modeling, and Mitigation of Lead Impacts from General Aviation

by

Stephen Neil Feinberg

A dissertation presented to the
Graduate School of Arts and Sciences
of Washington University in
partial fulfillment of the
requirements for the degree
of Doctor of Philosophy

December 2015
St. Louis, Missouri

Table of Contents

List of Figures

List of Tables

List of Acronyms

100LL	100 octane low lead
ACRP	Airport Cooperative Research Program
AEDT	Aviation Environmental Design Tool
AERMOD	American Meteorological Society/Environmental Protection Agency Regulatory Model
APA	Centennial Airport
ASOS	Automated Surface Observing System
ATADS	Air Traffic Activity Database
avgas	Aviation Gasoline
Br	Bromine
CDC	Center for Disease Control
C_O	observed concentration
C_P	predicted concentration
EDMS	Emissions and Dispersion Modeling System
EPA	Environmental Protection Agency
FAA	Federal Aviation Administration
FAC2	fraction of modeled values within a factor of two of the measured values
FBO	fixed base operator
g/gal	grams per gallon
g/L	grams per liter
ICP-MS	Inductively Coupled Plasma-Mass Spectrometry
ISH	Integrated Surface Hourly

LTO	landing and takeoff operation
$\mu g/m^3$	micrograms per cubic meter
MDL	method detection limit
MOGAS	motor vehicle gasoline
NAAQS	National Ambient Air Quality Standards
NCDC	National Climatic Data Center
NEI	National Emissions Inventory
ng/m^3	nanograms per cubic meter
NMSE	normalized mean square error
NTA	Nonparametric Trajectory Analysis
NWR	Nonparametric Wind Regression
PAO	Palo Alto Airport
Pb	Lead
PM	Particulate Matter
PM_{10}	Particulate Matter less than 10 micrometers in aerodynamic diameter
$PM_{2.5}$	Particulate Matter less than 2.5 micrometers in aerodynamic diameter
RVS	Richard Lloyd Jones Jr. Airport
SCAQMD	South Coast Air Quality Management District
SMO	Santa Monica Airport
STC	supplemental type certificate
TEL	tetraethyllead
TGO	touch and go
TIM	time-in-mode

TSP	Total Suspended Particulate
UFP	Ultrafine Particles
VSCC	Very Sharp Cut Cyclone
WHO	World Health Organization
XRF	X-Ray Fluorescence

Acknowledgments

I would like to express my thanks to my advisor, Dr. Jay Turner, for all of his time, continued guidance, and support during my time at Washington University. His enthusiasm for exploring data and solving problems brought me into and led me through my research experience. I would also like to thank Dr. Richard Axelbaum, Dr. Pratim Biswas, Dr. Rex Couture, Dr. Zorimar Rivera-Núñez, and Dr. Brent Williams for their service as committee members and research guidance. The projects in Chapters 3-5 were funded by the Airport Cooperative Research Program of the Transportation Research Board, Project Numbers 02-34 and 02-57. Jim Lyons, Jeremy Heiken and Marc Valdez (Sierra Research, Inc.) are gratefully acknowledged for their collaborations on these projects; it has been a pleasure to work with them.

I would also like to thank all of the research and department staff for their help throughout my learning experience. Furthermore, I would like to extend my gratitude to my former and current colleagues at Washington University, specifically my colleagues in the Turner lab, Dr. Li Du, Dr. Varun Yadav, Chris Peng and Kelsey Haddad for creating a friendly and collaborative learning environment. Finally, I would like to thank my family and friends outside of the department and university for their continual support and encouragement.

Stephen Neil Feinberg

Washington University

December 2015

ABSTRACT OF THE DISSERTATION

Measurement, Modeling, and Mitigation of Lead Impacts from General Aviation

By

Stephen N. Feinberg

Doctor of Philosophy in Energy, Environmental & Chemical Engineering

Washington University in St. Louis, 2015

Professor Jay R. Turner, Chair

Airborne lead (Pb) has been regulated as a criteria pollutant by the United States Environmental Protection Agency (EPA) since the Clean Air Act and its amendments in the 1970s. During the 1970s, atmospheric Pb emissions were dominated by the combustion of leaded automobile fuel and metals manufacturing. Over time, those emissions have decreased greatly and according to the EPA the largest emitter of Pb today is piston-engine aircraft. Additionally, in 2008 the EPA reduced the National Ambient Air Quality Standard (NAAQS) for Pb by an order of magnitude. These combined factors served as the impetus for further study of general aviation Pb emissions by the EPA, local and regional air planning agencies, and airports.

This dissertation is focused on characterizing Pb impacts at and around general aviation airports because of piston-engine aircraft activity. It includes a detailed analysis of Pb emissions and concentrations by both measurement and modeling. On-site particulate matter (PM) sampling was conducted at three general aviation airports across the United States with varying size, meteorological, and layout characteristics. Those airports were Richard Lloyd Jones Jr. Airport (RVS) in Tulsa, OK, Centennial Airport (APA) in Denver, CO, and Santa Monica Airport (SMO) in Santa Monica, CA. Airborne PM samples collected at these airports were digested and analyzed for Pb by inductively coupled plasma-mass spectrometry (ICP-MS) and a

subset of samples were analyzed by X-ray fluorescence (XRF) to examine both Pb and Bromine (Br). Measurement data were used to characterize Pb at airports by examining differences in Pb concentrations at sampling locations upwind and downwind of piston-engine aircraft activity on the airport footprints. Specific analyses included upwind-downwind differences in total Pb concentrations, differences in Pb-Br correlations for samples with predicted high and low aircraft emissions impacts, and differences in Pb isotope ratios measured in the high and low impact samples. The analysis showed that Pb-Br correlation and especially Pb isotope ratios, could serve as markers for identifying Pb impacts from aircraft. Measured Pb concentrations were also used to validate the modeling performed as part of this work.

Further analysis of Pb impacts was conducted by performing air dispersion modeling of Pb emissions at airports. Modeling of Pb impacts is critical because Pb measurements are usually only collected at a single or limited number of locations at or near an airport. Initially, Pb emissions at APA were modeled using the Federal Aviation Administration's (FAA) Emission and Dispersion Modeling System (EDMS), without having detailed information about aircraft activity at the airport. Subsequently, field campaigns were conducted at RVS, APA, and SMO to collect detailed on-site activity data and to characterize the aircraft fleet. These data were collected concurrently with the on-site Pb sampling. The airport-specific data collection was used to generate a spatially and temporally resolved emission inventory which was used as input to the EPA's AERMOD air dispersion model to estimate Pb concentration fields at and around each of the three airports. Modeled concentrations agreed well with measured values at RVS and SMO, while comparisons at APA were inferior but still acceptable by conventional air quality modeling permeance metrics. The modeling was also used to determine the aircraft operations most significantly contributing to Pb hotspots.

The on-site data collection and air quality modeling framework was then applied to a fourth airport, Palo Alto Airport (PAO) in Palo Alto, CA. Data collection was conducted over a shorter period of time than the other airports. The modeled results at PAO showed excellent comparison to on-site concentrations measured by the local air agency, even though the data collection, other than total daily activity, did not occur at the same time as the modeled period. The model setups for RVS, SMO, and PAO were then used to evaluate two mitigation strategies: moving some activity areas away from others to reduce converging emissions; and replacing leaded aviation gasoline with motor vehicle gasoline in planes that are certified to use it. Moving activity areas significantly reduced maximum Pb concentrations at RVS and SMO with a smaller reduction at PAO, while using motor vehicle gasoline significantly reduced concentrations across the full airport footprints at all three airports.

Chapter 1: Introduction

1.1 Introduction

1.1.1 Lead as a Pollutant

Lead (Pb) is one of the oldest known pollutants, with clinical diagnosis of Pb poisoning dating back to Hippocrates and ancient Greece (Waldron, 1973). However, the regulation of Pb as a pollutant has been much more recent. The Clean Air Act first classified Pb as an air pollutant in 1970. In 1978, the National Ambient Air Quality Standard (NAAQS) for Pb was established and set to 1.5 micrograms per cubic meter ($\mu g/m^3$) as a three-month quarterly average. In 2008 the Pb NAAQS was reduced by an order of magnitude to 0.15 $\mu g/m^3$ as a three-month rolling average.

Lead is known to impact multiple bodily systems, including neurological, cardiovascular, renal, and reproductive systems (U.S. EPA 2013). Lead is distributed in the body in the brain, liver, kidneys, bones and blood. While impacts are greatest in the body's organs, it is most often measured in blood because it is easier to sample and measure. At high levels in blood (> 50 micrograms per deciliter), Pb can result in both acute and chronic poisoning, resulting in pain, weakness, and gastrointestinal and neurological problems. However, at lower concentrations, Pb can also have negative impacts. One of the more well studied effects of Pb is the reduction of IQ in children. Multiple studies have shown associations between elevated blood Pb levels and reduced IQ at different stages of childhood development (Bellinger and Needleman 2003, Canfield et al. 2003, Lanphear et al. 2005). Blood-Pb levels as low as 5 micrograms per deciliter (µg/dL) were shown have negative IQ impacts (Lanphear et al. 2005). Additionally, childhood elevated blood Pb levels have also been associated with reduced IQ in adulthood (Mazumdar et

al. 2011). Lead affects the brain by inhibiting calcium in the nervous system, interfering with synapses in the cerebral cortex and causing the release of neurotransmitters. Lead is also able to cross the blood-brain barrier and accumulate in astroglial cells which maintain homeostasis and provide protection and support to neurons in the brain and spinal cord, via Pb binding proteins, where it is toxic (Flora and Tiwari 2012).

Lead also impacts the cardiovascular system and is associated with increased blood pressure and hypertension. Martin et al. (2006) examined Pb concentrations in both blood and bone (tibia) and found a positive correlation between both of these concentrations and elevated systolic and diastolic blood pressure. Additionally, Peters et al. (2007) found that bone Pb concentrations when combined with stress, is associated with increased hypertension risk in adults who were originally nonhypertensive. Cardiovascular effects of Pb are also linked to the renal system (U.S. EPA 2013). In the kidneys, Pb can cause both acute and chronic nephropathy, which in turn can cause hypertension and renal failure (Flora and Tiwari 2012).

The reproductive system in humans is also impacted by Pb. One impact Pb has on the reproductive system is the delay of puberty among girls (Gollenberg et al. 2010, Selevan et al. 2003, Wu et al. 2003). Pb exposure has also been shown to cause damage to sperm DNA (Nava-Hernandez et al. 2009) and reduce sperm production rate in rodents (Sokol and Berman 1991). Toxicological studies have linked male reproductive effects to oxidative stress induced by exposure to Pb (U.S. EPA 2013).

Multiple studies have shown that exposure to Pb is controlled more by ingestion than by inhalation (Carrizales et al. 2006, Cornelis et al. 2006). Lead pipes used in water delivery systems and leaded paint have been traditional sources of ingested Pb. However, airborne Pb can

result in ingestion via dry and wet deposition to soils and water systems. Hand-to-mouth contact has been shown to be the primary route of Pb ingestion by children (Lanphear et al. 1998). In addition to direct ingestion of Pb, humans can also be exposed by consumption of plants and animals exposed to Pb.

According to both the Center for Disease Control (CDC) and World Health Organization (WHO), no level of lead in the body is considered safe ("Lead" 2015, "Lead Poisoning and Health" 2015). Each year, the WHO estimates that there are over 140,000 deaths and about 600,000 cases of intellectual impairment in children worldwide because of Pb exposure ("Lead Poisoning and Health" 2015). Additionally, the CDC estimates there are at least 4 million homes with children who have high Pb exposures and about half a million children age 5 and younger with blood-Pb levels greater than 5 μg/dL ("Lead" 2015). Airborne Pb is of particular concern because it may be deposited into soil and water systems, where it accumulates. This can lead to human exposures due to ingestion of these systems, particularly by children.

1.1.2 History of Atmospheric Pb Emissions

Peak domestic emissions of Pb to the atmosphere occurred in the 1970s. The predominant source of Pb emissions during this period was combustion of automobile gasoline. Lead was added to automobile fuel to reduce engine knock and boost octane levels and engine compression. As catalytic converters became more prolific, leaded fuel was slowly replaced by unleaded gasoline because lead poisons the catalysts in the converters. With increased research and awareness of the effects of Pb on health, the sale of leaded gasoline was banned in the United States in 1996. The phase out of Pb in gasoline resulted in a 98% reduction in domestic Pb emissions from 1970 to 1995 (U.S. EPA 2013).

In the 1990s, after significant reduction of Pb emissions, the predominant emitter of Pb in the United States became metal processing. However, during the 1990s and 2000s, metal processing emissions were significantly reduced because of enhanced emission controls. In 1995, metal processing was responsible for 45% of Pb emissions in the United States, but by 2008 it was only responsible for 19% of nationwide emissions. By 2008, there was only a single primary Pb smelter operating in the United States, located in Herculaneum, MO (U.S. EPA 2013). However, this facility ceased operations of its Pb smelter at the end of 2013 as part of an agreement with the United States Environmental Protection Agency (EPA) ("Metal Production" 2015). There are still Pb recycling and recovery smelting operations in the United States and other metal smelters also emit Pb. Figure 1-1, from the 2013 Integrated Science Assessment for Lead, shows the change in Pb emissions by source from 1990 to 2011 (U.S. EPA 2013). Resuspended soil is not included in these estimates, but it cannot be excluded as a source

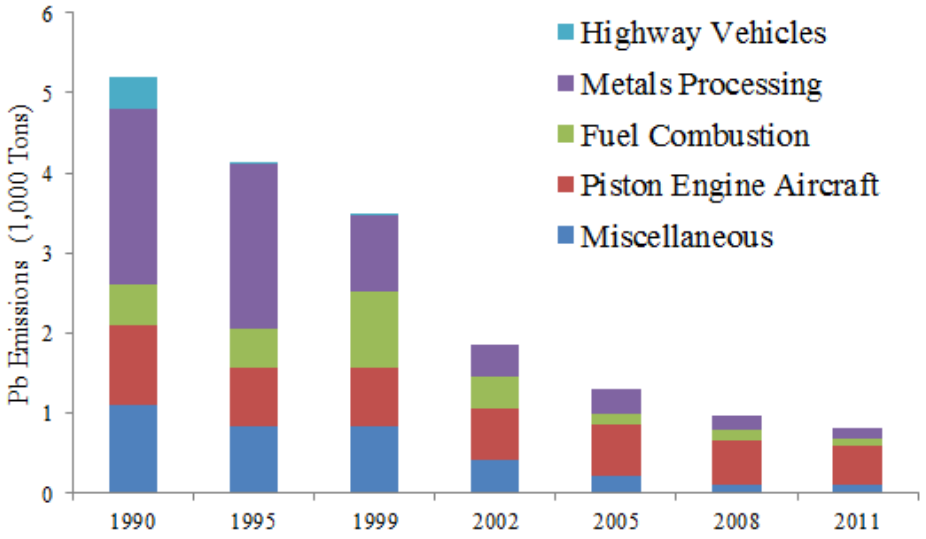

Figure 1-1 EPA estimated annual U.S. Pb emissions over time (adapted from U.S. EPA 2013).

of airborne Pb. Resuspended soil is a more significant contributor in locations with both current and previous major emission sources.

According to the 2011 National Emissions Inventory (NEI), piston-engine aircraft were the largest emitter of Pb in the United States, contributing 60% of the total nationwide emissions (U.S. EPA 2015a). Like in automobiles, piston-engine aircraft use Pb as an additive to reduce engine knock and increase octane level and engine compression ratios. Aircraft also have additional requirements in fuel properties, such as vapor pressure and flash point. In addition to increasing the octane rating of fuel, Pb is added to aviation gasoline (avgas) because it helps reduce the vapor pressure, allowing the fuel to stay liquid at high altitudes. The Pb emitted after the combustion of avgas will be the focus of this dissertation.

1.1.3 Aviation Pb Emissions

The most common leaded avgas is 100 octane low lead (100LL), which has a maximum allowable Pb content of 0.56 g Pb/L. Avgas is used by piston-engine aircraft, which include propeller planes and helicopters. Conversely, jet aircraft do not use avgas and have insignificant Pb emissions because jet fuel has very little to no Pb. Lead is added to avgas in the form of tetraethyllead (TEL). This is the same additive that was previously used in leaded automobile gasoline. There is only one supplier of the TEL additive (Innospec) and it supplies TEL-B, which also contains ethylene dibromide ("Octane Additives" 2015). Ethylene bromide is added as a scavenger for Pb. When avgas combusts in an aircraft engine, Pb reacts with oxygen to form lead oxide. Lead oxide is not very volatile, and therefore solid lead oxide deposits will form within an aircraft engine. These deposits lead to engine fouling, especially around the spark plugs, where temperatures are lower compared to the rest of the engine. Ethylene dibromide is added to avgas because it reacts with lead oxide to form lead bromide, which is much more volatile. Lead

bromide is emitted from aircraft engines as a gas. Once it cools in the atmosphere, lead bromide goes back into the solid phase, forming particulate matter ("Lead Fouling" n.d.).

While piston-engine aircraft emissions are spread across large distances through flight, they tend to be concentrated at airports. In 2008, out of 550 tons of Pb emitted by piston-engine aircraft, 254 (46%) were emitted at or near airports (U.S. EPA 2013). The concentration of Pb emissions at airports has prompted further evaluation of their impacts. In 2010, the EPA released new rules for ambient Pb air monitoring to assess compliance with the 2008 revisions to the Pb NAAQS (U.S. EPA 2010). These rules emphasized monitoring at airports to evaluate whether aviation activity could result in Pb NAAQS violations. Such localized emissions could possibly result in Pb high concentration zone ("hotspots") that could have detrimental impacts on the air quality of neighboring communities.

A limited number of studies have monitored Pb at airports. A study at Buttonville Airport near Toronto, Canada, included measurements of particulate matter with diameters less than 10 micrometers (PM_{10}) and 2.5 micrometers ($PM_{2.5}$) at the ends of the two runways and at a background site 10 kilometers away (Conor Pacific Environmental Technologies, Inc. 2000). Ten 24-hour integrated samples were taken at each of the sampling locations. The airport samples had on average four times higher concentration than the background site, while maximum daily concentrations were 25 times greater at the airport. The mean daily PM_{10} Pb concentration at the airport was 30 ng/m^3 with a maximum daily concentration of 302 ng/m^3 at the end of a runway. The Pb was found to be primarily in the fine particle fraction, which suggests it originated from combustion sources rather than resuspended soil.

Another study conducted in 2013 at McClellan-Palomar Airport near San Diego, CA, measured Pb concentrations at multiple locations around the airport to examine the gradient of Pb hotspots (San Diego Air Pollution Control District 2013). This study used low-volume samplers to collect 24-hour ambient Pb samples at ten locations for ten sampling days. The sampling location with the highest average concentration was next to a runup area with an average concentration of 121 ng/m^3. Runup areas are the locations where pilots perform engine testing and other aircraft testing operations before takeoff. To examine the gradient of Pb impacts, there were three "gradient sites" located 310 ft., 620 ft., and 930 ft. to the east of the runup area site. The average concentrations at these sites were 15, 10 and 7 ng/m^3, respectively. These measurements highlight how quickly the high concentrations decrease with increasing distance from aircraft activity.

Lead and ultrafine particles (UFP) were measured at two general aviation airports in California's South Coast Air Basin (South Coast Air Quality Management District 2010). Sampling was performed near runways and in neighboring communities at Van Nuys Airport and Santa Monica Airport for two different three month periods. Total Suspended Particulate (TSP – particles up to nominally 40-50 micrometers in diameter) Pb concentrations were much greater near the airport runways than in the neighboring communities. Daily average TSP Pb concentrations were nine times greater at Santa Monica Airport than other sites within the South Coast Air Basin. The sampling location with the highest impact had an average daily concentration of 85 ng/m^3 approximately 30 to 40 meters from the end of the runway. Real-time UFP measurements revealed significant particle emissions not only during takeoffs and landings but also while aircraft idled on runways. Like the study in Buttonville, combustion rather than resuspended soil was determined to be the primary source of airborne Pb.

Another study has modeled aviation activities to estimate near-field Pb impacts at and around Santa Monica Airport (Carr et al. 2011). This was the first study to model emissions and impacts by collecting time-in-mode aircraft activity information from on-site surveys and engine operation manuals. The EPA's AERMOD dispersion model was used to predict concentration fields. Airborne Pb monitoring was performed around the airport for two four-day periods during winter and a weeklong period during summer. A total of six days from these two periods (three each) were used for model-to-monitor comparison. Modeling results compared favorably to the measurements with a mean difference of 40% during the winter period and a mean difference of 20% during the summer period. The study found that modeled three-month average impacts around the runway could potentially exceed the current Pb NAAQS of 150 ng/m^3. Modeled Pb concentrations greater than 10 ng/m^3 were estimated for distances up to 900 meters downwind of the airport. Aircraft runup activities were deemed the largest contributor to Pb concentrations at the location of highest impact (i.e. hotspot), while only accounting for about 11% of total aircraft Pb emissions. This finding is consistent with runup activities centralized in one or two locations near the start of the runway and thus are zones of concentrated emissions.

1.2 Motivation for Dissertation Research

Increased relative contribution of airports to total nationwide lead emissions has led to increased airport scrutiny. As previously mentioned EPA reduced the Pb NAAQS from a three-month average of 1.5 $\mu g/m^3$ to 0.15 $\mu g/m^3$ in 2008, and in 2010 revised requirements for ambient Pb monitoring around facilities known to have substantial Pb emissions. The monitoring requirements included general aviation airports. Originally, EPA required ambient Pb monitoring at any airport estimated to emit 1.0 ton of Pb a year, or more. Eventually, an additional 15 airports with estimated emissions between 0.5 and 1.0 ton per year were also monitored for Pb

(U.S. EPA 2015b). Of the 17 airports studied by EPA, two were found to have maximum three-month average Pb concentrations greater than the standard, McClellan-Palomar Airport in San Diego, CA and San Carlos Airport in San Carlos, CA. Two additional airports, Palo Alto Airport in Palo Alto, CA and Reid-Hillview Airport in San Jose, CA were found to have maximum three-month average concentrations greater than half of the standard, and therefore will require further monitoring.

There is significant uncertainty in the EPA Pb emission inventories. There are numerous factors which play a role in an airport's emissions that can vary widely from airport to airport. However, EPA was required to develop a methodology that was applicable to all airports, leading to assumptions which introduce significant uncertainty on an airport-to-airport basis. Key areas that require assumptions in the EPA methodology include the volume of aircraft activity, type of aircraft activity, type of aircraft, engine load and fuel burn rate by activity type, times spent performing different activities, and gasoline Pb content. While it would be onerous to collect these data from every airport, collecting such data at airports where Pb emissions and concentrations are of concern is feasible.

There are only a limited number of studies focused on Pb emissions at airports. Even fewer studies are reported in peer reviewed literature. The lack of study partly results from the relatively recent interest in airport Pb emissions. The FAA and EPA developed the Emissions and Dispersion Modeling System (EDMS) in the 1980s to model and analyze air quality impacts at airports; however, it is more focused on commercial airports. EDMS does not include Pb as a pollutant to be modeled, and it also does not include some activities that are common at general aviation airports, such as runups. Additionally, airport emissions are relatively complex to spatially and temporally distribute. Daily landing and takeoff counts are available from airports

with air traffic control towers; however, these data are generally not available on an hourly basis which is needed for meaningful air quality dispersion modeling. Spatially allocating emissions at airports is also difficult, as many have multiple runways and taxiways where activities can occur. Previous research has shown that pollutant hotspot concentrations are sensitive to the specific location of emissions, especially for near-field impacts (Feinberg et al. 2011).

Recent work has showed living in proximity to airports is related to increased blood-Pb levels. A geospatial analysis of six counties in North Carolina revealed small but significant positive relationships between child blood lead levels and residential proximity to general aviation airports (Miranda et al. 2011). The association was strongest at distances up to 500 meters from the airport boundary and was statistically significant (95% confidence interval) at distances up to 1,500 meters. As previously discussed, increased blood-Pb levels are of significant public health concern. This finding contributes to the motivation to model Pb emissions and Pb concentration fields at general aviation airports. However, as previously mentioned, such modeling has been very limited.

1.3 Thesis Objectives and Structure

This dissertation seeks a greater understanding of the Pb emissions and impacts from piston-engine aircraft at general aviation airports. This includes the measurement and modeling of Pb emissions at airports. From the information learned by measurement and modeling, this work also seeks to evaluate mitigation strategies for reducing potential Pb impacts and health effects.

The remainder of this dissertation is presented in the order of study. The broad objective was to characterize and model lead emissions and impacts for the purposes of quantifying

potential exposures and assessing mitigation strategies. Initial modeling was conducted to examine the importance of different model input parameters as well as perform a base case modeling scenario where site-specific data are unavailable for use in detailed modeling. Site-specific data was then collected to characterize and strengthen connections between aircraft activity and Pb impacts and also provide necessary emission inventory parameters required for the development of more robust emission estimates and model results. Mitigation strategies were also examined based on the information learned and methods developed after collecting site-specific data and performing modeling with the new methodologies.

The first objective of this research was to perform modeling of an airport lacking detailed site-specific data relating to the location, timing, and types of different aircraft activity. This work is presented in Chapter 2, where Centennial Airport (APA) in Denver, CO was modeled using the FAA's EDMS program. This airport was chosen because it has a large number of operations and EPA-mandated Pb measurements. For this project, important parameters such as type, location, and frequency of activity by piston-engine aircraft were estimated via conversations with airport operators. One parameter included in these discussions was the location of runup operations. As previously discussed, they are particularly important in the formation of high concentration hotspots (Conor Pacific Environmental Technologies, Inc. 2000, Carr et al. 2011). This is because they are periods of high fuel burn rate that occur in small, designated areas, which are often located near runway ends. Other important parameters discussed with airport operators were the location and frequency of touch and go operations (TGOs). A touch and go is a flight training exercise where an aircraft lands on a runway and subsequently takes off again without leaving the runway. These are important operations to

characterize because they do not have the associated taxi, idling, and runup emissions that are included in normal landing and takeoff operations (LTOs).

The study modeled daily Pb concentrations across the airport footprint for the full year of 2011. The author was responsible for all model development and data analysis. This work was performed as part of the Airport Cooperative Research Program's Graduate Research Award Program on Public Sector Aviation Issues, which provided a one year research contract. EDMS was used to generate the emissions inventory for all of the activities. While EDMS does not account for lead by itself, emissions were estimated by generating custom aircraft and manually adding an emission factor of 0.56 grams of Pb per liter of fuel, the maximum allowable Pb content in 100LL. EDMS does not include runup emissions; therefore, those emissions had to be manually included. Since complete runup emission parameters were unknown, these emissions were used as an adjustable parameter to fit modeled concentrations to Pb concentrations measured on-site. By using the runup as an adjustable parameter, the project was able to estimate concentrations at other locations around the airport footprint. The work also examined the impact of using different meteorological data sets on modeled Pb concentrations. This work was published in the *Transportation Research Record: Journal of the Transportation Research Board.* While the modeling results compared well with the measured concentrations, using runup emissions as an adjustable parameter is not ideal grouping because grouping all of the uncertainty into a single parameter may provide the right answer for the wrong reasons. Additionally, knowing the true contributors to high concentrations is important for future work to mitigate Pb concentrations. Subsequent research, presented in Chapters 3 and 4, describe research to develop a more robust evaluation of airport Pb impacts. As a result of this subsequent

research, several of the assumptions made in this initial modeling were determined to be inaccurate, showing the importance of collecting site-specific data.

The second objective of this dissertation was to measure and characterize Pb at general aviation airports, which is discussed in Chapter 3. Airborne particulate matter (PM) samples were collected from three general aviation airports of varying size and aircraft activity, and analyzed for Pb content. The three airports that were used in this study were Richard Lloyd Jones Jr. Airport (RVS) in Tulsa, OK; Centennial Airport (APA) in Englewood, CO; and Santa Monica Airport (SMO) in Santa Monica, CA. Both total Pb concentration and Pb isotopic composition of airborne PM samples were measured by inductively coupled plasma-mass spectrometry (ICP-MS). Soil and avgas samples were also analyzed for Pb isotopic composition using ICP-MS. Some airborne PM samples were also analyzed for Pb, Bromine (Br) and other elements using X-Ray Fluorescence (XRF). All airborne, soil, and avgas sample collection, ICP-MS analysis, and data analysis was performed by the author. The XRF analysis was performed by Cooper Environmental Services in Beaverton, OR. A draft of this research and its findings is in preparation to be submitted for publication. The findings help to strengthen claims that measured Pb is indeed from aircraft activity and add to a limited body of knowledge about Pb at airports. However, these measured concentrations are difficult to interpret in the absence of modeling because of the potentially steep concentration gradients. These measured concentrations also serve as a basis for validating the modeling developed and performed, which is presented in Chapter 4.

The third objective of this work was to develop a more robust modeling framework for estimating Pb impacts from airports. As previously noted, there is very limited literature available that focuses on the modeling of Pb at airports. Chapter 4 presents the activity data

collection, development, and results of modeling performed at RVS, APA and SMO. A refined emission inventory methodology was developed and implemented, and the AERMOD air quality dispersion model was used to determine Pb concentration fields at each airport. Modeled concentrations were evaluated using airborne Pb concentrations measured on-site, which are presented in detail in Chapter 3. The spatial extent of impacts across the airport footprints and beyond their boundaries was also examined. This chapter also evaluates the relative impacts of different types of aircraft activity (runup, taxiing, takeoffs, etc.) at the sampling locations used in the study. The author was responsible for collecting and summarizing model and emission inventory parameters, running the airport models and data analysis. Collaborators at Sierra Research, Inc. were responsible for the development of the emission inventory and initial model setup, with significant input from the author. A manuscript of this work has been submitted for publication.

The final objective of this dissertation was to evaluate different mitigation strategies to reduce the potential impacts of Pb from aircraft and airports. Two different strategies are evaluated in Chapter 4. These strategies are moving the runup areas away from other high emitting activities, which could reduce peak hotspot concentrations, and replacing avgas with motor vehicle gasoline (MOGAS) in aircraft with engines that have been tested, certified, and approved to use it. MOGAS is currently not widely available at most general aviation airports. These strategies were evaluated by modeling Pb impacts at RVS, SMO, and a third, new airport, Palo Alto Airport (PAO) in Palo Alto, CA. PAO was selected because it is one of the four airports that must continue to monitor Pb concentrations because previous measurements exceeded more than half of the Pb NAAQS. In order to evaluate the mitigation strategies at PAO, on-site activity data was collected. We were not permitted to collect airborne PM samples, but

the EPA-mandated sampling conducted by the local air quality agency provided an opportunity to evaluate the site-specific data collection and modeling methodology at an airport not previously studied. It also motivated an assessment of the most critical emissions estimation and modeling parameters required to obtain high-quality modeling results. The mitigation strategies of moving runup areas and including MOGAS were evaluated by adjusting source locations and average aircraft Pb emission rates, respectively. The author was responsible for on-site data collection at PAO, with assistance from Mr. Chris Peng, another student at Washington University. The author was also responsible for implementation of mitigation strategies and performing the modeling and data analysis. Initial model setup was assisted by colleagues at Sierra Research, Inc. This modeling will be used as part of an analysis, which also includes an economic evaluation, to fully examine prospective airport Pb mitigation strategies.

This dissertation also includes a major appendix, focused on the evaluation of Nonparametric Trajectory Analysis (NTA). NTA was originally developed by Henry et al. (2011) and the goal to conduct this work was included as a task in the Thesis Proposal. NTA uses high-time resolution (5 minutes or less) air quality and meteorology data to determine the expected concentration at a receptor when the wind passes over other locations. It can be used to determine potential source locations, and potentially is an improvement over 1-D Nonparametric Wind Regression (NWR, Henry 2002) as it adds a distance component to its results. The Thesis Proposal suggested using Monte Carlo simulations to remove artifacts observed when using the conventional analysis methodology. This work was tangential to the main theme of Pb impacts from airports; therefore, it appears as an appendix.

1.4 References

Bellinger, D. and H. L. Needleman (2003). "Intellectual impairment and blood lead levels." New England Journal of Medicine **349**(5): 500.

Bressler, J. P. and G. W. Goldstein (1991). "Mechanisms of lead neurotoxicity." Biochemical Pharmacology **41**(4): 479-484.

Canfield, R. L., C. R. Henderson, Jr., D. A. Cory-Slechta, C. Cox, T. A. Jusko and B. P. Lanphear (2003). "Intellectual impairment in children with blood lead concentrations below 10 micrograms per deciliter." New England Journal of Medicine **348**(16): 1517-1526.

Carr, E., M. Lee, K. Marin, C. Holder, M. Hoyer, M. Peddle, R. Cook and J. Touma. (2011). "Development and evaluation of an air quality modeling approach to assess near-field impacts of lead emissions from piston-engine aircraft operating on leaded aviation gasoline." Atmospheric Environment **45**(32): 5795-5804.

Carrizales, L., I. Razo, J. I. Téllez-Hernández, R. Torres-Nerio, A. Torres, L. E. Batres, A. C. Cubillas and F. Díaz-Barriga (2006). "Exposure to arsenic and lead of children living near a copper-smelter in San Luis Potosi, Mexico: Importance of soil contamination for exposure of children." Environmental Research **101**(1): 1-10.

Conor Pacific Environmental Technologies, Inc. Airborne Particulate Matter, Lead and Manganese at Buttonville Airport. Prepared for Environment Canada under CPE Project 041-6710. Final Report, 2000

Cornelis, C., P. Berghmans, M. van Sprundel and J. C. Van der Auwera (2006). "Use of the IEUBK model for determination of exposure routes in view of site remediation." Human and Ecological Risk Assessment **12**(5): 963-982.

Cullen, C., A. Singh, A. Dykeman, D. Rice and W. Foster (1993). "Chronic lead exposure induces ultrastructural alterations in the monkey seminal vesicle." Journal of Submicroscopic Cytology and Pathology **25**: 127-135.

Feinberg, S. N., V. Yadav, J.G. Heiken and J. R. Turner. (2011). "Midwest rail study: Modeled near-field impacts of emissions of fine particulate matter from railyard activities." Transportation Research Record **2261**: 106-114.

Flora, G., D. Gupta and A. Tiwari (2012). "Toxicity of lead: A review with recent updates." Interdisciplinary Toxicology **5**(2): 47-58.

Gollenberg, A. L., M. L. Hediger, P. A. Lee, J. H. Himes and G. M. Buck Louis (2010). "Association between lead and cadmium and reproductive hormones in peripubertal U.S. girls." Environmental Health Perspectives **118**(12): 1782-1787.

Henry, R. C., A. Vette, G. Norris, R. Vedantham, S. Kimbrough, and R.C. Shores. (2011). "Separating the air quality impact of a major highway and nearby sources by nonparametric trajectory analysis." Environmental Science and Technology **45**(24): 10471-10476.

Henry, R. C., Y. S. Chang, C.H. Spiegelman. (2002). "Locating nearby sources of air pollution by nonparametric regression of atmospheric concentrations on wind direction." Atmospheric Environment **36**(13): 2237-2244.

Lanphear, B. P., R. Hornung, J. Khoury, K. Yolton, P. Baghurst, D. C. Bellinger, R. L. Canfield, K. N. Dietrich, R. Bornschein, T. Greene, S. J. Rothenberg, H. L. Needleman, L. Schnaas, G. Wasserman, J. Graziano and R. Roberts (2005). "Low-level environmental lead exposure and children's intellectual function: An international pooled analysis." Environmental Health Perspectives **113**(7): 894-899.

Lanphear, B. P., T. D. Matte, J. Rogers, R. P. Clickner, B. Dietz, R. L. Bornschein, P. Succop, K. R. Mahaffey, S. Dixon, W. Galke, M. Rabinowitz, M. Farfel, C. Rohde, J. Schwartz, P. Ashley and D. E. Jacobs (1998). "The contribution of lead-contaminated house dust and residential soil to children's blood lead levels: A pooled analysis of 12 epidemiologic studies." Environmental Research **79**(1): 51-68.

“Lead” 2015. Centers for Disease Control, U.S. Department of Health. Accessed October 9, 2015. http://www.cdc.gov/nceh/lead

“Lead Fouling” Accessed October 9, 2015. http://www.shell.com/global/products-services/solutions-for-businesses/aviation/aeroshell/knowledge-centre/technical-talk/techart18-30071600.html

“Lead Poisoning and Health” 2015, World Health Organization. Accessed October 9, 2015. http:// http://www.who.int/mediacentre/factsheets/fs379/en/

Martin, D., T. A. Glass, K. Bandeen-Roche, A. C. Todd, W. P. Shi and B. S. Schwartz (2006). "Association of blood lead and tibia lead with blood pressure and hypertension in a community sample of older adults." American Journal of Epidemiology **163**(5): 467-478.

Mazumdar, M., D. C. Bellinger, M. Gregas, K. Abanilla, J. Bacic and H. L. Needleman (2011). "Low-level environmental lead exposure in childhood and adult intellectual function: A follow-up study." Environmental Health **10**(1): 24.

"Metal Production." 2015. Accessed September 24, 2015. http://www.doerun.com/what-we-do/metal-production

Miranda, M. L., R. Anthopolos, and D. Hastings. (2011). "A Geospatial Analysis of the Effects of Aviation Gasoline on Childhood Blood Lead Levels." Environmental Health Perspectives **119**(10): 1513-1516.

Nava-Hernandez, M. P., L. A. Hauad-Marroquin, S. Bassol-Mayagoitia, G. Garcia-Arenas, R. Mercado-Hernandez, M. A. Echavarri-Guzman and R. M. Cerda-Flores (2009). "Lead-, cadmium-, and arsenic-induced DNA damage in rat germinal cells." DNA and Cell Biology **28**(5): 241-248.

"Octane Additives." 2015. Accessed September 29, 2015 http://www.innospecinc.com/our-markets/octane-additives/octane-additives

Peters, J. L., L. Kubzansky, E. McNeely, J. Schwartz, A. Spiro, III, D. Sparrow, R. O. Wright, H. Nie and H. Hu (2007). "Stress as a potential modifier of the impact of lead levels on blood pressure: The Normative Aging Study." Environmental Health Perspectives **115**(8): 1154-1159.

San Diego Air Pollution Control District. Lead Gradient Study at McClellan-Palomar Airport. Final Report, 2013

Selevan, S. G., D. C. Rice, K. A. Hogan, S. Y. Euling, A. Pfahles-Hutchens and J. Bethel (2003). "Blood lead concentration and delayed puberty in girls." New England Journal of Medicine **348**(16): 1527-1536.

Sokol, R. Z. and N. Berman (1991). "The effect of age of exposure on lead-induced testicular toxicity." Toxicology **69**(3): 269-278.

South Coast Air Quality Management District. General Aviation Airport Monitoring Study. Final Report, 2010

U.S. EPA. 2013 Final Report: Integrated Science Assessment for Lead. U.S. Environmental Protection Agency, Washington, DC, EPA/600/R-10/075F, 2013.

U.S. EPA. 2015a. "2011 National Emissions Inventory data and documentation." From http://www.epa.gov/ttn/chief/net/2011inventory.html.

U.S. EPA. 2015b. *Program Overview: Airport Lead Monitoring* (4 pp, EPA-420-F-13-003, January 2015) http://www.epa.gov/otaq/regs/nonroad/aviation/420f13032.pdf

U.S. EPA. 40 CFR Part 58 - Revisions to Lead Ambient Air Monitoring Requirements, Final Rule. Published at 75 FR 81126. December 27, 2010

Waldron, H. A. (1973). "Lead poisoning in the ancient world." Medical History **17**(4): 391-399.

Wu, T., G. M. Buck and P. Mendola (2003). "Blood lead levels and sexual maturation in U.S. girls: The Third National Health and Nutrition Examination Survey, 1988-1994." Environmental Health Perspectives **111**(5): 737-741.

Chapter 2: Dispersion Modeling of Lead Emissions from Piston-Engine Aircraft at General Aviation Facilities

This chapter has been published in the Transportation Research Record: Journal of the Transportation Research Board (S.N. Feinberg and J.R. Turner, number 2325, pages 34-42 (2013)).

2.1 Abstract

In 2008 the National Ambient Air Quality Standard (NAAQS) for lead was tightened by an order of magnitude. Additionally, general aviation is now the largest source of lead emitted to the atmosphere. The accuracy of modeled lead impacts from general aviation airports is unclear due to uncertainties in both emissions estimation and dispersion modeling. It is important to understand how well such modeling can perform when there is limited data on the aircraft activities at an airport. This study evaluated the level of accuracy that can be achieved by using aggregate activity information and using simple assumptions about the nature of activities to estimate impacts at an airport with lead monitoring.

Dispersion modeling of general aviation lead emissions was performed for Centennial Airport to estimate near-field impacts from airport operations in 2011. Emissions were estimated using the Federal Aviation Administration's Air Traffic Activity System and Emission and Dispersion Modeling System (EDMS). The annual emission estimates for 2011 was 0.43 tons, which is much lower than the 0.73 tons estimated by the 2008 National Emissions Inventory. Sensitivity analyses were conducted by varying several emission parameters. Modeled concentrations at the on-site lead sampler were quite sensitive to the amount of runup emissions. Concentrations modeled with Automated Surface Observing System meteorology have greater

correlation with on-site measured values than concentrations modeled with Integrated Surface Hourly meteorology. Three-month average impacts modeled at the on-site lead sampling location ranged from 10 ng/m^3 to 20 ng/m^3, all well below the lead NAAQS of 150 ng/m^3.

2.2 Introduction

General aviation activities are the largest source of lead emissions to the air and are receiving increased attention following the revisions in 2008 to the National Ambient Air Quality Standards (NAAQS) for lead (U.S. EPA 2011). In 2010, the Environmental Protection Agency (EPA) released new rules for ambient lead air monitoring to assess compliance with the new lead standard (U.S. EPA 2010a). These rules emphasized monitoring at airports to evaluate whether aviation activity could result in violations of the lead NAAQS. Such localized emissions could possibly result in lead "hotspots" that could have detrimental impacts on the air quality of neighboring communities. In addition to monitoring, emission and dispersion modeling can provide insights on the extent of lead impacts from airports.

Lead emissions at airports result from the combustion of leaded aviation gasoline (avgas) in piston-engine aircraft, which include propeller planes and helicopters. Lead is present in the fuel as an antiknock agent. Conversely, lead emissions from jets are not significant as jet fuel contains very little to no lead. The most common avgas is 100 octane low lead (100LL). A gallon of 100LL can contain up to 2.12 grams of lead, most of which is emitted as particles when combusted (ASTM International 2005).

A limited number of studies have monitored lead at airports. A study at Buttonville Airport near Toronto, Canada, included measurements of particulate matter with diameters less than 10 micrometers (PM_{10}) and 2.5 micrometers ($PM_{2.5}$) at the ends of the two runways and at a background site 10 kilometers away (Conor Pacific Environmental Technologies, Inc. 2000).

Ten daily integrated samples were taken at each of the sampling locations. The airport samples had on average 4 times higher concentration than the background site, while maximum daily concentrations were 25 times greater at the airport. The mean daily PM_{10} lead concentration at the airport was 30 ng/m^3 with a maximum daily concentration of 302 ng/m^3 at the end of a runway. Additionally, the lead was primarily in the fine particle fraction, which suggests it originated from combustion sources rather than resuspended soil.

Lead and ultrafine particles (UFP) were measured at two general aviation airports in California's South Coast Air Basin (South Coast Air Quality Management District 2010). Sampling was performed near runways and in neighboring communities at Van Nuys Airport and Santa Monica Airport for two different three month periods. Total Suspended Particulate (TSP) lead concentrations were found to be much greater near the airport runways than in the neighboring communities. Daily average TSP lead concentrations were nine times greater at Santa Monica Airport than other sites within the South Coast Air Basin. The sampling location with the highest impact measured an average daily concentration of 85 ng/m^3 approximately 30 to 40 meters from the end of the runway. Real-time UFP measurements revealed significant particle emissions not only during takeoffs and landings but also while idling on runways. Again, combustion, not resuspended soil, was determined to be the primary source of airborne lead.

Another recent study modeled aviation activities to estimate near-field lead impacts at and around Santa Monica Airport (Carr et al. 2011). This study modeled emissions and impacts by collecting time-in-mode aircraft activity information from on-site surveys and engine operation manuals. Additional monitoring was performed around the airport for winter and summer sampling periods. Results compared favorably to the measurements during the winter period with a mean difference of 40%. The study found that modeled three-month average

impacts could potentially exceed the current NAAQS for lead of 150 ng/m^3 around the runway. Modeled lead concentrations of greater than 10 ng/m^3 were estimated for distances up to 900 meters downwind of the airport. Aircraft runup activities were deemed the largest contributor to lead impacts, while only accounting for about 11% of total aircraft lead emissions.

In the case of general aviation airports, activity data such as aircraft type, timing of take-offs, and location of activity may be highly aggregated or unavailable. These activities must be allocated to the hourly level to be consistent with dispersion modeling. Lead emissions from piston-engine aircraft activity and resulting concentrations must be better characterized to understand the impacts of general aviation activity on overall air quality. The Federal Aviation Administration's (FAA) Emissions and Dispersion Modeling System (EDMS), a popular tool to develop emission inventories, has the American Meteorological Society/Environmental Protection Agency Regulatory Model (AERMOD) embedded to perform dispersion modeling; however, it is focused mostly on commercial airports and does not contain emission estimates for lead. To model impacts, EDMS required manual inputs for lead emission factors.

Dispersion modeling can be a very useful tool to screen for lead impacts at general aviation airports where they may be of concern. It is important to understand model performance when there is limited data on the aircraft activities at an airport. Thus, the study summarized in this paper was conducted to estimate impacts at an airport with on-site lead monitoring and to evaluate the level of accuracy that can be achieved by using aggregate activity information and using simple assumptions about the timing, location and type of activities.

This study modeled lead concentrations at Centennial Airport (APA) near Denver, Colorado. According to the 2008 National Emissions Inventory (NEI), Centennial Airport emitted 0.73 tons of lead (U.S. EPA 2012a). On-site lead sampling commenced in April 2010.

Samples are collected on a one-in-six-day schedule, with 59 valid sampling days during 2011. Hourly lead concentrations at the sampling site were modeled for the full year 2011. Multiple scenarios were modeled to understand the varying impacts of important parameters such as fleet makeup, number of touch-and-gos and amount of runup emissions. Additionally, the sensitivity of impacts to the meteorological data sets used for modeling was evaluated by using both the National Climatic Data Center's (NCDC) Integrated Surface Hourly (ISH) and Automated Surface Observing System (ASOS) data sets for Centennial (NOAA National Climatic Data Center 2012a, NOAA National Climatic Data Center 2012b). ISH meteorology is the dataset that historically has been used for dispersion modeling. It records data every hour; however, the data for a given hour is typically a spot reading is often taken for only one minute. EPA now recommends using ASOS data for dispersion modeling conducted with AERMOD. ASOS data are reported as two-minute averages each minute, which can later be rolled up into hourly averages using the EPA's AERMINUTE meteorological processor (U.S. EPA 2012b).

2.3 Methods and Experimental Design

Centennial Airport has three main runways. Figure 2-1 shows the layout of the airport including the location of the sampling site as well as a wind rose for hourly winds in 2011. Annual and monthly total operations, as well as day-of-week profiles, were obtained from the FAA's Air Traffic Activity System (ATADS). These data structures are consistent with the operational profiles used by EDMS. While ATADS does not provide information on the location of activity and whether the operations are from jets or piston-engine planes, many of these details were determined through conversations with airport management (Robert Olislagers, unpublished data). The majority of piston engine landings and takeoffs (LTOs) occur on Runway 10 (the east/west runway) taking off toward the east and piston-engine aircraft account for about

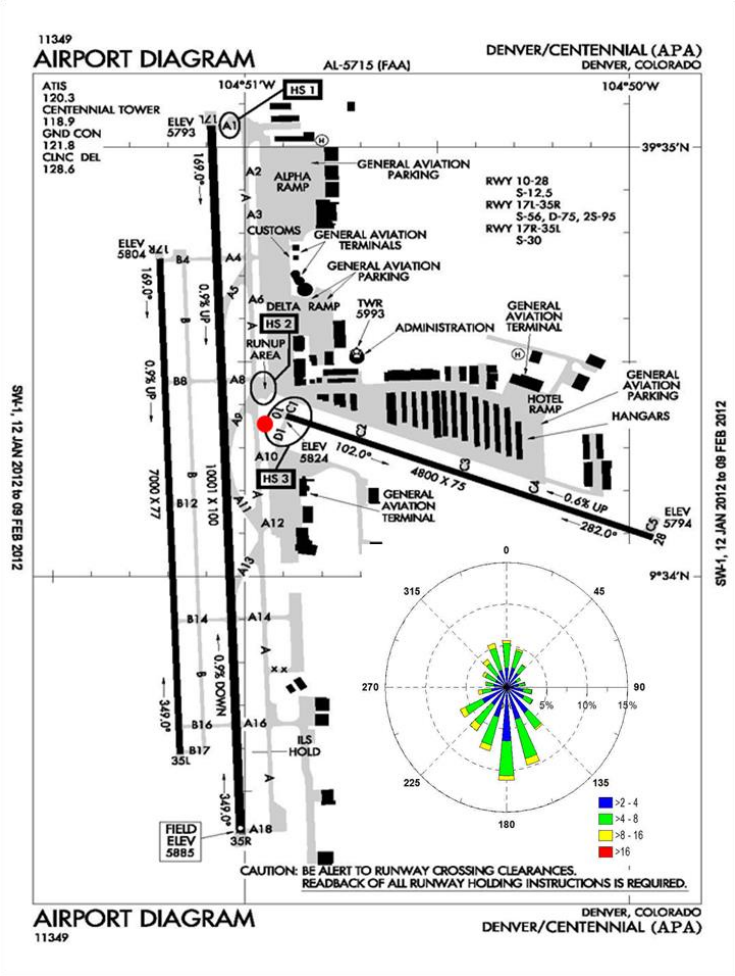

Figure 2-1 Diagram of Centennial Airport layout with the location of the on-site lead sampler. Diagram from FAA (U.S. FAA). Inset is a wind rose of hourly ISH winds (m/s) measured at Centennial in 2011. The wind rose orientation is consistent with the airport diagram orientation. Calm and missing winds made up 15% of hours.

40% of the aircraft activity. Touch-and-gos at Centennial most often occurs on the far west runway (17R/35L). Most of runups occur just northwest of the start of Runway 10, which is labeled on Figure 2-1. The lead sampler is located about 100 meters southeast of the start of Runway 10 and 200 meters south of the runup area, in a zone of estimated high lead impact. Measurement data from the Denver Municipal Animal Shelter $PM_{2.5}$ Chemical Speciation Network site, which is about 10 miles northwest of the airport, was used to evaluate background lead levels in the area (U.S. EPA 2012c). Background lead levels were below the median

detection limit of 2.8 ng/m^3on more than half of the days, and the average lead level was less than 5% of the average level at Centennial of 16 ng/m^3.

EDMS was used to generate the emissions inventory for all of the activities. Default EDMS parameters were used for emissions estimation and dispersion modeling when more specific data are otherwise unavailable. While EDMS does not account for lead by itself, emissions were estimated by generating custom aircraft and manually adding an emission factor of 2.12 grams of lead per gallon of fuel. The custom aircraft used to represent single-engine planes was based on a Cessna Skyhawk, while the aircraft used to represent twin-engine aircraft was based on a Cessna Golden Eagle. Other than the lead emission factor, all other factors for the custom aircraft were unchanged. Since EDMS does not account for runup, the runup was modeled as an additional volume source with an initial vertical dispersion parameter of 10 meters and lateral dispersion parameter of 20 meters. Runways and taxiways were modeled with the default EDMS dispersion width of 20 meters. Other important factors, including the fleet makeup, amount of runup and number of touch-and-gos, varied based on the scenario being modeled. Lead impacts were initially modeled at the sampling location to make model-to-monitor comparisons. Subsequently, spatial concentration fields within and beyond the airport boundary were modeled using input parameters that maximized the agreement with measurements.

2.3.1 Development of the Base Case

A base case modeling scenario was developed using readily available data and some simple assumptions. This was not intended to be the most accurate case for modeling, but rather a starting point for model-to-monitor comparisons. Since there was no time-of-day activity information available, the time-of-day profile was chosen to be uniform between the hours of

7:00 AM to 7:00 PM local standard time. No activity was assigned to the nighttime hours. None of the operations were modeled as touch-and-gos for the base case scenario, and all of the LTOs were modeled using Runway 10. An additional scenario was modeled using different runways based on conditional winds; however, the modeled annual average concentration at the monitor was within 5% of the base case modeled concentration and all subsequent model runs were conducted using only Runway 10. Since the percentages of single- and twin-engine planes were unknown, they were assumed to be 81% and 19%, respectively, based on planes housed at the airport (AirNav 2012). Because EDMS does not calculate runup, it was estimated as a percentage of total emissions from LTOs. For the base case, runup emissions were estimated to be 3%, based the 2008 NEI guidelines for time-in-mode emissions for an IO-320 engine. Base case dispersion modeling was performed using both ISH and ASOS meteorology.

2.3.2 Sensitivity Studies

Several sensitivity studies were performed, using ISH meteorology, to assess the effects of different factors on the range of modeled impacts. The first sensitivity study assessed the impact of different time-of-day activity profiles on modeled concentrations at the sampling site. Three different diurnal activity profiles were evaluated. Each included a different number of peaks in activity, ranging from one to three peaks in a day. Figure 2-2 shows the weighted diurnal profile of airport activity for these three models. The weighted activity value was defined as the ratio of activity in a given quarter-hour to the activity in the highest quarter-hour. The 1-peak model started with activity at about half its maximum value at the beginning of the day, ramped up linearly to a peak at midday, and then fell back to half its maximum value by the end of the day.

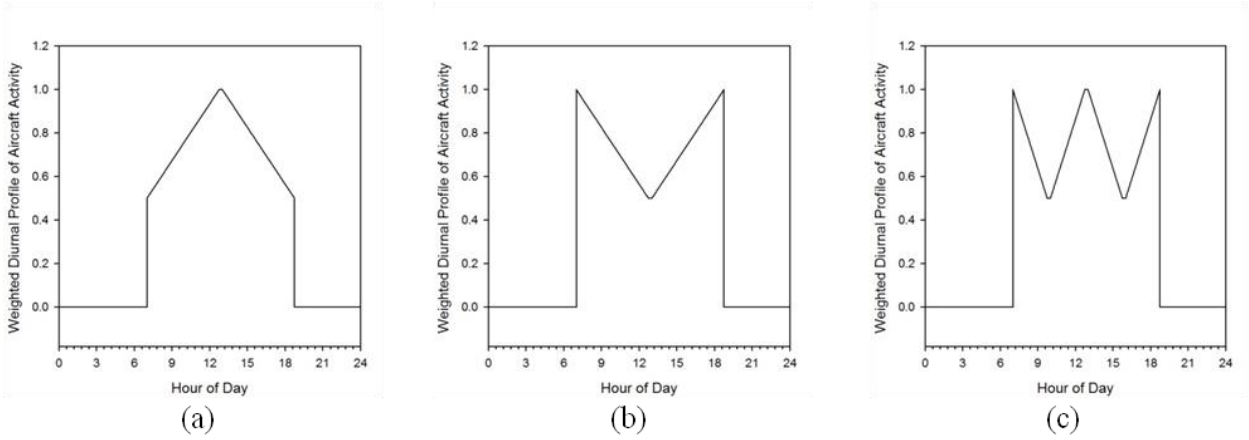

Figure 2-2 Weighted diurnal profile of aircraft activity for the 1-peak (a), 2-peak(b) and 3-peak (c) models.

The 2-peak model was similarly constructed, with peaks at the beginning and end of the day and about half of the peak activity level at midday. The 3-peak scenario had peaks at the beginning, middle and end of the day. Another sensitivity study evaluated the impact of varying the fraction of single- and twin-engine aircraft. In addition to the base case scenario, two scenarios were modeled with 10% and 30% of aircraft operations attributed to twin-engine aircraft. A third sensitivity study analyzed the impact of touch-and-go operations. Touch-and-go activity was modeled as 10% to 50% of total piston-engine aircraft operations in 10% increments. Since touch-and-gos occur on a different runway than LTOs at Centennial, the spatial allocation of emissions also changes as the touch-and-go percentage is changed. For this study, the runup activity also had to be scaled based on the level of touch-and-go activity, because touch-and-go operations do not have corresponding runups. A final sensitivity study varied the amount of runup emissions. Scenarios were modeled with runup accounting for 1%, 5%, and 10% of total emissions. Each of these studies were then compared to the measurement data at the airport to determine which cases produced the most consistent results and which were likely not feasible.

2.4 Results and Discussion

2.4.1 Base Case Model

Dispersion modeling of airport activities was performed for each hour in 2011 at Centennial Airport. Total annual lead emissions estimated by EDMS were 0.49 tons, significantly lower than the 0.73 tons estimated by the 2008 NEI. While operations decreased 9% from 2008 to 2011, the difference between these two emission estimates largely arises from differences in methodology. While EDMS emissions are estimated based on aircraft operations at the specific airport, NEI emissions are based on the assumption that 72% of LTOs were performed by piston-engine aircraft at all airports (U.S EPA 2010b). The 2011 modeled annual average lead concentration at the monitoring location was 28 ng/m^3 using ISH meteorology and 34 ng/m^3 using ASOS meteorology. These levels are about twice the measured annual average of 16 ng/m^3. While only 3% of lead emissions were assigned to runup, 60% of the lead modeled at the sampling site resulted from runup activity. Using ASOS meteorology, the modeled impacts from runup alone exceeded the measured impacts in 2011. While runup impacts are expected to be high based on the proximity to the sampling site, these modeled values suggest that runup emissions were significantly overestimated for the base case.

Figure 2-3a shows a scatter plot of ISH modeled daily concentrations and measured daily concentrations, while Figure 2-3b shows a scatter plot of ASOS modeled daily concentrations and measured daily concentrations. Both ISH and ASOS modeled concentrations consistently overestimated the measured values, although ASOS overestimated the concentrations more than ISH. Both modeled concentrations showed moderate correlation with the measured results when comparing daily average values. Measured and ISH concentrations had a Pearson correlation of 0.47, while measured and ASOS concentrations had a Pearson correlation of 0.55. The mean

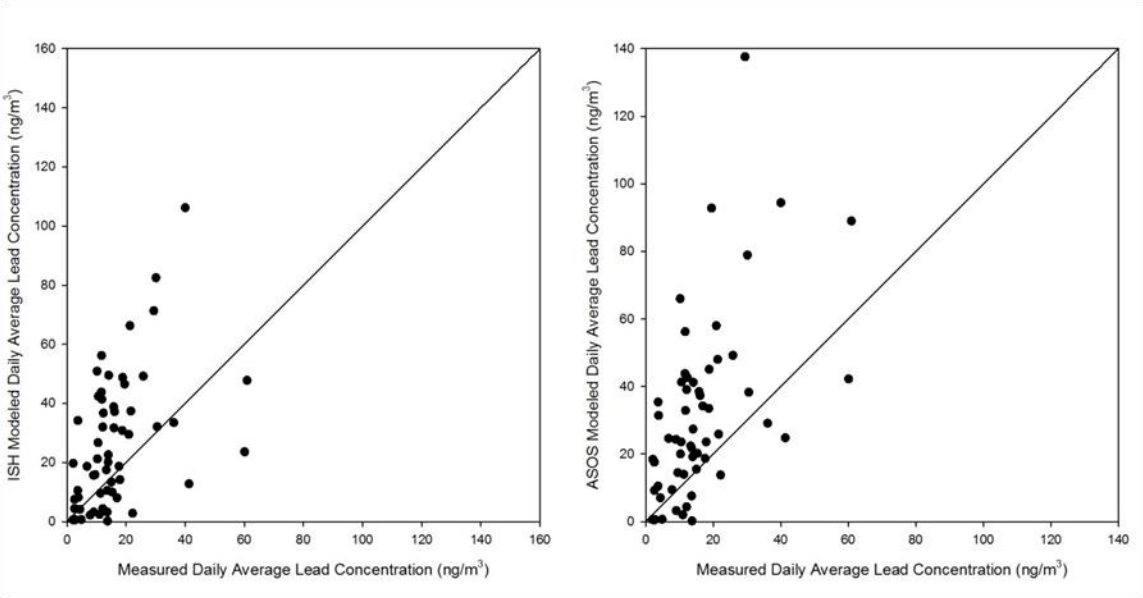

Figure 2-3 Scatter plots of measured daily lead concentrations versus base case ISH modeled daily concentrations (a) and ASOS modeled daily concentrations (b).

ratio of measured concentrations to ISH modeled concentrations was about 2 on a daily basis, and the mean ratio for ASOS concentrations was about 2.4. Figure 2-4a shows the monthly average measured and modeled lead concentrations at the monitor. The monthly modeled averages were calculated using only the days with valid sampling data. The base case scenarios

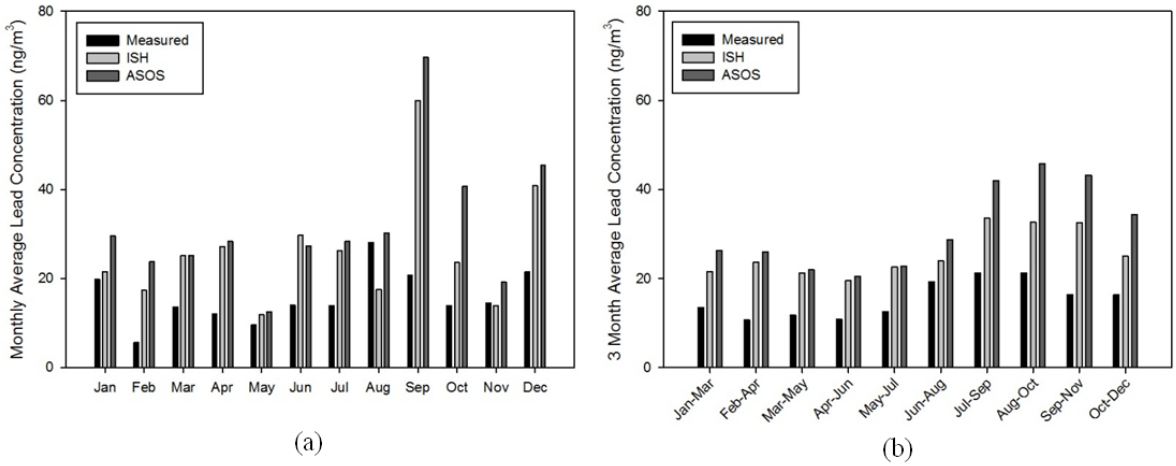

Figure 2-4 Measured and Base Case modeled monthly average lead concentrations (a) and 3-month average concentrations (b) at the Centennial lead sampler.

modeled with the two wind datasets yielded modeled concentrations consistently higher than measured concentrations for the majority of months. In September, the ISH modeled concentration was more than twice the measured concentration, and the ASOS modeled concentration was more than three times the measured value. Gaussian plume models tend to overestimate on the microscale, which could account for some of the overestimation; however, this study assumed that the biases resulted from the location of activities and their emission rates. While the monthly estimates can be noisy because of the few (typically five to six) sample days per month, the overall trend of excess modeled concentrations implies that there is an overestimation of emissions for the base case scenario. Figure 2-4b **s**hows rolling three-month average concentrations to match the averaging time for the lead NAAQS. Both ISH and ASOS modeled three-month concentrations are higher than the measured concentrations for all of the three-month periods in 2011. Additionally, ASOS modeled three-month concentrations are consistently higher than ISH modeled concentrations. Similar to the monthly average concentrations, these results suggest that the estimated emissions in the base case are too high and/or the spatial and temporal allocations of activity are misplaced. These variations were evaluated by the sensitivity studies performed in this study. Even with the model bias toward overestimation, modeled three-month average concentrations were all much lower than the NAAQS standard of 150 ng/m^3.

2.4.2 Sensitivity Studies

A total of thirteen sensitivity studies on four activity variables were also modeled for 2011. These studies were performed to determine which variables had a significant impact on modeled concentrations and their range of feasible values. Table 2-1 summarizes the sensitivity studies and the variables' impact on annual average concentrations at the Centennial sampling

Table 2-1 Summary of Modeled Annual Average Concentrations from Sensitivity Studies

Variable	Base Case	Diurnal Pattern[1]			Fleet Makeup[2]		Touch and Gos[3]			Run-Up[4]		
Value	-	1	2	3	10	30	10	30	50	1	5	10
Annual Average (ng/m^3)	28	28	28	28	23	34	25	20	14	16	38	67
Difference from Base Case (%)	-	-0.1	-0.3	-0.4	-17	-21	-10	-30	-49	-43	34	141

site. While a different diurnal activity pattern will certainly affect hourly modeled concentrations, the annual average modeled concentrations were relatively insensitive to diurnal activity patterns because over longer periods the hourly differences average out. Monthly averages also exhibit relatively small variations from the base case modeled values.

Increasing and decreasing the percentage of operations due to twin-engine aircraft had significant impacts on modeled concentrations. Decreasing the fraction of twin-engines from 19% to 10% resulted in a 17% decrease in modeled impacts, while increasing the percentage to 30% increased the modeled impacts by 21%. This corresponds to about a 1.9% increase in emissions for each 1% increase in the percentage of twin-engine aircraft, which suggests that there could be significant uncertainty in emissions and concentrations in the absence of data showing the actual percentage of activity. However, since twin-engine aircraft make up a relatively small fraction of the overall piston-engine aircraft fleet, the bias is likely well constrained.

Changing the amount of touch-and-gos also resulted in a wide variation of modeled impacts. Table 2-1 shows a subset of the sensitivity studies performed varying touch-and-go activity. For every 10% increase in touch-and-gos, there was an approximate 10% decrease in modeled concentrations at the sampling site. This is expected since most touch-and-gos at Centennial are performed at the far west runway. Lead emissions from the west runway originate

far enough away from the sampling site that they are too disperse to have large impacts there. Touch-and-go activity levels likely will vary widely by airport, depending on the presence of flight schools, and these activities may affect the spatial allocation of emissions.

Changes in runup resulted in very significant changes in modeled concentrations at the lead monitor. Decreasing runup emissions to 1% of total emissions reduced the modeled annual concentration by 43%, while increasing runup emissions to 10% raised the modeled annual concentration by 141%. Runup occurs in a relatively small spatial footprint, which in the case of Centennial, is close to the sampling site near the centroid of the airport footprint. The beginnings of runways are often located close to the runup areas, and this combination of activities likely gives such areas the highest lead concentrations on an airport footprint. Airports where these zones are near public spaces may warrant an evaluation of impacts, and in such cases it may be important to refine the runup emissions estimate. This may be difficult, as there are many factors that influence runup emissions such as engine type and length of time spent performing runup.

An additional sensitivity study was performed to better constrain the number of touch-and-gos and amount of runup emissions at Centennial. Full year 2011 modeling was performed using ASOS meteorology, varying the amount of touch-and-go operations between 10% and 50% of total operations. For each case, the amount of runup emissions was adjusted to optimize agreement between the twelve monthly-average modeled and measured concentrations using objective functions: minimizing the mean squared error, minimizing the mean absolute error, and making the mean ratio equal to one. The mean ratio is the mean of the modeled over monitored daily-average ratios. Figure 2-5 shows the amount of runup emissions, as a percentage of total non-touch-and-go emissions, required to optimize these figures of merit as a function of the fraction of touch-and-go activity. Of the three approaches to reconciling the model-to-monitor

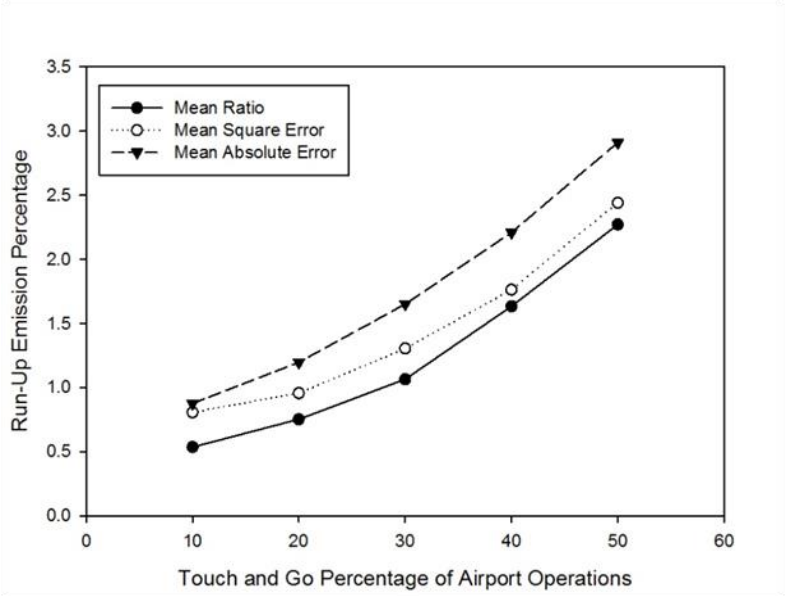

Figure 2-5 Optimized runup emission percentage as a function of touch and go operations and optimized figure of merit.

concentrations, optimizing the mean ratio resulted in the least amount of runup emissions, while minimizing the mean absolute error resulted in the greatest amount of runup emissions. For each, large increases in touch-and-go activity required small increases in the amount of runup emissions needed for optimization, which varied from 0.5% to 3% of total non-touch-and-go emissions. All of the calculated amounts of runup emissions were found to be lower than the amount of emissions used in the base case. This again suggests that the base case overestimated the amount of emissions from runup.

Airport administration at Centennial estimated that about 40% of aircraft operations were touch-and-gos in 2011 (Lorie Hinton, unpublished data). With this parameter now better constrained, modeling was performed to estimate runup emissions based on minimizing the mean square error between monthly average modeled and measured concentrations. Runup emissions were used as an adjustable parameter to match the model to the measurements. Using this refined model, hourly lead concentrations were estimated for the full year 2011 using both

ISH and ASOS meteorology with a touch-and-go percentage of 40% and best-fit runup percentage emissions as 1.8% of total non-touch-and-go emissions. Total lead emissions for 2011 were estimated to be 0.43 tons. Again, this is significantly lower than the 2008 estimate by the NEI (U.S. EPA 2012a).

The refined model showed better correlation between modeled and measured daily average concentration than the base case. ASOS modeled daily concentrations again correlated better with measured values than ISH modeled daily concentrations. Measured and ISH modeled daily concentrations had a Pearson correlation of 0.55, while measured and ASOS modeled daily concentrations had a Pearson correlation of 0.66. Figure 2-6a shows a scatter plot of measured and ASOS modeled concentrations. The improved correlation is visually apparent when compared to the scatter plot of the base case ASOS modeled daily values (Figure 2-3b). Additionally, the scatter is now well distributed about the one-to-one line. The wide spread

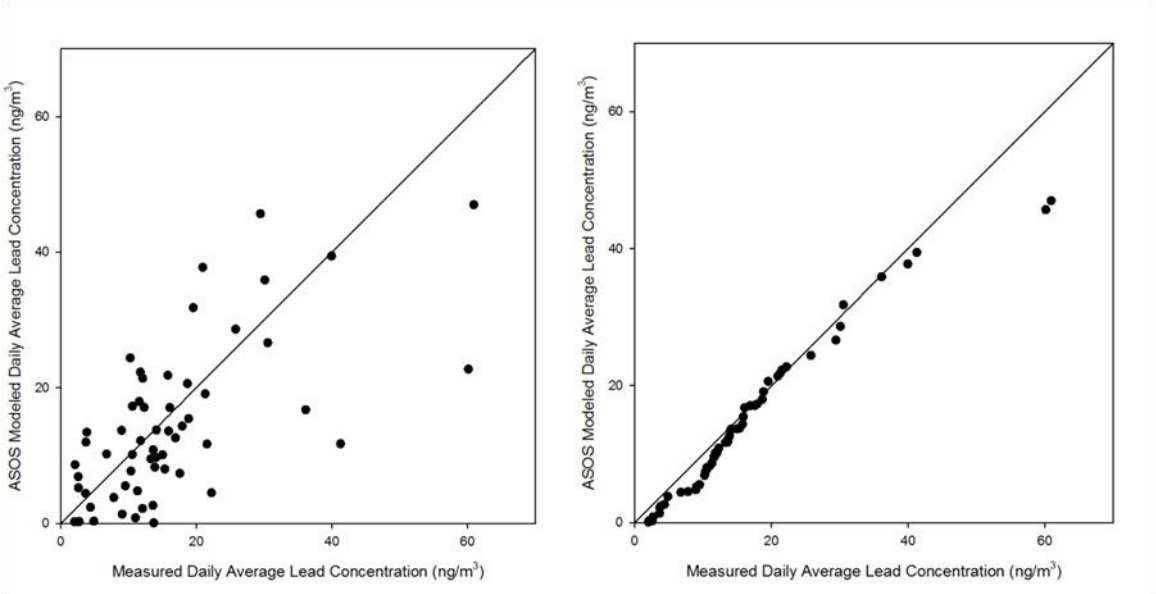

Figure 2-6 Scatter plots of measured daily lead concentrations versus refined ASOS modeled daily concentrations (a) and sorted measured daily concentrations versus sorted ASOS concentrations (b). Note that the axes are one half the scale used in Figure 2-4.

around the one-to-one line shows the difficulty in modeling short time periods with aggregated activity information. Figure 2-6b shows a scatter plot of measured and ASOS modeled daily average concentrations when both data sets are sorted and paired based on rank. The scatter is very tightly correlated along the one-to-one line. This suggests that even though the exact daily averages are difficult to model, the distribution of values is very well characterized by this modeling approach, and long term modeled averages will likely be accurate.

Figure 2-7a shows monthly average measured and monitored concentrations at the sampling site at Centennial for this refined model. Monthly average modeled concentrations were calculated using only days with concurrent sampling. Both ISH and ASOS modeled concentrations were closer to the measured concentrations than in the base case; however, ASOS generally showed better agreement with measurements than ISH. For all months, monthly averaged ASOS modeled concentrations were within a factor of two of the measured concentrations. The largest differences in modeled and measured monthly average concentrations were in January and August. These two months each contained a single day where measured concentrations were significantly higher than modeled values. Further

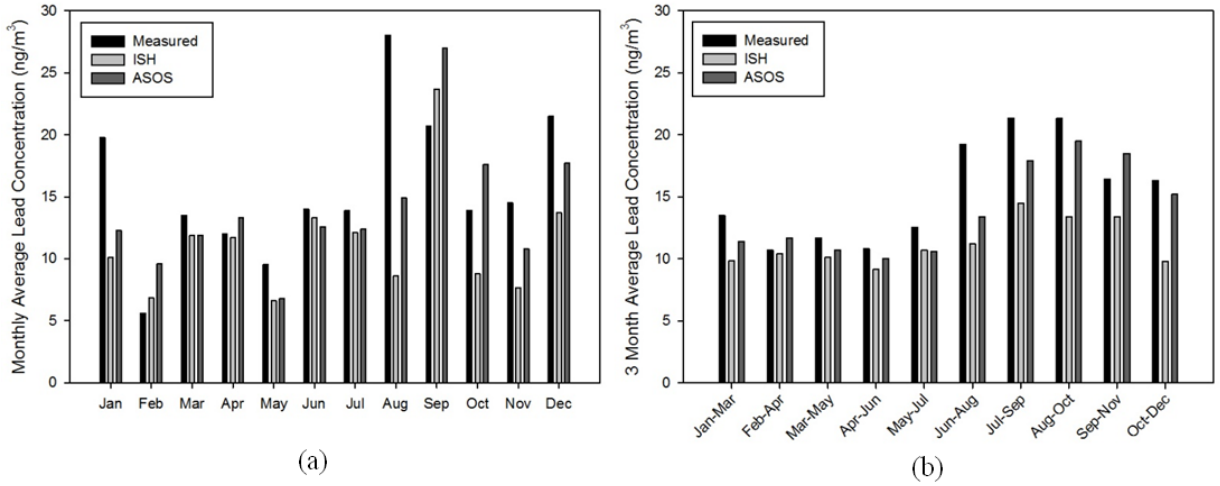

Figure 2-7 Measured and Refined model monthly average lead concentrations (a) and 3-month average concentrations (b) at the Centennial lead sampler.

examination of these two days did not reveal explanations for such large differences between measured and modeled concentrations. However, such day-specific differences are to be expected when modeling with limited activity pattern data. Figure 2-7b shows the three-month average measured and modeled concentrations. There was strong agreement between measured and modeled three-month average concentrations using the refined model. Similar to the monthly average concentrations, ASOS modeled values generally agreed better with measurements than ISH modeled values. Measured and modeled three-month average concentrations were well below the NAAQS standard.

The refined method was then used to model lead concentrations around the airport. Hourly concentrations were modeled using a 200 meter grid. An additional 50 meter grid was modeled in a 650 by 400 meter section around the sampling site, runup area and start of Runway 10. Figure 2-8 shows the monthly average concentrations around Centennial Airport for September 2011, the month with the highest modeled lead concentration at the sampling site in 2011. The white circle represents the lead sampling site. Note that the sampling site is not in the area of highest concentration for this month, because it is upwind of the high emissions zone, or in general, during prevailing winds. The highest lead levels are actually north of the monitor. The highest modeled monthly averages were found to be around the start of Runway 10 and the runup area. However, it is important to consider that Gaussian plume tend to models overestimate concentrations at locations very close to sources (De Nevers 2000). For this reason, AERMOD has an exclusion zone around volume sources (44 meters in this case) where concentrations are not modeled (U.S. EPA 2012d). Given this information, concentrations are likely higher immediately around the runup area than are shown by the modeling. The highest modeled September average around the airport was found to be 27 ng/m^3. Three-month averages

Figure 2-8 Modeled average September lead impacts in ng/m^3 using the refined model. Background image from Google Earth™.

were also calculated across the airport. The largest modeled three-month average was 25 ng/m^3 between October and December, approximately 150 meters north of the runup area. Significant impacts did not extend much past the runup area and the beginning of Runway 10. Modeled impacts outside the airport boundary all were less than 5 ng/m^3 in September, which was true for all other months. Centennial is a somewhat special case because a large part of the general aviation activity occurs near the centroid of the airport. Other airports with greater activity levels near their boundaries will have higher lead impacts extending past their footprint.

2.5 Conclusion

Dispersion modeling performed at Centennial Airport in Colorado shows that accurate modeling of measured lead impacts can be achieved using aggregate activity data and EDMS. The base case model significantly overestimated lead impacts at the on-site sampling location. Concentrations modeled at this location were extremely sensitive to the amount of runup activity, because the runup area is very close to the lead sampling site. A refined model was developed using insights provided by the airport operations personnel. The percentage of total emissions assigned to runup activities was used as an adjustable parameter to fit the model to the monitored data. Using a single estimate for the runup emissions percentage significantly improved monthly average model-to-monitor comparisons over the year. Runup activity levels were used to tune the model-to-monitor reconciliation and, while the comparison was favorable, there might be other sources of bias in the emissions estimation and activity allocations that are being lumped into this fitting parameter. More work is needed to evaluate the applicability of EDMS – which uses the AERMOD implementation of the Gaussian plume model – when the receptors of interest are close (e.g., within a hundred meters) of the high emission source zones. Despite these caveats, the methodology used for this study provides a framework for modeling impacts at other airports.

Annual average concentrations modeled using ASOS meteorology were about 20% higher than those obtained using ISH meteorology. ASOS modeled daily average concentrations exhibited significantly better correlation with measurements performed at the airport than ISH modeled concentrations. This suggests that ASOS is the preferable meteorological dataset for modeling. While it is difficult to accurately model day-specific measured concentrations using only aggregate activity information, this modeling approach showed that it is possible to make

accurate predictions for longer time scales. Despite the relatively high levels of general aviation activity at Centennial Airport, modeled concentrations showed that impacts were well below the lead NAAQS for 2011. Concentrations were highest near runup and take-off areas with steep gradients when moving away from these zones. Thus, airports with runup and take-off areas in close proximity to public spaces may warrant evaluation. While this study has focused on modeled concentration values within the context of the lead NAAQS, broader concerns have been raised about the impact of general aviation lead emissions on neighboring communities (Miranda et al. 2011) and dispersion modeling could be a valuable tool towards assessing the impacts.

2.6 Acknowledgments

This study was funded by the Airport Cooperative Research Program's Graduate Research Award Program. The authors would like to thank Larry Goldstein (Manager, ACRP Graduate Research Award Program). Paul Hamilton, Mike Kenney, and Robert Samis served on the review panel for this project and their valuable feedback is gratefully acknowledged. The authors would also like to thank Robert Olislagers and Lorie Hinton for providing insights on the operations at Centennial Airport.

2.7 References

AirNav. 31 May 2012. Centennial Airport. Accessed June 5, 2012. http://www.airnav.com/airport/KAPA/

ASTM International, 2005. Annual Book of ASTM Standards Section 5: Petroleum Products, Lubricants, and Fossil Fuels, vol. 05.01, Petroleum Products and Lubricants (I): pp. D 56 e D 3230.

Carr, E.; Lee, M.; Marin, K.; Holder, C.; Hoyer, M.; Pedde, M.; Cook, R. and J. Touma. Development and Evaluation of an Air Quality Modeling Approach for Lead Emissions from

Piston-Engine Aircraft Operating on Leaded Aviation Gasoline. Atmospheric Environment 45 (2011) 5795-5804

Conor Pacific Environmental Technologies, Inc. Airborne Particulate Matter, Lead and Manganese at Buttonville Airport. Prepared for Environment Canada under CPE Project 041-6710. Final Report, 2000

De Nevers, Noel. (2000). Air Pollution Control Engineering. Boston. McGraw Hill

Miranda, M. L.; Anthopolos, R; and D. Hastings. A Geospatial Analysis of the effects of Aviation Gasoline on Childhood Blood Lead Levels. Environmental Health Perspectives 119 (2011) 1513-1516

NOAA National Climatic Data Center, 2012a. Global Surface Hourly Database. Available at http://hurricane.ncdc.noaa.gov/pls/plclimprod/poemain.accessrouter

NOAA National Climatic Data Center, 2012b. ASOS 1-Minute Data. Available at http://www.ncdc.noaa.gov/oa/climate/climatedata.html

South Coast Air Quality Management District. General Aviation Airport Monitoring Study. Final Report, 2010

U.S. EPA, 2012a. 2008 National Emissions Inventory Data. Available at http://www.epa.gov/ttnchie1/net/2008inventory.html

U.S. EPA, 2012b. AERMINUTE Version 11325. Available at http://www.epa.gov/scram001/metobsdata_procaccprogs.htm

U.S. EPA, 2012c. Chemical Speciation Network Lead – Daily. Available at http://www.epa.gov/ttn/airs/airsaqs/detaildata/downloadaqsdata.htm

U.S. EPA. 40 CFR Part 58 - Revisions to Lead Ambient Air Monitoring Requirements, Final Rule. Published at 75 FR 81126. December 27, 2010a

U.S EPA. Calculating Piston-Engine Aircraft Airport Inventories of Lead for the 2008 National Emissions Inventory. EPA-420-B-10-044, 2010b

U.S. EPA. Haul Road Workgroup Final Report Submission to EPA-OAQPS. Accessed August 30, 2012d. Available at http://www.epa.gov/scram001/reports/ Haul_Road_Workgroup-Final_Report_Package-20120302.pdf

U.S. EPA. Integrated Science Assessment for Lead. EPA/600/R-10/075A, 2011

U.S. FAA. Denver/Centennial Airport Diagram. Accessed July 9, 2012. Available at https://www.faa.gov/airports/runway_safety/diagrams/

Chapter 3: Measurement and Characterization of Lead Impacts at General Aviation Airports

3.1 Abstract

Combustion of aviation gasoline (avgas) is the largest emitter of lead (Pb) to the atmosphere in the United States. In this study, ambient particulate matter (PM) was sampled and analyzed for Pb content at three general aviation airports of varying size and aircraft activity. The three airports were Richard Lloyd Jones Jr. Airport (RVS) in Tulsa, OK; Centennial Airport (APA) in Englewood, CO; and Santa Monica Airport (SMO) in Santa Monica, CA. For all airports, PM-Pb concentrations were higher downwind of aircraft ground operations and especially downwind of high activity areas that included taxiing, takeoffs, and runups. In addition to Pb concentration, bromine (Br) concentration and lead isotope ratios were also examined. PM-Br and PM-Pb were highly correlated for samples downwind of aircraft ground operations, which is consistent with avgas-Pb origins. The Pb isotopic compositions for PM samples collected at sites with expected high avgas-Pb impacts are distinct from those for samples collected at sites with expected low impacts. Furthermore, PM-Pb isotopic compositions for the high-impact sites are consistent with avgas samples collected at the airports, while the isotopic compositions for the low-impact sites are generally consistent with soil samples collected at the airports.

3.2 Introduction

Lead (Pb) emissions to the atmosphere have historically been associated with combustion of automobile gasoline and metals manufacturing. However, recently the dominant emitter of Pb in the United States has become the combustion of aviation gasoline (avgas) in piston-engine

aircraft (U.S. EPA 2013a). Additionally, in 2008 the National Ambient Air Quality Standard (NAAQS) for Pb was reduced by a factor of ten to 0.15 $\mu g/m^3$. This has influenced the U.S. EPA to begin monitoring ambient Pb levels at general aviation airports that are estimated to emit more than 1 ton per year (U.S. EPA 2013b). Of the 17 airports initially monitored by this program, two recorded exceedances of Pb NAAQS at the site of monitor placement within the airport footprint.

While most airports do not violate the new lead standard, at least one study has reported adverse health effects from Pb in avgas. Miranda et al. (2011) found elevated blood-Pb levels in children living within 1000 m of airports using avgas compared to background levels, with greater effects for those living within 500 m of the airports. There was not a significant increase in blood Pb levels for those living greater than 1000 m from the airports. Elevated blood-Pb levels in children are associated with reduced IQ and academic achievement.

There have been relatively few studies measuring airborne Pb at general aviation airports. One study performed at Buttonville airport in Toronto, Canada (Conor Pacific Environmental Technologies, Inc. 2000) measured airborne Pb at the ends of two runways and at a background site. On average, concentrations measured at the runway ends were 4 times greater than the background site and were at maximum 25 times greater than the background site. The average Pb concentration at the airport from particles with a diameter of 10 micrometers or less (PM_{10}) was measured to be 30 ng/m^3. Additionally, the Pb was found primarily in the fine fraction, suggesting the measured lead was from combustion sources.

Another study conducted in 2013 at McClellan-Palomar Airport measured Pb concentrations in multiple areas around the airport in effort to examine the gradient of Pb high concentration zones, or "hotspots" (San Diego Air Pollution Control District 2013). This study used low-volume samplers to collect 24-hour airborne Total Suspended Particulate (TSP)

samples at ten locations for ten sampling days. The sampling location with the highest average concentration was next to a runup area with an average Pb concentration of 121 ng/m^3. To examine the gradient of Pb impacts, there were three "gradient sites" located 310 ft., 620 ft., and 930 ft. to the east of the runup area site. These sites are downwind of aircraft operations during prevailing winds. The average concentrations at these sites were 15, 10 and 7 ng/m^3, respectively. These measurements highlight the decrease in Pb concentration with increasing distance from aircraft activity.

The South Coast Air Quality Management District (SCAQMD) conducted a study in 2006-2007 to assess the impact of airport operations for a suite of air pollutants, including PM-Pb at two airports in southern California (South Coast Air Quality Management District 2010). Winter and summertime Pb levels were measured at Van Nuys Airport and Santa Monica Airport. TSP Pb levels were greatest near the runway ends, with an average concentration of 85 ng/m^3. Concentrations measured at Santa Monica airport were on average nine times greater than at other TSP sites within the South Coast Air Basin.

Another study modeled near-field impacts at and around Santa Monica Airport, while also collecting samples for comparison to the model (Carr et al. 2011). Aircraft activity data were collected to perform detailed daily modeling of Pb impacts. The study conducted a total of 15 days of TSP sample collection using MiniVol samplers. Six of these days were used for model-to-monitor comparison. Similar to the SCAQMD study, the highest concentrations were both measured and modeled to be near the runways and runup areas, and while runup activities accounted for only 11% of the total emissions, they were deemed the largest contributor to Pb impacts. Pb levels of up to 10 ng/m^3 were modeled up to 900 m downwind of the airport boundary.

This study performed nominally one month of daily ambient Pb measurements at each of three airports across the United States. Listed below are the three airports selected for field studies and the dates the studies were performed.

- Richard Lloyd Jones Jr. (RVS), Tulsa, OK; March 27 to April 28, 2013
- Centennial Airport (APA), Englewood, CO; May 15, 2013 to June 10, 2013
- Santa Monica Airport (SMO), Santa Monica, CA; July 3, 2013 to July 30, 2013

These airports have distinctive characteristics. RVS and APA are among the busiest general aviation airports nationwide and have relatively large footprints with multiple runways. However, the spatial distribution of runup and landing and takeoff (LTO) activity patterns are quite different because of the runway layouts, and wind directions were more variable at APA than RVS. SMO is a much smaller airport but with concentrated runup and LTO activity patterns and a history of being the subject of PM-Pb special studies.

The primary reason for collecting these samples was to reconcile new airport Pb emission inventory methodology development; however, this manuscript will focus on the measurement and characterizations of the ambient Pb at these airports. In addition to measuring the total Pb concentration, this study also examined Pb isotopic ratios and bromine concentrations. Halide compounds such as ethylene dibromide and ethylene dichloride are part of the tetraethyllead (TEL) additive blended into avgas. These compounds scavenge Pb in the engine and the resulting exhaust emissions are bromolead compounds such lead bromide ($PbBr_2$) and lead bromochloride (PbBrCl). There is only one supplier of the TEL additive (Innospec) and it supplies TEL-B, which contains only ethylene bromide ("Octane Additives" n.d.). The Br/Pb

ratio in ambient particulate matter has long been used as an indicator for combustion of leaded fuels and, in particular, motor gasoline (Harrison and Sturges 1983). These additional measurements should provide insight on the total Pb measured and help to quantify the impacts of avgas versus background Pb levels. Previous studies have only reported total Pb concentrations. The examination of Pb/Br ratios and isotopic concentrations in this study could identify these characteristics as potential markers for avgas combustion in future source apportionment studies.

3.3 Methods

Airborne PM samples were collected daily and analyzed for Pb. At each airport, four PM sampling sites were selected based on the location of piston-engine aircraft activities, historical winds data, and Pb concentration fields generated from preliminary dispersion modeling. PM-Pb hot spots were predicted downwind of runup areas and such locations were given high priority. Relatively flat terrain was desired, and it was necessary to stay clear of FAA-restricted areas; for SMO, the siting of samplers in previous studies was also considered. At each airport, the four sampling sites included two "primary" sites and two "secondary" sites. Aircraft generally takeoff into the wind which results in high takeoff impacts directly downwind of the start of runways. Therefore, the downwind primary sites were located downwind of runup/takeoff areas for prevailing winds. Upwind primary sites were placed in a location chosen to capture background PM-Pb levels for prevailing winds. Characteristics for the each of the sites are described in the supplemental material. Up to four PM samplers were operated during each sampling event. Figure 3-1 shows the placement of the sampling sites at RVS. Maps of the other airports and descriptions of all sampling sites are provided in the supplemental information. A $PM_{2.5}$ sampler was always operated at each of the two primary sites, and the remaining two PM samplers were

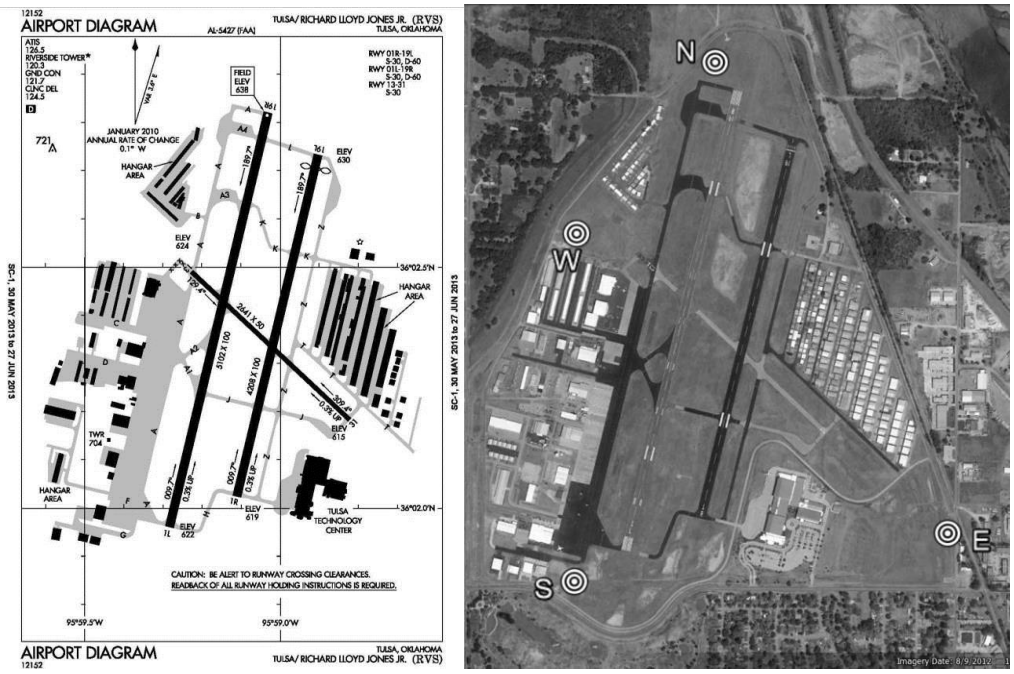

Figure 3-1. Airport Diagram and PM sampling locations at RVS.

used in one of the three configurations: (i) collocated $PM_{2.5}$ sampling at the primary sites (to establish $PM_{2.5}$-Pb measurement precision); (ii) TSP sampling at the primary sites; or (iii) $PM_{2.5}$ sampling at the secondary sites. PM samples were collected using Model PQ100 portable samplers (BGI, Waltham, MA). The samplers were used with BGI Very Sharp Cut Cyclones (VSCC) to achieve $PM_{2.5}$ cutpoints. A louvered inlet with PM_{10} impactor—the standard configuration for ambient PM_{10} sampling—was used upstream of the $PM_{2.5}$ cyclone. TSP samples were collected using PQ100 samplers with BGI TSP inlets. The primary sites at RVS were the North and East sites, at APA they were the Central and East sites, and at SMO they were the Northeast and Southwest sites. Soil and avgas samples were also collected from each airport.

Twelve-hour integrated PM samples were collected each day during the 12-hour period of highest piston-engine aircraft activity based on discussions with the airport authorities. Twelve-hour samples were chosen over 24-hour samples because piston-engine aircraft activity

is very low at night and thus the additional 12 hours of sampling would increase the relative contribution from background Pb to the time average concentration. Reduction of the background contribution to sampled Pb concentration was important, as the original reason for collecting airborne PM samples was to evaluate a new airport emission inventory methodology (Heiken et al. 2014). Filter holders containing the Teflon® filter media (Measurement Technology Laboratories PT47P Filters) were installed in the samplers each morning immediately prior to the start of sampling and retrieved each evening immediately following the end of sampling. While Pb is nonvolatile, bromine (Br) is also of interest and it is relatively volatile so cold transport and storage was adopted. Samples were transported to and from the field sites in coolers with ice packs and were stored in a freezer after sampling.

For each airport study, a subset of samples was analyzed by X-Ray Fluorescence (XRF) at Cooper Environmental Services (CES, Beaverton, OR) to obtain data for a range of elements. All samples—including those analyzed by XRF, which is a non-destructive method—were digested and analyzed for Pb using Inductively Coupled Plasma – Mass Spectrometry (ICP-MS). Filter samples were digested using the methodology presented by Du and Turner (2015). Two sequential digestions were performed using a hot block at 90 °C with nitric acid and hydrofluoric acid for the first digestion and boric acid for the second digestion. Digestion solutions were diluted to a known volume and filtered to remove any remaining particulate matter. Soil samples were analyzed by resuspending soil and collecting $PM_{2.5}$ onto a Teflon® filter and performing the same ICP-MS analysis as the ambient filters; the methodology is described by Li and Turner (2015). Avgas samples were also analyzed for isotopic compositions by ICP-MS; however, the gasoline samples cannot be directed injected into the ICP-MS and thus Pb was extracted using the methodology presented by Lord (1994).

3.4 Results and Discussion

At each airport one sampling site was designated as a primary downwind site and another site as the primary upwind site. Figure 3-2 shows the paired upwind (x-axis) and downwind (y-axis) $PM_{2.5}$-Pb concentrations at each of the three airports. At RVS (Figure 3-2a) there was significant day-to-day variability in wind direction; however, there was often little intraday variability in wind direction and thus a prevailing direction could be assigned to most days. Meteorology used was taken from the Automated Surface Observation System (ASOS) database for RVS. The 1-minute data was averaged to form 15-minute average winds. Wind direction persistence was examined by assigning each 15-minute average wind direction to a quadrant centered on the cardinal wind directions. A wind direction was assigned to a sampling event if at least two-thirds of the 15-minute average winds were from a given quadrant; otherwise the winds were deemed to be variable. At RVS with winds from the south, the North (downwind) site measured concentrations at least 5 times that of the East (upwind) site. There were three events with $PM_{2.5}$-Pb at the East site significantly higher than at the North site. These three events had prevailing winds from the west which led to aircraft emissions impacts at the East site. For other

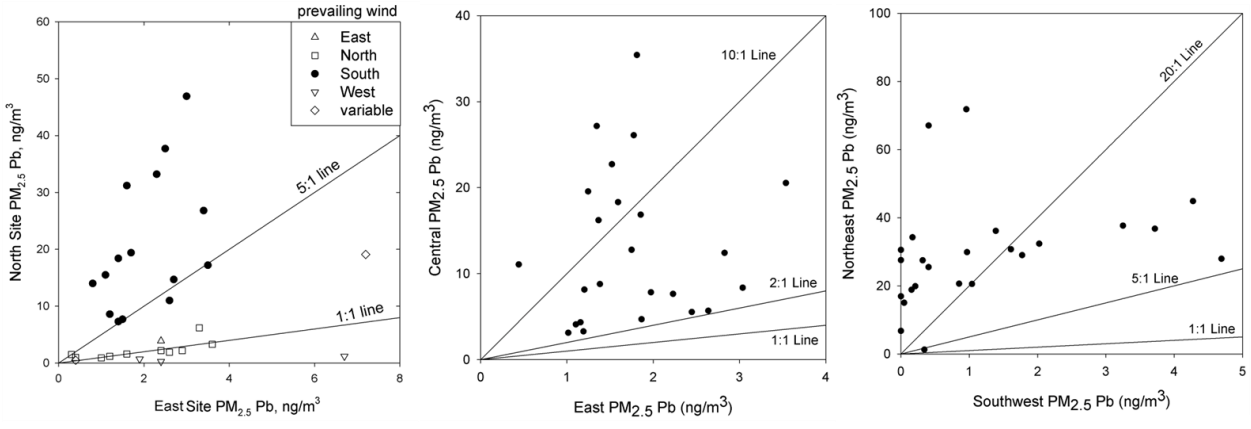

(a) (b) (c)

Figure 3-2 Upwind and downwind $PM_{2.5}$-Pb concentrations at RVS (a), APA (b), and SMO (c).

wind directions, and when the wind was variable, the measured concentrations at the two sites were similar. There were a subset of days winds from the north and sampling at the South location shown in Figure 3-1. In these cases PM-Pb was elevated at the South site which is near a runup and takeoff area for operations when winds are from the north. A comparison of the concentrations at the North and South sites for all days with measurement at the South site is presented in the supplementary material.

Figure 3-2b compares the $PM_{2.5}$-Pb at the Central (downwind) and East (upwind) sites at APA. The minimum ratio of Central site concentration to East site concentration was 2.2. The Central site was located such that it would be impacted from activities across the airport and the East site was located far enough away so it should generally not measure impacts from the airport. While it is difficult to stratify the data based on wind direction because of the within-sample wind variations, the highest ratios usually occurred for higher wind frequencies from the south or west. This pattern clearly indicates the downwind Central site is impacted by aircraft operations. In contrast, for sampling events with a higher frequency of northerly or easterly winds the ratios of $PM_{2.5}$-Pb at the Central and East sites are usually lower but still greater than unity.

Figure 3-2c compares $PM_{2.5}$-Pb at the Northeast (downwind) and Southwest (upwind) sites at SMO. Of the 30 data pairs, 29 (97%) have downwind to upwind ratios of greater than five, and 20 (67%) have a ratio of greater than 20. These high ratios result from consistent winds from the southwest and concentrated activity at the northeast end of the airport. This pattern clearly indicates the downwind Northeast site is impacted by aircraft operations. The concentrations at this site were less than those measured by previous studies (South Coast Air Quality Management District 2010, Carr et al. 2011); however, there are many possible reasons

for this difference, including different sampling efficiencies between samplers and possible analytical biases.

In addition to $PM_{2.5}$, TSP samples were also collected. Most of the PM-Pb at the high impact sites is in the $PM_{2.5}$ size range, consistent with direct exhaust emissions from piston-engine aircraft, but there is considerable Pb in the $PM_{TSP-2.5}$ size range. The median TSP-Pb/$PM_{2.5}$-Pb ratio across all three airports was 1.3 with a narrow interquartile range of 1.2 and 1.4 for the 25^{th} and 75^{th} percentiles, respectively. While coarse mode particles are not the dominant contributor to PM-Pb, they cannot be neglected.

For this study, Br/Pb ratios were examined for evidence of Pb from piston-engine aircraft exhaust emissions. Figure 3-3 shows the relationship between $PM_{2.5}$-Br and $PM_{2.5}$-Pb as measured by XRF stratified by airport (a) and expected airport impact (b). In Figure 3a, all but

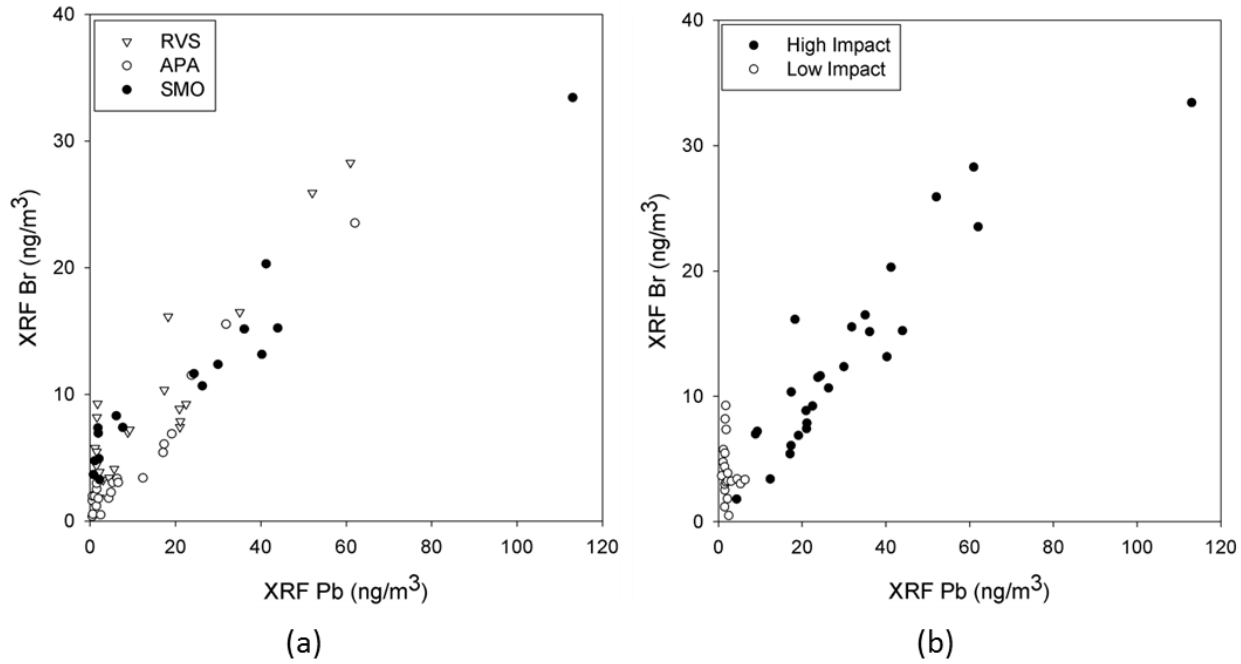

Figure 3-3 $PM_{2.5}$ Br and Pb Measured by XRF and stratified by airport (a) and expected airport impact (b).

one sample are above a distinct edge with Br/Pb ~ 1/3. At low Pb concentrations, the samples can be enriched in Br which is consistent with soil impacts.

Figure 3-3b shows the same data after classifying each sample as having expected high or low aircraft exhaust impacts. First, concentrations less than three times the XRF method detection limit (MDL) values were screened out for this analysis. Next, expected high-impact samples were identified on an airport-by-airport basis. At RVS, expected high-impact samples were those collected at either the North or South sites, depending on the wind pattern. Samples from the East site or upwind of the airport based on the daily winds were categorized as low impact. Samples collected at RVS on days with variable winds are not included in Figure 3-3b. At APA, all samples from the Central site were categorized as high impact while samples from the East site were considered low impact. At SMO, all samples from the Northeast site were categorized as high impact and the samples from the Southwest site were considered low impact. High and low impact designations were made without consideration of measured Pb concentration.

Br and Pb are highly correlated for the high impact samples ($r = 0.92$). In contrast, Pb was weakly correlated with markers for resuspended soil, especially for the high impact samples ($r = 0.00$ and 0.01 for Si-Pb and Ca-Pb, respectively). The strong correlation of Pb with Br and weak correlation of Pb with soil markers such as Ca and Si provide support that the $PM_{2.5}$-Pb originates from combustion of leaded fuel. The median adjusted downwind Br/Pb ratio is 0.30 with 25^{th} and 75^{th} percentile ratios of 0.24 and 0.39, respectively. These ratios are much smaller than the expected ratio of 0.772 if all the lead was present as $PbBr_2$. They are also less than the ethyl ratio. This discrepancy may be caused by direct volatilization of Br in the atmosphere or after reaction on the particle surface (Harrison and Sturges 1983). .

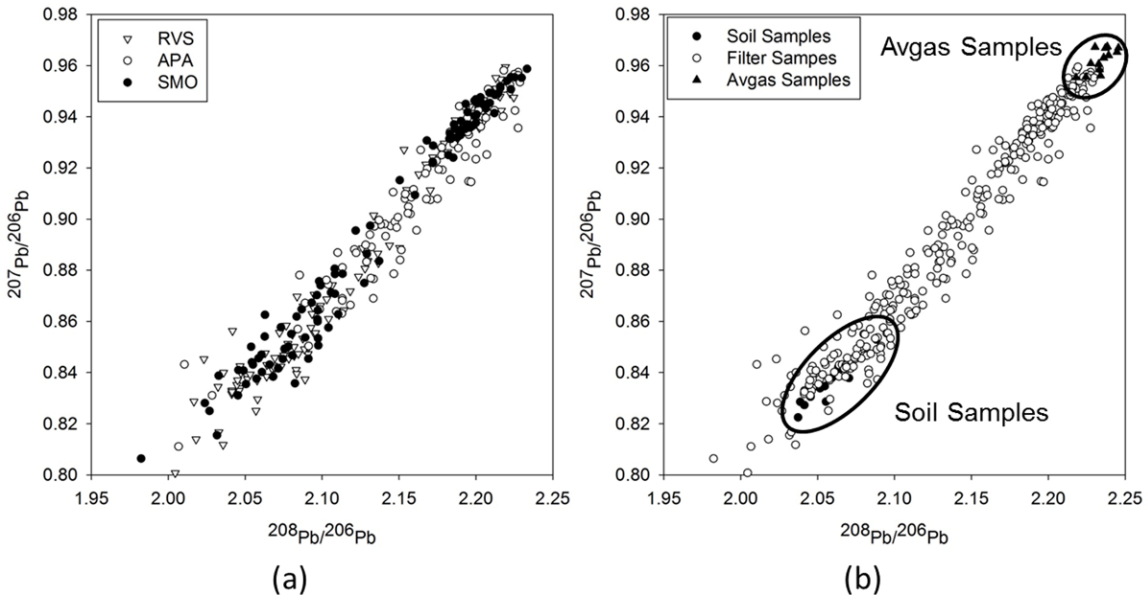

Figure 3-4 Pb Isotope ratios for Airborne PM-Pb, Soil, and Avgas Samples collected at the three airports.

All PM-Pb samples were analyzed for Pb isotopes. While precise quantification of Pb isotopes is best performed using a high resolution ICP-MS, the ICP-MS available to this project was adequate for at least semi-quantitative analyses. Figure 3-4a shows the $^{207}Pb/^{206}Pb$ versus $^{208}Pb/^{206}Pb$ ratios for all airborne PM samples collected in this study with the data stratified by airport. All of the samples lie along a line, albeit it with some scatter, which generally supports the notion of a two-source model for Pb. Four resuspended soil samples from each airport and 15 total avgas samples were also analyzed. Figure 3-4b shows the $^{207/206}Pb$ versus $^{208/206}Pb$ for all airborne PM samples and the soil and avgas samples collected for each airport. The avgas ratios are similar to measured ratios of lead mined in Australia (Townsend et al. 1998), which is reported to be the source of the lead used in avgas. Isotope ratios for resuspended soil are generally consistent with crustal material in the continental United States (Reimann et al. 2011) and are more similar to each other than to Australian lead. Therefore, samples with high Pb ratios likely contain more avgas contribution while samples with low ratios are likely indicative of

background ambient Pb and in particular resuspended soil. It is not clear whether the soil samples include significant Pb originating from the use of avgas. However, isotopic compositions of soil samples collected at different locations within and between the three airports are indistinguishable. This suggests that avgas Pb does not dominate the Pb in these soils. A potential confounder to the soils analysis is that the airport topsoil samples can have dramatically different histories, and in some cases there was evidence of soil being moved.

Collocated sample isotope ratios were highly correlated, with $r^2 = 0.90$ for $^{208}Pb/^{206}Pb$ and $r^2 = 0.94$ for $^{207}Pb/^{206}Pb$. The collocated precisions of $^{208}Pb/^{206}Pb$ and $^{207}Pb/^{206}Pb$, measured by the standard deviation of paired samples, were 11% and 10%, respectively. While the data are highly correlated, there was high scatter suggesting that even if the end member compositions are appropriately identified, caution should be used when quantitatively apportioning airborne PM-Pb to the end members. There was more scatter among samples with lower total Pb concentration. This scatter is likely a limitation of not using a high-resolution ICP-MS instrument. If this scatter were reduced, it is like that the relative source contributions of avgas and soil could be determined from the isotope ratios.

The isotope ratios of collocated $PM_{2.5}$ and TSP samples were also examined. For the high-impact data, there was no consistent trend in the directional difference of the $PM_{2.5}$-Pb and TSP-Pb isotope ratios and the differences were generally small. This pattern suggests that there was relatively little contribution of resuspended soil to the total Pb concentrations and isotope ratios.

Figure 3-5 shows the same data but now stratified into samples expected to have low or high impacts from piston-engine aircraft emissions. Concentrations less than three times the ICP-MS MDL for Pb were screened out for this analysis, and the classification scheme used for the

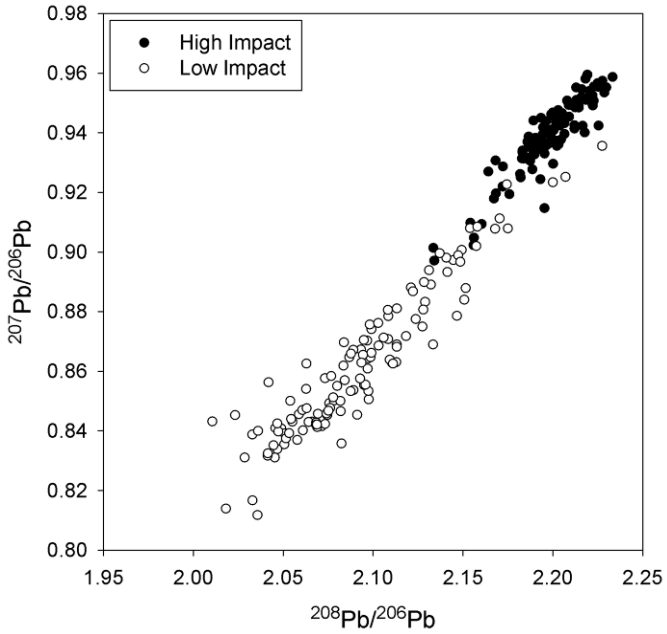

Figure 3-5 Pb isotope ratios for airborne PM-Pb with samples stratified as high or low expected impacts from aircraft exhaust.

Br/Pb ratios analysis was used for this analysis. Most of the high-impact samples are clustered towards the avgas end member, whereas most low-impact samples are at greater distances from the avgas end member. This pattern is consistent with Pb in high-impact samples being dominated by avgas combustion. The threshold composition between high- and low-impact samples is $^{208}Pb/^{206}Pb \sim 2.15$. All of the low-impact samples with $^{208}Pb/^{206}Pb$ above this threshold are from APA. It is not clear why those samples from APA had elevated $^{208}Pb/^{206}Pb$ ratios.

Correlation was also observed between Pb isotope ratios and total lead concentration. Figure 3-6 shows total Pb concentration versus the $^{208}Pb/^{206}Pb$ ratio for airborne PM samples collected at the three airports. High Pb concentrations correspond to high $^{208}Pb/^{206}Pb$ ratios, suggesting that lead from avgas combustion is the primary driver of the high PM-Pb measured at each airport.

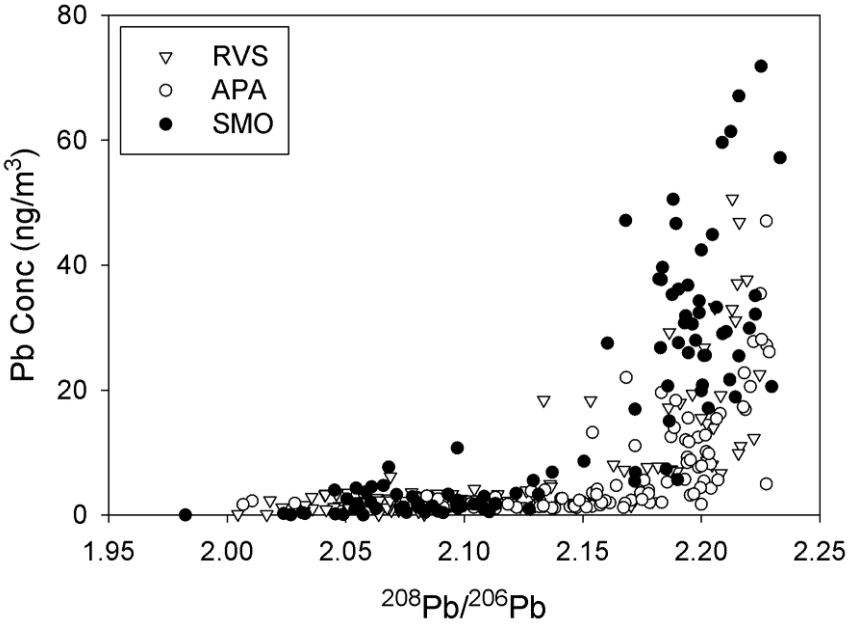

Figure 3-6 Pb total concentration versus the $^{208}Pb/^{206}Pb$ Ratio for PM samples collected at the three airports.

It should be noted that PM data collection focused on size ranges and averaging times that do not support direct comparisons to the Pb NAAQS. Nonetheless, none of the individual 12-hour PM-Pb values exceeded the three-month average NAAQS of 150 ng/m^3, and the highest observed 12-hour concentration was a TSP-Pb value of 72 ng/m^3 at SMO. Study-average $PM_{2.5}$-Pb values at the highest concentration sites were 15 ng/m^3 at APA, 21 ng/m^3 at RVS, and 30 ng/m^3 at SMO. However, based on study findings that concentrations below the NAAQS can impact blood lead levels (Miranda et al. 2011), these levels could still be of concern and warrant further evaluation.

This characterization of airport Pb emissions and impacts serves to inform potential future Pb studies. Pb-Br correlations, as well as Pb isotope ratios could potentially be used as markers for piston-engine aircraft emissions in future studies. The World Health Organization (WHO) states that there is no tolerable intake level for Pb (World Health Organization 2010);

therefore, any information on the sources and potential targets for reduction of Pb emissions is important.

There are a significant number of aircraft activities that contribute to Pb concentrations at an airport. Modeling has been conducted in order to evaluate the relative contribution of different aircraft activities to the sites used in these studies (Feinberg et al., *submitted*). Overall, the largest contributors to concentrations measured at the downwind sampling locations were taxiing, takeoffs and runups.

3.5 Acknowledgements

This study was funded by the Airport Cooperative Research Program (ACRP), project number 02-34. The authors would like to thank Marci Greenberger and the ACRP project panel. The authors would also like to thank James Lyons, Jeremy Heiken and colleagues at Sierra Research Inc., Mike Kenney and Paul Sanford of KB Environmental Services, Jeff Condray of the Tulsa Airport Authority, Steve Mushrush and the airport operations staff at RVS, Robert Olislagers and the airport operations staff at APA, and Stelios Makrides and the airport operations staff at SMO.

3.6 References

Carr, E.; Lee, M.; Marin, K.; Holder, C.; Hoyer, M.; Pedde, M.; Cook, R. and J. Touma. Development and Evaluation of an Air Quality Modeling Approach for Lead Emissions from Piston-Engine Aircraft Operating on Leaded Aviation Gasoline. *Atmospheric Environment.* **2011,** 45 5795-5804

Conor Pacific Environmental Technologies, Inc. Airborne Particulate Matter, Lead and Manganese at Buttonville Airport. Prepared for Environment Canada under CPE Project 041-6710. Final Report, 2000

Du, L. and Turner, J. Using $PM_{2.5}$ lantanoid elements and nonparametric wind regression to track petroleum refinery FCC emissions. *Science of the Total Environment* **2015**, 529, 65-71.

Feinberg, S.N., J.G. Heiken, M.P. Valdez, J.M. Lyons, and J.R. Turner. "Modeling of Lead Concentrations and Hotspots at General Aviation Airports." *Transportation Research Record*, submitted.

Harrison, R.M. and W.T. Sturges. The measurement and interpretation of Br/Pb ratios in airborne particles. *Atmospheric Environment* **1983,** 17, 311-328.

Heiken, J., Lyons, J., Valdez, M., Matthews, N., Sanford, P., Turner, J and Feinberg, N. "Quantifying Aircraft Lead Emissions at Airports." Transportation Research Board. Web-Only Document 21. October 2014. http://onlinepubs.trb.org/Onlinepubs/acrp/acrp_webdoc_021.pdf

Lord, C.J. Determination of lead and lead isotope ratios in gasoline by inductively coupled plasma mass spectrometry. *Journal of Analytical Atomic Spectrometry* **1994**, 9, 599-603.

Miranda, M.L; Anthopolos, R.; Hastings, D. A Geospatial Analysis of the Effects of Aviation Gasoline on Childhood Blood Lead Levels. *Environ. Health Perspect.* **2011**, 119 (10), 1513-1516; DOI 10.1289/ehp.1003231

Octane Additives; http://www.innospecinc.com/market/octane-additives

Reimann, C., Smith, D.B., Woodruff, L.G., and B. Flem. Pb-Concentrations and Pb-Isotope Ratios in Soils Collected Along an East-West Transect Across the United States. *Applied Geochemistry.* **2011**, 26 (9-10), 1623-1631.

San Diego Air Pollution Control District. Lead Gradient Study at McClellan-Palomar Airport. Final Report, 2013

South Coast Air Quality Management District. General Aviation Airport Monitoring Study. Final Report, 2010

Townsend, A.T., Z. Yu, P. McGoldrick, and J.A. Hutton. "Precise lead isotope ratios in Australian Galena samples by high resolution inductively coupled plasma mass spectrometry." *Journal of Analytical Atomic Spectrometry* **1998,** 13, 809-813.

U.S. EPA. 2013a. *Integrated Science Assessment for Lead.* EPA600-R-10-075F

U.S. EPA. 2013b. *Program Update on Airport Lead Monitoring* (4 pp, EPA-420-F-13-032, June 2013) http://www.epa.gov/otaq/regs/nonroad/aviation/420f13032.pdf

World Health Organization, 2010. *Exposure to Lead: A Major Public Health Concern*. http://www.who.int/ipcs/features/lead.pdf

3.7 Supplemental Material

3.7.1 PM Sampling locations

Figure 3-7 and Figure 3-8 shows the PM sampling locations at APA and SMO, respectively.

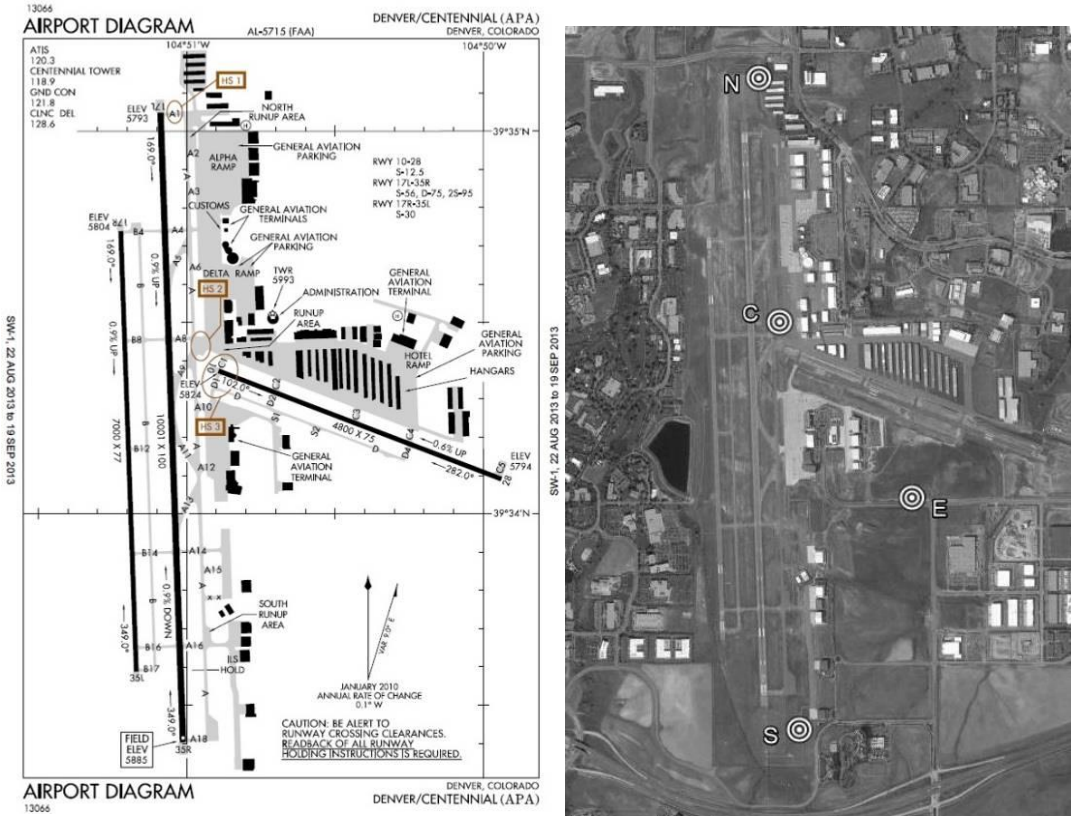

Figure 3-7 Airport diagram and PM sampling locations at APA.

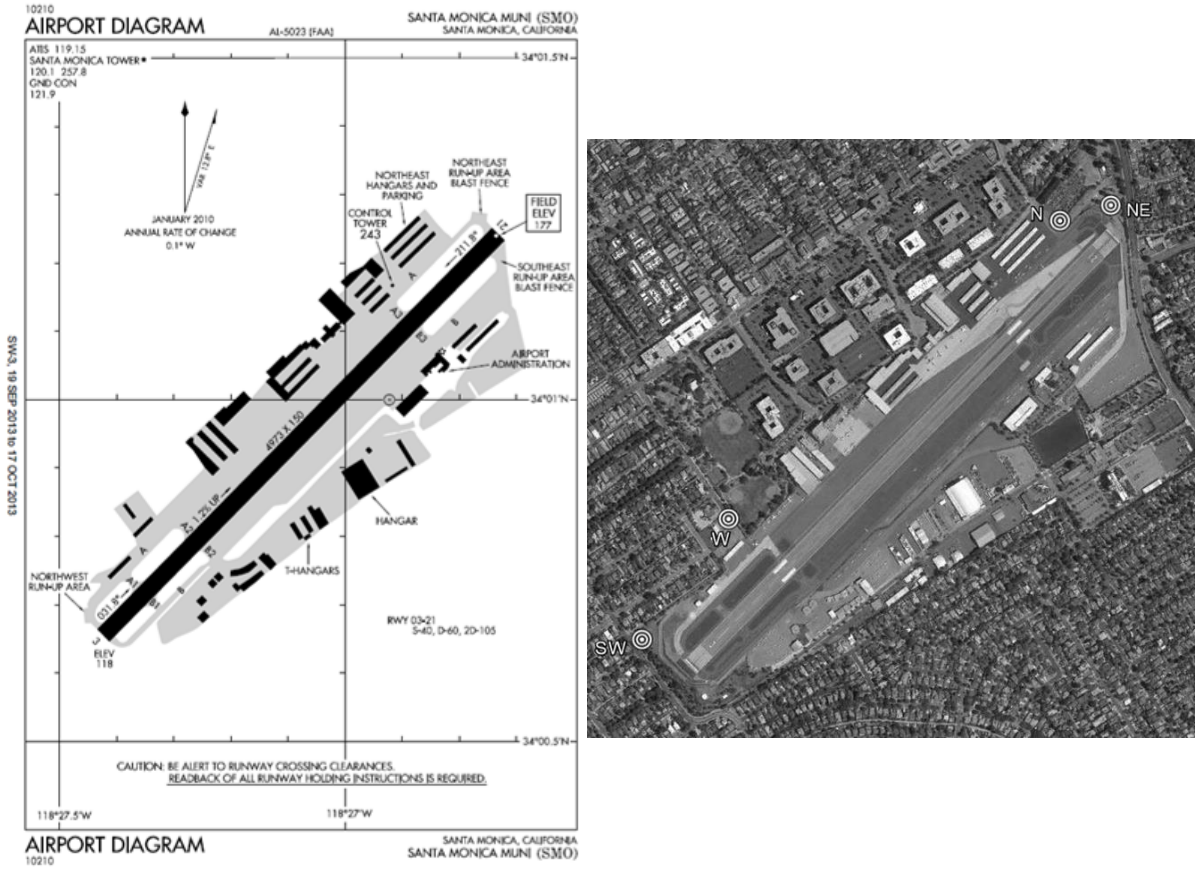

Figure 3-8 Airport diagram and PM sampling locations at SMO.

Tables 3-1 through 3-3 summarize key characteristics of each of the sampling locations for RVS, APA, and SMO, respectively. At RVS, The North site (N) is the downwind primary site with presumably high impacts from runup, taxiing and idling, and takeoff activities on runway 19R for prevailing southerly winds. The East site (E) is the upwind primary site and should capture background Pb concentrations regardless of wind direction with the exception of westerly winds, which were rare during the study. The South (S) site is impacted by climb-out from runway 19R for southerly winds and runup, taxiing and idling, and takeoffs from runway 1L for northerly winds. Emissions from ground-based operations west of the runways might impact this site for northerly winds. The West site (W) is potentially

Table 3-1 Airborne PM Sampling Locations for the RVS Study

Site	Location with Respect to Nearest Runway	Comments
North Downwind Primary	~125m NW of 19R	For prevailing southerly winds, this site was impacted from runway 19R runups and take-offs, as well as idling and taxiing. (Lat: 36.047435° Long: -95.984719°)
East Upwind Primary	~500m SE of 31	For winds from the south, east, and north, this site is upwind of all ground-based activities. It is ~700m east of runway 1R and may be modestly impacted by aircraft operations for winds from the west. (Lat: 36.033631° Long: -95.976139°)
West Downwind Secondary	~250m NW of 13	For prevailing southerly winds, this site was impacted by the southern half of runways 19L and 19R and ground-based activities on the west side of the airport. (Lat: 36.042370° Long: -95.989708°)
South Upwind Secondary	~200m SW of 1L	For winds from the south, east, and west, this site is upwind of all ground-based activities. For northerly winds, it was impacted by ground-based activities on the west site of the airport including runups and take-offs for runway 1L, as well as idling. (Lat: 36.032130° Long: -95.989700°)

Table 3-2 Airborne PM Sampling Locations for the APA Study

Site	Location with Respect to Nearest Runway	Comments
Central Downwind Primary	~250m NW of 10	For prevailing southerly winds, this site was impacted by runway 10 runups and take-offs. It was also impacted by taxi and idle activities around the center of the airport. (Lat: 39.574860° Long: -104.849210°)
East Upwind Primary	~1km SE of 10	For winds from the south, east, and north, this site is upwind of all ground-based activities. It is ~850m east of runway 35R and was modestly impacted by aircraft operations for winds from the west. (Lat: 39.566290° Long: -104.840830 °)
North Downwind Secondary	~300m NW of 17L	For prevailing southerly winds, this site was impacted by the northern portions of runways 35L and 35R and ground-based activities on the east side of the airport. (Lat: 39.586810° Long: -104.850550°)
South Upwind Secondary	~250m SE of 35R	For winds from the south, east, and west, this site is upwind of all ground-based activities. For northerly winds, it was impacted by ground-based activities on the east side of the airport, including runups and take-offs for runway 35R. (Lat: 39.555010° Long: -104.847950°)

Table 3-3 Airborne PM Sampling Locations for the SMO Study

Site	Location with Respect to Nearest Runway	Comments
Northeast Downwind Primary	~100m N of 21	For prevailing southwesterly winds, this site was impacted from runway 21 runups and take-offs. It was also significantly impacted by taxiing and idling on Taxiways A and B. (Lat: 34.021490° Long: -118.445531°)
Southwest Upwind Primary	~150m NW of 3	For winds from the southwest, this site is upwind of all ground-based activities but may be impacted by climb-out. It may be impacted by aircraft operations for winds from the east. (Lat: 34.011560° Long: -118.458439°)
North Downwind Secondary	~150m W of 21	For prevailing southwesterly winds, this site was impacted by takeoffs and runups on runway 3, as well as most ground-based activities on Taxiways A and B. (Lat: 34.021030° Long: -118.447011°)
West Upwind Secondary	~400m NE of 3	For winds from the southwest, this site is upwind of all activities on runway 21 and the northeast side of the airport. It may be impacted by activities at the southwest end of the airport. For southeasterly winds, it is potentially impacted by ground-based activities at the southern end of the airport. In contrast to the other three sites that were sited in open fetch, the West site was near obstructions (buildings, trees). (Lat: 34.014300° Long: -118.456050°)

impacted by ground-based operations on the west side of the airport for southerly winds and runway operations for easterly winds, which were rare during the study.

At APA, the Central site (C) is the downwind primary site, with presumably high impacts from runup and takeoff activities on runway 10 for prevailing southerly winds as well as taxiing on taxiway A. Although information provided prior to the field campaign suggested there was little piston-engine aircraft activity on runway 17L/35R, we were subsequently informed that there is considerable piston-engine activity on this runway that may lead to significant impacts at the Central site. The East site (E) is the upwind primary site and should capture background Pb

concentrations because of its distance from airport activity. The South site (S) is impacted by climb-out from runway 17L for southerly winds and runup, taxiing and idling, and takeoffs from runway 35R for northerly winds. Emissions from ground-based operations east of the runways might impact this site for northerly winds. The North site (N) should be impacted primarily by climb-out from runway 35R for northerly winds and runup, taxiing and idling, and takeoffs from runway 17L for southerly winds.

At SMO, The Northeast site (NE) is the downwind primary site, with presumably high impacts from runup, taxiing and idling, and takeoff activities on runway 21 for prevailing southwesterly winds. In contrast to RVS and APA, it was not possible to locate the upwind primary site on the airport footprint far removed from aircraft activities. The Southwest site (SW) is the upwind primary site and should, to a large extent, capture background Pb concentrations; however, it might be influenced by climb-out, for prevailing southwesterly winds. The North site (N) is impacted by taxiing and climb-out from runways 3 and 21 for southwesterly winds. Emissions from ground-based operations north of the runway might impact this site for prevailing winds. The West site (W) should be impacted primarily by climb-out from runway 3 for southwesterly winds and ground-based activities for southerly and southeasterly winds.

3.7.2 Measured Pb Concentrations

Tables 3-4 through Table 3-6 show the airborne Pb concentrations measured by ICP-MS at RVS, APA, and SMO, respectively. At RVS, of the 99 $PM_{2.5}$ samples, 93 (94%) had a Pb concentration at least three times the $PM_{2.5}$ median field blank level. Of the 18 TSP samples, 16 (89%) had Pb concentrations at least three times higher than the median TSP field blank. At APA, of the 80 analyzed $PM_{2.5}$ samples, 79 (99%) had a Pb concentration at least

Table 3-4 Airborne Pb Concentrations Observed at RVS

Date	Pb Concentration, ng/m^3					
	North		East			
	Primary	Collocate	Primary	Collocate	South	West
03/27/2013	{49.6}	{50.1}	4.3	2.6		
03/28/2013	37.7	32.9	2.5	2.4		
03/29/2013	19.1	18.3	7.2	8.0		
03/30/2013	8.6	8.0	1.2	--		
03/31/2013	1.2	1.1	1.2	0.9		
04/01/2013	3.3	2.2	3.6			
04/02/2013						
04/03/2013	2.2	2.3	2.9			
04/04/2013	6.2	2.8	3.3			
04/05/2013	46.9	50.7	3.0			
04/06/2013	17.2	--	3.5			
04/07/2013	7.3	7.0	1.4			
04/08/2013	14.0		0.8		--	
04/09/2013	18.4		1.4		2.4	
04/10/2013	0.5		0.4		0.3	
04/11/2013	0.7		1.9		7.6	0.8
04/12/2013	1.9		2.6		29.2	1.8
04/13/2013	33.2		2.3		2.2	--
04/14/2013	11.0		2.6		1.2	2.1
04/15/2013	1.6	[3.4]	1.6	[3.4]		
04/16/2013	0.9	[3.3]	1.0	[2.2]		
04/17/2013	15.5	[18.0]	1.1	[2.0]		
04/18/2013	0.3	[0.4]	2.4	[2.2]		
04/19/2013	1.2		6.7		9.9	1.2
04/20/2013	31.2		1.6		1.4	7.1
04/21/2013	7.7		1.5		1.4	2.9
04/22/2013	19.4		1.7		2.1	4.9
04/23/2013	1.0		0.4		12.3	0.6
04/24/2013	2.2	[4.2]	2.4	[3.3]		
04/25/2013	26.8	[37.1]	3.2	[3.1]		
04/26/2013	3.9	[4.6]	2.4	[3.2]		
04/27/2013	1.5	[1.9]	0.3	[0.6]		
04/28/2013	14.7	[22.5]	2.7	[2.0]		

Notes: The row following each interior horizontal line is a Monday. Data are $PM_{2.5}$-Pb unless otherwise noted. [ ] = TSP;{ } = samplers moved during the sampling period; "--" = invalid sample; and empty cells indicate no sample collection.

Table 3-5 Airborne Pb Concentrations Observed at APA

Date	Pb Concentration (ng/m^3)						
	Central		East				Central
	Primary	Collocate	Primary	Collocate	North	South	Secondary
05/15/2013	16.2		1.4		2.0		--
05/16/2013	22.7		1.5		5.4		4.3
05/17/2013	27.2		1.3		12.0		4.0
05/18/2013	20.5		3.5		2.3		9.3
05/19/2013	8.1		1.2		1.3	3.5	
05/20/2013	7.7		2.2		1.5	1.9	
05/21/2013	35.4		1.8		1.2	3.4	
05/22/2013	8.4		3.0		2.3	2.0	
05/23/2013	47.1		0.4		6.6	0.2	
05/24/2013	18.3	[25.5]	1.6	[2.2]			
05/25/2013	16.9	[21.7]	1.9	[2.6]			
05/26/2013	12.4	[22.0]	2.8	[2.1]			
05/27/2013	12.8	[12.5]	1.8	[1.8]			
05/28/2013	26.1	[27.7]	1.8	[2.1]			
05/29/2013	3.1		1.0		1.0	0.9	
05/30/2013	4.7		1.9		1.6	1.1	
05/31/2013	4.3		1.2		0.3	2.0	
06/01/2013	4.1		1.1		4.9	1.3	
06/02/2013	7.8	[10.1]	2.0	[1.7]			
06/03/2013	8.8	[1.2]	1.4	[2.6]			
06/04/2013	3.3	[4.0]	1.2	[1.8]			
06/05/2013	11.1	[9.8]	0.4	[0.0]			
06/06/2013	17.3	15.4	5.6	4.9			
06/07/2013	19.6	--	1.2				
06/08/2013	5.7	5.5	2.6	2.4			
06/09/2013	[13.2]	[11.7]	[2.3]	[3.8]			
06/10/2013	[13.9]	[15.5]	[1.9]	[0.9]			

Notes: The row following each interior horizontal line is a Monday. Data are $PM_{2.5}$-Pb unless otherwise noted. [ ] = TSP; "--" = invalid sample; and empty cells indicate no sample collection.

Table 3-6 Airborne Pb Concentrations Observed at SMO

Date	Pb Concentration, n/m^3					
	Northeast		Southwest			
	Primary	Collocate	Primary	Collocate	North	West
07/03/2013	29.0		1.7			
07/04/2013	16.9		< 0		3.3	
07/05/2013	< 0		3.3		6.8	
07/06/2013	36.8		3.7		8.6	
07/07/2013	27.5	[35.3]	0.3	[4.5]		
07/08/2013	20.5	[50.5]	1.0	[2.5]		
07/09/2013	25.5	[39.6]	0.4	[2.9]		
07/10/2013	37.7	[46.6]	3.2	[3.9]		
07/11/2013	27.9	[37.8]	4.7	[2.9]		
07/12/2013	30.7		1.6		7.3	0.0
07/13/2013	--		--		10.7	7.6
07/14/2013	71.8		1.0		5.4	1.7
07/15/2013	6.8		< 0		5.5	< 0
07/16/2013	29.9		1.0		5.6	1.7
07/17/2013	30.5		< 0		3.4	--
07/18/2013	32.4	[42.4]	2.0	[0.8]		
07/19/2013	44.9	[61.4]	4.2	[2.3]		
07/20/2013	27.6	[26.8]	< 0	[1.7]		
07/21/2013	34.2	[47.1]	0.1	[0.9]		
07/22/2013	20.6	21.6	0.9	0.6		
07/23/2013	19.9	20.8	0.2	0.3		
07/24/2013	18.9	25.4	0.2	1.3		
07/25/2013	15.0	17.1	0.0	0.9		
07/26/2013	36.1	31.9	1.4	1.2		
07/27/2013	67.1	32.1	0.4	0.5		
07/28/2013	[33.2]	[35.1]	[1.0]	[1.4]		
07/29/2013	[26.0]	[29.3]	[1.7]	[1.8]		
07/30/2013	[59.6]	[57.2]	[2.0]	[1.0]		

Notes: The row following each interior horizontal line is a Monday. Data are $PM_{2.5}$-Pb unless otherwise noted. [ ] = TSP; and empty cells indicate no sample collection. 2.8 ng/m^3 was subtracted from the underlined samples through to correct for laboratory contamination; negative concentration values after applying this correction are denoted by "< 0". Samples denoted with a dash (--) were invalidated because of contamination.

three times the $PM_{2.5}$ median field blank; of the 26 TSP samples, 24 (92%) had Pb concentrations at least three times higher than the median TSP field blank. At SMO, of the 57 analyzed $PM_{2.5}$ samples, 45 (79%) had a Pb concentration at least three times the $PM_{2.5}$ median field blank. Additionally, 29 (97%) of the 30 analyzed $PM_{2.5}$ samples collected at the North and Northeast sites had a Pb concentration at least three times the $PM_{2.5}$ median field blank. Of the 30 TSP samples, 26 (87%) had Pb concentrations at least three times higher than the median TSP field blank. These results demonstrate that acceptable detectability was achieved for the airborne Pb data.

As discussed in Section 3.4, days at RVS were categorized by wind direction. Figure 3-9 shows polar plots of the measured lead concentration and daily average wind direction at the North (a) and East (b) sites. Daily average wind directions were calculated as the wind speed weighted resultant vector average wind directions. Days classified as variable (wind frequency less than 0.75 from a given quadrant) are not included in these plots. Similar to what is shown in Figure 3-2, concentrations at the North site were greater when the wind was from the south. Conversely, concentrations measured at the East site did not show clear dependence on wind directions. The lack of concentration dependence on wind direction is desired for a background monitoring location.

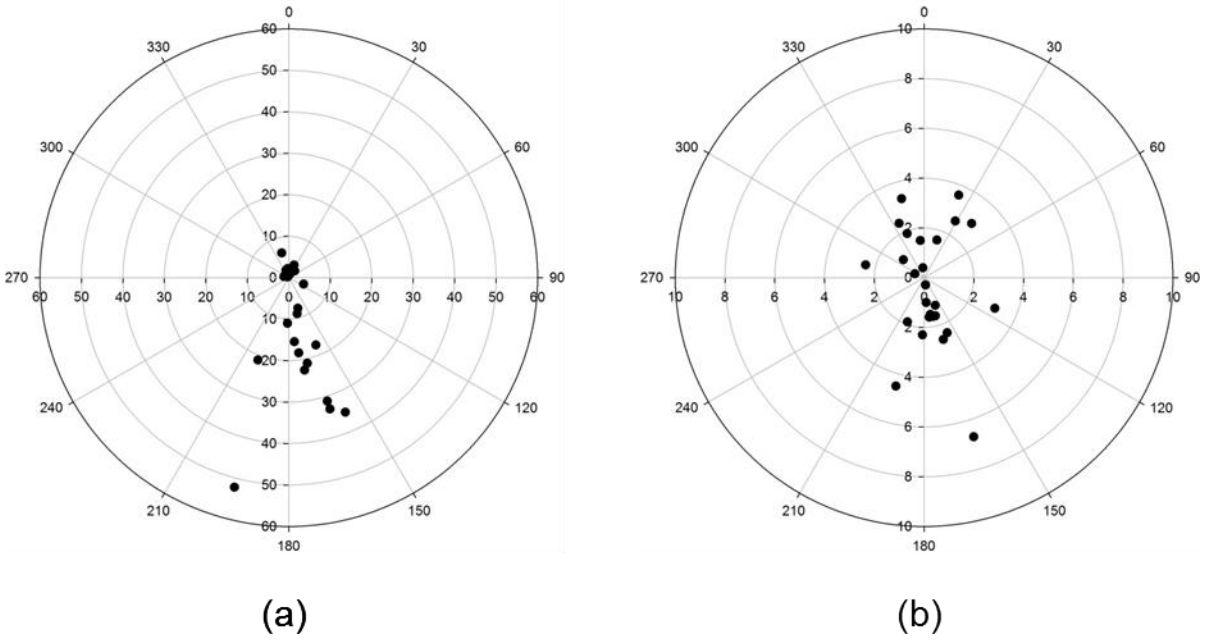

Figure 3-9 $PM_{2.5}$-Pb concentrations (radial axis, ng/m^3) versus wind direction at the RVS North (a) and East (b) sampling locations. The concentration scale for the East sampling location is one-sixth that of the North sampling location.

3.7.3 PM-Pb analysis by XRF with comparison to ICP-MS

Twenty-two airborne $PM_{2.5}$ samples from each airport were sent to Cooper Environmental Services (CES) for elemental analysis by XRF. Fourteen field blanks, including at least four from each airport, and six laboratory blanks were also analyzed, with the latter used to develop the spectral blank correction for the specific make and model of filters used in this study. Samples were analyzed by CES Protocol C which is the most sensitive of the three routine protocols offered with a Pb MDL of 0.24 ng/m^3 effective ambient concentration. Pb effective ambient concentrations for each of the 14 field blanks were less than 0.5 ng/m^3.

Figure 3-10 compares ambient $PM_{2.5}$-Pb measured by XRF and ICP-MS. Samples with ICP-MS $PM_{2.5}$-Pb less than three times the ICP-MS MDL of 0.2 ng/m^3 were excluded. The data are highly correlated with $r^2 = 0.99$ (N = 57). The regression intercept is statistically

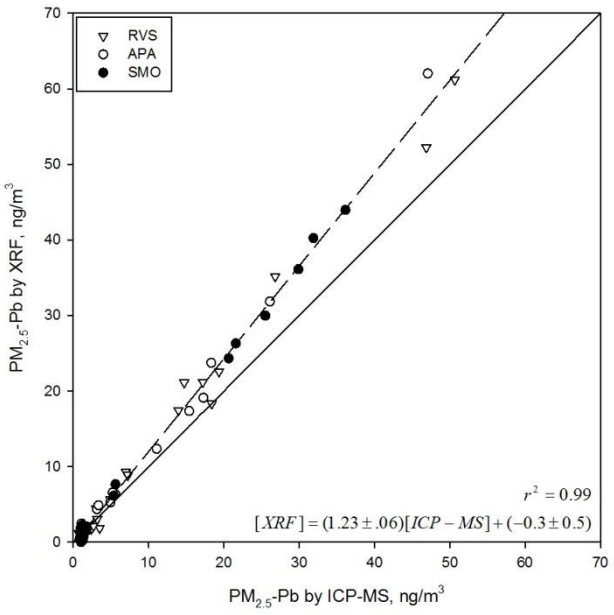

Figure 3-10 $PM_{2.5}$-Pb measured by XRF and ICP-MS. Regression coefficients including 95% confidence intervals are from a constant variance Deming regression. The solid line is the 1:1 line and the dashed line is the regression line.

indistinguishable from zero but from the regression slope the XRF data are biased 20% high compared to the ICP-MS data. The quantitative SRM recoveries provide compelling evidence for the accuracy of the ICP-MS data. Measurement differences in Pb are not unusual. For example, in the South Coast Air Quality Management District airport study (South Coast Air Quality Management District 2010), XRF and ICP-MS data were highly correlated ($r^2 = 0.97$) with regression slope of 1.06 and intercept of 25.6 ng/m^3. Compared to this study, the SCAQMD-reported slope is closer to unity, but the intercept is much larger.

3.7.4 Pb Isotope Ratios of Collocated Samples

Data from collocated PM sampling can be used to gauge measurement precision. Shown in Figure 3-11 are the $^{208}Pb/^{206}Pb$ ratios and $^{207}Pb/^{206}Pb$ ratios for the collocated airborne PM samples collected at the three airports. Collocated sample isotope ratios are highly correlated,

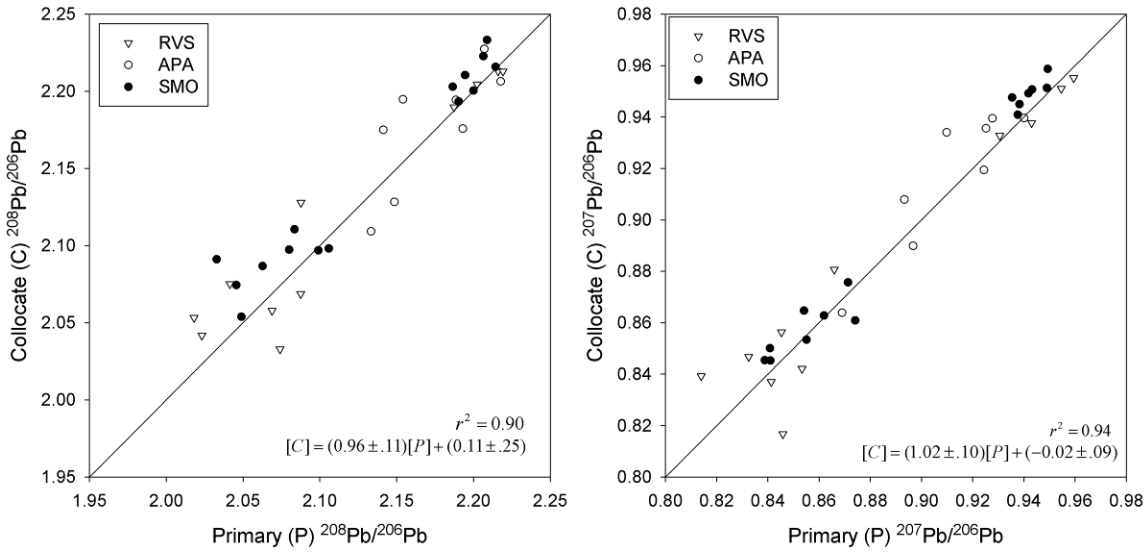

(a) (b)

Figure 3-11 Pb isotope ratios for collocated PM samples collected at the three airports.

with $r^2 = 0.90$ for $^{208}Pb/^{206}Pb$ and $r^2 = 0.94$ for $^{207}Pb/^{206}Pb$. As previously mentioned this scatter is likely a limitation of not using a high-resolution ICP-MS instrument.

Chapter 4: Modeling of Lead Concentrations and Hotspots at General Aviation Airports

4.1 Abstract

Lead (Pb) is a well-known air pollutant that can lead to a variety of adverse health impacts including neurological effects in children that lead to behavioral problems, learning deficits, and lowered IQ. According to the U.S. EPA, piston-engine aircraft contribute more than half of nationwide atmospheric Pb emissions (U.S. EPA 2013a). The most concentrated areas of piston-engine aircraft activity are at general aviation airports. While there is now monitoring for Pb emissions at several airports across the United States, there have only been a limited number of studies focused on modeling Pb emissions. Determining the spatial extent of Pb concentrations at airports and the primary contributors to high concentration areas can help airports and environmental agencies plan and mitigate impacts. In this study, aircraft operations were observed at three general aviation airports across the country to develop spatially and temporally resolved emission inventories. The three airports were Richard Lloyd Jones Jr. Airport (RVS) in Tulsa, OK; Centennial Airport (APA) in Englewood, CO; and Santa Monica Airport (SMO) in Santa Monica, CA. A refined emission inventory methodology was developed and implemented, and the AERMOD air quality dispersion model was used to determine Pb concentration fields at each airport. Modeled concentrations were evaluated using airborne Pb concentrations measured on-site. Modeled concentrations were shown to have very good agreement with measured values at RVS and SMO, and were biased high at APA. Maximum modeled Pb concentrations occurred near runup areas and runway ends for each of the three

airports. The primary contributors to these maximum concentrations were activities within runup areas, taxiing, and takeoffs.

4.2 Introduction

Concerns regarding the adverse health effects of environmental exposure to lead (Pb) resulted in its classification as an air pollutant pursuant to the Clean Air Act Amendment of 1970, followed by the requisite enactment of a health-based National Ambient Air Quality Standard (NAAQS) for Pb in 1978 (set at 1.5 $\mu g/m^3$ based on quarterly average concentration). In October 2008, the U.S. Environmental Protection Agency (EPA) promulgated revisions to the Pb NAAQS that lowered the acceptable level by an order of magnitude to 0.15 $\mu g/m^3$ based on a rolling three-month average concentration. Additionally, in December 2010 EPA revised requirements for Pb monitoring around facilities known to have substantial Pb emissions. These facilities include airports with sufficient piston-powered aircraft activity that they are estimated to have annual Pb emissions of 1.0 ton or more. EPA also engaged a monitoring study of 15 additional airports with estimated annual Pb emissions between 0.5 and 1.0 ton to investigate whether airports with this range of Pb emissions, and that meet additional criteria described by EPA, may have the potential to cause violations of the Pb NAAQS (U.S. EPA 2013b). After a year of sample collection, two airports were found to have three-month average lead concentrations greater than the Pb NAAQS and another two were found to have concentrations greater than half of the Pb NAAQS and the EPA will continue to require Pb monitoring these four airports (U.S. EPA 2015).

A geospatial analysis of six counties in North Carolina revealed small but significant positive relationships between child blood lead levels and residential proximity to general aviation airports (Miranda et al. 2011). The association was strongest at distances up to 500

meters from the airport boundary and was statistically significant (95% confidence interval) at distances up to 1,500 meters. This finding contributes to the motivation to model Pb emissions and Pb concentration fields at general aviation airports. To date, however, such modeling has been very limited. ICF International prepared a Pb emissions inventory based on 2008 piston-engine aircraft activity at Santa Monica Airport (SMO) (ICF International and T&B Systems 2010, Carr et al. 2011). Activity data were collected at the airport and used as inputs to the 2008 National emissions inventory (NEI) methodology to estimate Pb emissions. The ICF methodology applied at SMO included two modes of operation that were previously unaccounted for in the then-existent methodologies – aircraft runup and landing. Aircraft engine runup is performed by piston-engine aircraft before takeoff to test engine performance. The inclusion of engine runup was a significant improvement because this mode corresponds to high emissions in a concentrated area which could lead to Pb hotspots. Indeed, sensitivity analysis conducted by ICF showed engine runup to be one of the most important factors contributing to total aircraft-related Pb hotspot concentrations at SMO. The study used the maximum allowable Pb content in avgas of 2.12 g/gal for estimating emissions. Two periods were modeled, a winter period and a summer period, and on-site airborne particulate matter (PM) samples were collected at multiple locations for each period. The on-site samples were analyzed for Pb and used for model-to-monitor comparisons. A total of six days were examined for model-to-monitor comparison, with a mean absolute bias of 40% for the winter period and 20% for the summer period. The model tended to overestimate concentrations at most sampling locations.

Modeling has also been performed for Centennial Airport (APA) in Colorado which has on-site airborne Pb sampling (Feinberg and Turner 2013). FAA's Emissions and Dispersion Modeling System (EDMS) was used with runup emissions added as an area source. EDMS is not

designed for modeling Pb emissions at general aviation airports, but the model was used by making assumptions about the emissions and their spatial and temporal allocation consistent with the very limited activity data that were available. Using the amount of runup emissions as an adjustable parameter, this study was able to model Pb concentrations that captured the distribution of concentrations measured at the airport. Sensitivity tests revealed that modeled concentrations at the Pb sampling site were very sensitive to the amount of runup emissions. A major limitation of this work was the fitting with a single adjustable parameter whereas there are several sources of uncertainty and possibly bias in the modeling inputs that are lumped into the fitted parameter value.

The data and analysis presented in this paper were collected as part of the Airport Cooperative Research Program (ACRP) project 02-34 entitled "Quantifying Aircraft Lead Emissions at Airports" (Heiken et al. 2014). The primary objective of this project was to review and improve upon existing methodologies to quantify and characterize aircraft-related Pb emissions at airports with significant populations of aircraft that use leaded aviation gasoline. To support the development of an improved methodology, month-long field studies were conducted at each of three selected airports to gather site-specific data for aircraft activity, the lead content of aviation gasoline used at the airport, and airborne Pb concentrations. The three airports selected for this study were: Richard Lloyd Jones Jr. Airport (RVS) in Tulsa, OK; APA; and SMO. Day-specific emissions were estimated and the refined methodology was evaluated through comparison of dispersion modeling results based on the inventory, generated from the site-specific data, to airborne Pb data collected during the field study. This paper focuses on the results of the modeling of airborne Pb concentrations arising from aircraft exhaust emissions.

4.3 Methods

4.3.1 On-site Data Collection

Field studies—each nominally one month in duration—were conducted in 2013 at each of the three airports. Data was collected from March 27 to April 28 at RVS, May 15 to June 10 at APA, and July 3 to July 30 at SMO. Detailed aircraft activity data were collected to inform the development of a spatially and temporally resolved emissions inventory (Heiken et al. 2014). Key activity data collected included landing and takeoff operations (LTOs), aircraft fleet inventory, and time in mode (TIM) for runup and other activities. Additionally, airborne PM samples were collected daily and analyzed for Pb. Airborne $PM_{2.5}$ (particulate matter less than 2.5 μm aerodynamic diameter) data are used in this paper because the focus is on aircraft exhaust emissions which falls within this size range. A limited number of Total Suspended Particulate (TSP) samples were also collected; this is the size range for the Pb NAAQS but is also influenced by Pb in resuspended dust and therefore less desirable for evaluating the aircraft emissions inventory.

Sampling locations were selected both downwind and upwind of the airport activity for prevailing winds. Downwind sampling locations were selected based on preliminary modeling performed before the field studies were conducted and upwind sampling locations were selected based on prevailing winds and distance from airport activity (Heiken et al. 2014). Twelve-hour integrated PM samples were collected each day. These sampling events were conducted during the 12-hour period of highest piston-engine aircraft activity based on discussions with the airport authorities (starting at 7 or 8AM local time depending on the airport). This approach was preferred over 24-hour integrated sampling for several reasons. Piston-engine aircraft activity is very low at night and thus the additional 12 hours of sampling would increase the relative

contribution from background Pb to the time average concentration. Background Pb can result from resuspension of deposited Pb in soil and atmospheric transport from other distant sources. The 24-hour time window for sampling also increases the likelihood of wind direction variability. This is not a hard constraint for modeling, but persistent winds do simplify the data interpretation. Finally, calm winds are more frequently observed at night and these periods are more difficult to model.

In order to assess the spatial and temporal distribution of aircraft LTO activities, video cameras were used to continuously record LTOs during each PM-Pb sampling event. LTO data were collected for all fixed-wing aircraft at each airport and at SMO the piston-engine aircraft fraction was also directly measured. At RVS and APA, the piston-engine aircraft fraction was not directly measured from the video data because aircraft in the video images were often too small to be conclusively identified as either piston engine or jet. During video playback, LTO activities were apportioned based on runway, hour of day, and activity type. Figure 4-1 shows the hourly distribution of total operations at RVS for all aircraft (not just piston-engine aircraft)

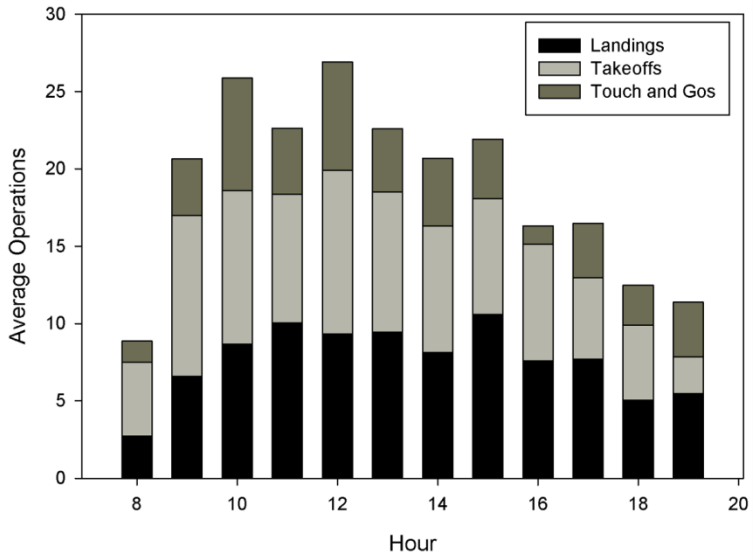

Figure 4-1 Hourly landing and takeoff operations at RVS averaged over the 21 days of data collection. Hour reported in local time.

as determined from the video camera data. (Throughout this manuscript figures and tables are provided for RVS with similar information for the other two airports provided elsewhere (Heiken et al. 2014).) Touch-and-go activities are counted as two operations each and are distinguished from normal takeoffs and landings. Over the study period there were, on average, 19 operations per hour. Total operations peaked between 10 AM and 12 PM, with the lowest levels of activity in the early morning.

To obtain the aircraft fleet inventory, LTOs were photographed for at each airport. Photographs were reviewed to develop a time-stamped inventory of LTO activities by tail ID. The FAA Registry was used to identify the aircraft and engine characteristics for each recorded tail ID (Federal Aviation Administration). Data were collected for all aircraft, not just piston-engine aircraft, to provide information about the distribution of activities between piston-engine airplanes and jets. The tail ID inventory was used to generate average fuel burn rates for all activities, and average TIM for aloft activity (climbout, approach, etc.). Some aircraft were observed multiple times over the 30 hours of data collection. At each of the three airports a small number of aircraft disproportionately contributed to total operations with 5% of the observed aircraft conducting one-third of the operations and 10-12% of the observed fleet conducting half of the operations.

In order to determine the time aircraft spent performing runups, these operations were manually observed for 15 hours at each airport. Data collection was scheduled to capture a range of conditions (time of day, day of week) and included the time aircraft spent in a runup area (visual observation), the duration of the magneto test (audible changes in engine noise during runup), and the aircraft tail ID. Some planes bypassed the runup area prior to takeoff and such instances were recorded. In some cases, the magneto test duration could not be determined

because of confounding sources of noise. Table 4-1 summarizes the runup results for each of the three airports. Figure 4-2(a) shows box plots of the total runup and magneto test TIM data at RVS, and Figure 4-2(b) shows cumulative distributions for these data. 57% of emissions from the runup areas were attributed to idling while 43% of was attributed to magneto testing. Reducing time spent idling in the runup areas would lead to reduced runup area contributions to Pb concentrations. Runup operation TIM was more variable than landing-and-takeoff TIM. Since

Table 4-1 Time in Mode Data Collected for Run-Up Operations at RVS, APA and SMO.

	RVS		APA		SMO	
	Total Run-Up	Magneto Testing	Total Run-Up	Magneto Testing	Total Run-Up	Magneto Testing
Number of Aircraft	109	76	53	42	41	36
Mean ± Std Dev (sec)	296 ± 150	69 ± 56	327 ± 189	97 ± 102	328 ± 215	61 ± 52
Median (sec)	284	50	287	71	244	42

Notes: Based on 15 hours of data collection at each airport. Means are reported with 1σ standard deviation values.

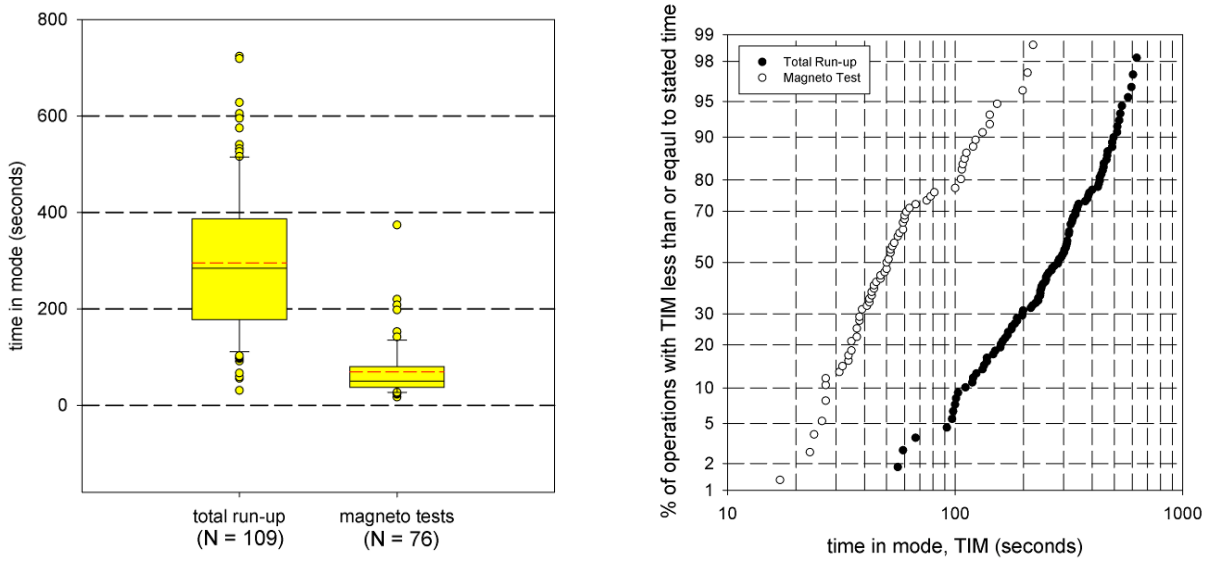

(a) (b)

Figure 4-2 Time-in-Mode data for total time in the runup area and duration of magneto testing at RVS, based on fifteen hours of data collection.

PM-Pb hot spots tend to be downwind of runup areas, so the runup TIM variability will lead to variability in the hot spot intensity.

Additional piston-engine aircraft activities such as taxiing, takeoffs, and landings were manually observed for 15 hours at each airport. Data collection was scheduled to capture a range of conditions (time of day, day of week). Observation points were chosen to maximize viewing of the entire airport footprint. Activities were tracked by aircraft and recorded by runway or taxiway. For example, a taxi-back would consist of the following data: landing time (time on runway between wheels down and turning onto taxiway); time taxiing and idling on each taxiway; and takeoff time (time on runway between starting rollout and wheels-up). Approach and climb-out times could not be adequately captured because of the difficulty in establishing aloft locations for the start of approach and end of climb-out. Instead, average TIM were estimated based on the tail ID inventory and aircraft operation manuals, and wheels-up and wheels-down locations on the runways were recorded to spatially allocate runway emissions. TIM for touch-and-go operations was recorded as the time between wheels down for the landing portion and wheels-up for the takeoff portion.

Avgas dispensed by all fixed base operators (FBOs) at the three airports is 100LL grade, which has a maximum Pb content of 2.1 g/gal (0.56 g/L). The actual Pb content in 100LL can be considerably lower, however, and thus avgas samples were collected at each airport and analyzed for Pb content. Avgas samples were collected from FBOs at RVS and APA. At SMO, however, the FBOs were unwilling to provide avgas samples for this study; therefore, samples were collected from two privately owned, SMO-based piston-engine aircraft. In general, avgas samples were collected from FBOs within days after new fuel deliveries; however, some samples were obtained from FBOs with low avgas sales volumes, resulting in samples drawn as long as

ten months after the most recent delivery. A total of 15 avgas samples were collected with analysis by Intertek Caleb Brett for Pb content using test method ASTM D5059. Pooling over the three airports, mean and median Pb concentrations in avgas were 1.6 g/gal and 1.3 g/gal, respectively, with a maximum Pb content of 2.1 g/gal. Mean and median Pb concentrations were considerably less than the maximum allowable Pb content of 2.1 g/gal that is used in the NEI methodology for estimating lead emissions.

4.3.2 Emission Inventory and Model Development

The emission inventory was spatially and temporally resolved by combining TIM, average fuel burn rate and avgas Pb content for each type of activity (landing, takeoff, or TGO) to calculate an emission rate per activity for each source type (takeoff, runup, taxiing, etc.) and location (runway, runup area, taxiway, etc.). Emissions were assigned to each hour by scaling per unit activity emissions to the activity counts observed from the video data. The resolved emission estimates were used to perform air quality modeling for each study site to evaluate how well modeled and measured ground-level lead concentrations compare at the sampling locations. The modeling was performed using the American Meteorological Society/Environmental Protection Agency Regulatory Model Improvement Committee modeling system, also known as AERMOD (version 13350). AERMOD is the dispersion modeling tool used in EDMS, and was also used to perform preliminary site modeling that determined the placement of the air samplers at the field study sites. EDMS was not used for modeling in this project because it does not include runup emissions and also does not allow for hour-specific activity and emissions estimations.

All Pb emission sources at each airport were characterized as line sources (represented as a string of volume sources) to represent the initial horizontal and vertical dispersion of the

emissions depending upon the operating mode. Average wind speeds were calculated over the period during which airport activity data are collected to allow calculation of an initial vertical dispersion parameter for each airport. Taxi/idle, take-off, climb-out, and approach/landing traffic for each type of aircraft were allocated to specific airport locations according to operating mode observations made during the activity data collection phase of the project. Specific parameters attributed to these sources are presented elsewhere (Heiken et al. 2014).

AERMOD was used to generate one-hour average modeled airborne Pb concentrations, which were converted into 12-hour average concentrations for purposes of comparison to the airborne PM-Pb measurement data.

4.4 Results and Discussion

4.4.1 Spatial Extent of Modeled PM-Pb Impacts

Hourly airborne PM-Pb concentration fields for each of the three airports were modeled using site-specific aircraft activity data. The modeled hourly concentrations were used to generate 12-hour average concentrations corresponding to the PM sampling events with valid aircraft LTOs data (collected from the video cameras); they do not include nighttime hours and days missing the hourly LTOs activity data. Study-average concentration fields were constructed by averaging the modeling results across all of the 12-hour sampling events (21-28 events per site).

Figure 4-3 shows the modeled study-average PM-Pb concentration fields for RVS (a), APA (b), and SMO(c), respectively. Consistent length scales are used to convey differences in the airport footprint sizes. Airport property boundaries are designated by a thick black line and the interior black lines are the runways. PM sampling sites are denoted by the black squares.

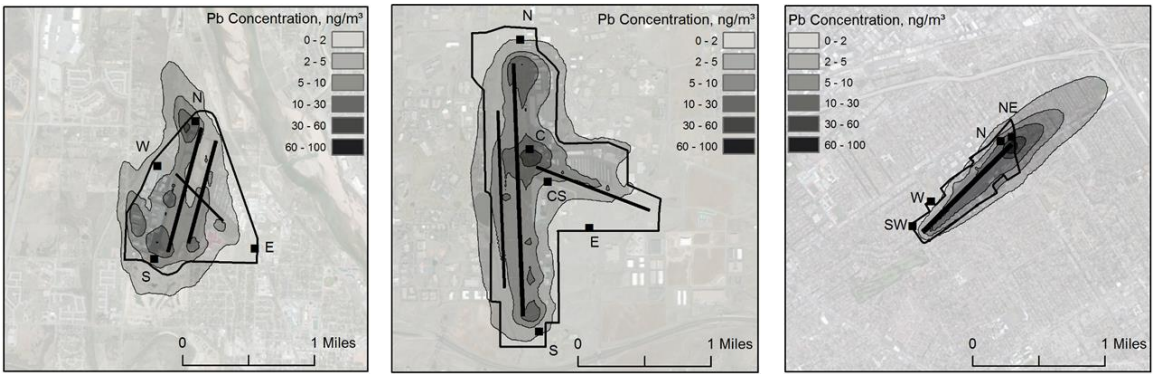

(a) (b) (c)

Figure 4-3 Modeled period-average PM-Pb concentrations at RVS (a), APA (b), and SMO (c).

Figure 4-3a shows the modeled study-average PM-Pb concentration fields at RVS. Modeled concentrations are highest near the runup areas and runway ends. The zone of Pb impacts, operationally defined as concentrations exceeding the 75th percentile measured $PM_{2.5}$-Pb background concentration of 3 ng/m^3, were generally confined to within the airport footprint with the exception of the northwest boundary. The North (N) sampling site (primary downwind site for prevailing southerly winds) was near the area of highest modeled concentrations at the airport. Modeling predicts very low impacts at the East (E) sampling site, consistent with the selection of this location as the primary upwind site for prevailing southerly winds.

Figure 4-3b shows the modeled study-average PM-Pb concentrations at APA. The zone of Pb impacts - operationally defined as concentrations exceeding the 75th percentile measured $PM_{2.5}$-Pb background concentration of 2 ng/m^3 - is again generally confined to within the airport footprint. Highest modeled study-average concentrations are at the center of the airport nearby multiple taxiways, a runup area, and the start of the east-west runway. The Central (C) sampling location is on the northern edge of the highest modeled concentrations. The East (E) monitor was sited to capture background conditions and the modeling confirmed very low study-average impacts from aircraft activities.

Figure 4-3c shows the modeled study-average Pb impacts at SMO. Its small spatial extent and activities near the airport fenceline lead to Pb impacts greater than the background—operationally defined as the 75th percentile measured $PM_{2.5}$-Pb background concentration of 2 ng/m^3—extending beyond the airport footprint. The highest study-average concentrations are near the northeast runup area and the start of a runway. The Northeast sampling location is located on the northern edge of the modeled Pb hotspot. The Southwest monitor was sited to capture background conditions, and the modeling suggests there might be modest aircraft activity contributions to the PM-Pb measured at this location.

4.4.2 Comparison of Modeled and Measured PM-Pb Concentrations

Modeled Pb concentrations were compared to measured $PM_{2.5}$-Pb concentrations with a focus on the primary downwind sites (N at RVS, C at APA, and NE at SMO). Measured $PM_{2.5}$-Pb concentrations were corrected for background using data from the primary upwind sites (E at RVS and APA, and SW at SMO). Days with wind patterns causing the primary upwind site to be impacted by aircraft activities, e.g., westerly winds at RVS, were excluded from the comparisons.

Figure 4-4 compares the modeled results from RVS (A), APA (b), and SMO (c) based on site-specific data to background-corrected measured concentrations for the primary downwind monitor. The data was background-corrected on a daily basis by subtracting the concentration of Pb measured at the primary upwind sampling locations. The first eight days of PM-Pb sampling at RVS were not modeled because of insufficient video camera data to capture airport operations. For RVS (Figure 4-4a), there was very good agreement between modeled and measured PM-Pb concentrations with the data well distributed about the 1:1 line. Modeled and measured concentrations were typically low at the other three sites at RVS (not shown). At these sites, six

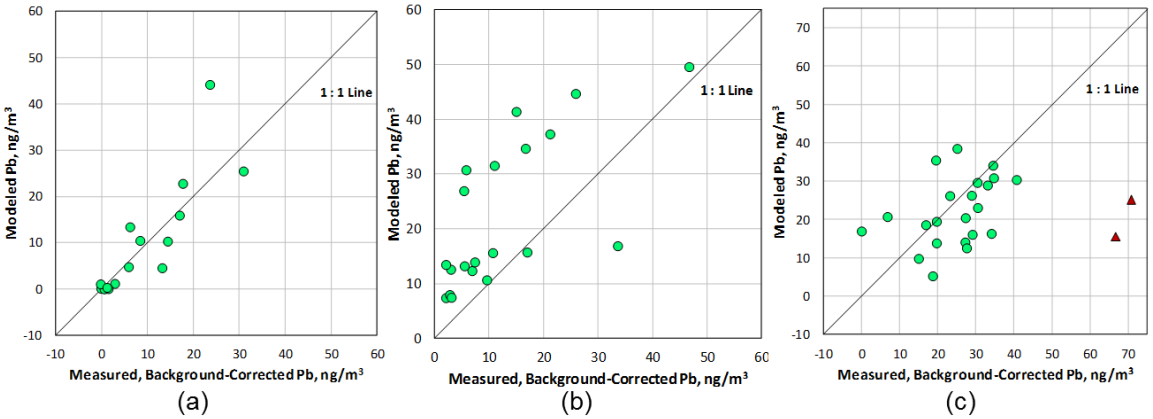

Figure 4-4 Modeled and measured $PM_{2.5}$-Pb concentrations at downwind locations at RVS (a), APA (b), and SMO (c).

of the nine samples with excess PM-Pb concentrations (defined as a background-corrected concentration greater than two times the propagated measurement precision) had modeled concentrations within a factor of two of the measured values. The model both overestimated and underestimated PM-Pb concentrations across these six days.

In contrast to RVS, there is a bias at APA with the modeled concentrations persistently higher than the measured concentrations (Figure 4-4b). The primary downwind sites at RVS and SMO were impacted by aircraft activities only for the prevailing wind direction; for other wind directions, the measured concentrations at the primary downwind sites approached background conditions. In contrast, the primary downwind site at APA was centrally located and therefore impacted by aircraft activities for a wide range of wind directions. This may be the reason for the poorer agreement between the modeled and measured concentrations. At APA, the primary downwind site was located north of the Runway 10 runup and takeoff areas, with the expectation that most piston-engine aircraft operations were on this runway. However, piston-engine activity was prevalent on the primary runway, 17L/1R, directly to the west of the Central site. As a result, shifting winds during the sampling period caused the modeling of APA to be very

sensitive to the specific spatial and temporal allocation of activity. Thus the hour-by-hour characteristics at the Central site could vary dramatically. Furthermore, the site was very close to the eastern edge of the main taxiway and modeling of Pb concentrations resulting from aircraft operating on this taxiway may have been affected by the short source-to-receptor distances.

Figure 4-4c compares the modeled results for SMO, based on site-specific data, to background-corrected measured concentrations for the primary downwind monitor. One day is not shown because of contamination during Pb analysis. There was good agreement between modeled and measured PM-Pb concentrations. Data are distributed about the 1:1 line but, overall, the model tended to underestimate PM-Pb impacts at the Northeast site. There were, however, two days (shown with triangles, both occurring on weekends) where the monitored concentrations were much greater than the modeled values. For both of these days, the monitoring location was about 100 meters away from the modeled plume centerline, and the concentrations on the centerline were well within a factor of two of the measured concentration.

Methods for comparing air quality models to measurements have been reviewed by Chang and Hanna (Chang and Hanna 2004). Several common performance measures are presented in Table 4-2. FAC2 is the fraction of model-predicted concentration values (C_P) within a factor of two of the measured (observed) concentration values (C_O), i.e. the fraction of data with $0.5 \leq C_P/C_O \leq 2$. FAC2 was ~75% at RVS and SMO and 45% at APA. The model over predicts the measurements for negative FB and the model under predicts the measurements for positive FB. Based on the ratio of means, the model is 11% high at RVS and 11% low at SMO, while the model is 76% high at APA. A NMSE of 0.5 corresponds to a mean bias of a factor of two. NMSE is higher at RVS (0.27) than at SMO (0.19) in large part because the concentration values are lower at RVS. NMSE accounts for both systematic errors (bias) and random errors. NMSE at

Table 4-2 Performance Measures for Comparing PM-Pb Model Predictions to Measurements

Performance Measure	RVS	APA	SMO
Number of Samples	9[1]	20	22[2]
Mean $PM_{2.5}$-Pb, ng/m^3			
– Measured	15.3	12.2	24.7
– Model Predicted	16.9	22.2	22.1
FAC2[3]	0.78	0.45	0.77
Fractional Bias, FB	-0.11	-0.55	+0.11
Ratio of Arithmetic Means	1.11	1.76	0.89
Normalized Mean Square Error, NMSE	0.27	0.69	0.19
– NSME systematic error contribution	0.01	0.33	0.01
– NSME random error contribution	0.26	0.36	0.18

1. Excludes seven samples with both measured and modeled $PM_{2.5}$-Pb less than 3 ng/m^3.
2. Excludes two samples with measured $PM_{2.5}$-Pb much greater than modeled concentrations (triangles in Figure 4-4c).
3. The fraction of model-predicted concentration values within a factor of two of the measured (observed) concentration values.

RVS and SMO are dominated by the random error component while at APA there are nearly equal contributions from the systematic and random error components.

4.4.3 Contributions of Discrete Activities to Pb Hotspot Formation

The modeled impacts from discrete airport activities and locations were grouped into the following nine source groups to determine their relative contributions across the airport in general and at the monitoring locations in particular. The source groups were defined based on a few key characteristics:

- Run-up – includes both magneto test and idling emissions in the run-up areas;
- Taxiways – includes emissions from both taxiing and idling on the taxiways as the planes move from hangars or tie-downs to runways and back;

- Takeoff – includes emissions from the beginning of movement on the runway until wheels-up;
- Climb Out – includes emissions from wheels-up until reaching traffic pattern altitude;
- Approach – includes emissions from traffic pattern altitude until wheels-down;
- Landing – includes emissions from wheels down until exiting the runway;
- Touch and Go – includes emissions from all phases of a touch and go (Approach, Ground Roll, and Climbout);
- Hangars – includes all emission activities within a hangar area such as taxiing and idling; and
- Helicopters – includes all phases of helicopter operation.

Modeling the lead emissions as individual source groups allowed for the evaluation of source group contribution to hotspot formation. Table 4-3 shows the source group contributions to airport-wide PM-Pb emissions and to modeled concentrations at the North monitor at RVS. Taxiways, takeoffs, and runup activities were the largest contributors to the modeled study-average PM-Pb concentration at the North sampling location. The taxiway contribution was higher than anticipated; however the small taxiway that connects the ends of the main taxiway and runway is much closer than the northwest runup area to the North monitor. Forty percent of the estimated emissions from this taxiway were from idling while waiting for takeoff clearance. Taxiways and takeoffs exhibited a wide range of contributions to absolute concentrations at the North monitor. This variability, combined with the good agreement shown in Figure 4-4a, suggest that the emission inventory and air quality modeling accurately represent these source groups at RVS. In contrast, the absolute contributions from runup activities are generally low and

Table 4-3 Airportwide PM-Pb Emissions and Modeled Contributions at the North Monitor, RVS

Source Group	Percentage of Total Emissions (%)	Period-Average Contribution at North Monitor (%)	Range of Contributions at North Monitor[1] (%)	Range of Contributions at North Monitor[1] (ng/m^3)
Runup	22%	12%	2% - 15%	0.1 – 3.9
Taxiways	12%	52%	50% - 57%	2.3 – 22.2
Takeoff	5%	25%	18% - 36%	1.6 – 13.3
Climbout	26%	3%	0% - 5%	0.0 – 0.9
Approach	17%	4%	2% - 7%	0.2 – 2.6
Landing	1%	1%	0% - 2%	0.0 – 0.2
Touch and Go	11%	2%	0% - 8%	0.0 – 0.8
Hangars	6%	1%	0% - 1%	0.0 – 0.3
Helicopters	1%	0%	0% - 0%	0.0 – 0.0

[1]Contributions for southerly winds only

with modest sample-to-sample variability. Thus, the RVS study alone does not robustly evaluate the runup portion of the emission inventory. At SMO, however, the runup contributions were relatively high with appreciable sample-to-sample variability which does provide for an evaluation of runups.

In addition to the North site data, there was one day at the South site during northerly winds with modeled runup contributions greater than 2 ng/m^3. For this day, the modeled and measured PM-Pb concentrations agreed very well. Like at RVS, runup, taxiways and takeoffs were the primary contributors to modeled concentrations at the downwind monitors at APA and SMO.

Figure 4-5 shows the study-average modeled total PM-Pb concentration (panel a, same as Figure 4-3a) and the individual PM-Pb contributions from taxiways, runup areas, and takeoffs at RVS. Taxiways (panel b) had moderate Pb impacts over large portions of the airfield, with highest impacts near the ends of runways and at highly trafficked intersections. Runup areas (panel c) have the highest contributions to the hotspots shown in panel (a); however,

Figure 4-5 Modeled total and source-group-specific PM-Pb concentrations at RVS. Airport property boundaries are designated by a thick black line; dark interior lines indicate runways.

concentration gradients were steep and the runup area impacts have relatively small spatial extent. Contributions from takeoffs (panel d) were constrained to the runway ends. Similar patterns were also observed at APA and SMO.

4.5 Conclusion

Site-specific activity data and aircraft fleet information were collected at three general aviation airports that each had distinguishing features in terms of airport layout and meteorology. Overall, aircraft activity patterns were similar across the three airports. These activity patterns were used to generate an emission inventory for each airport over the data collection period. The emission inventories were then spatially and temporally allocated in order to perform dispersion modeling using AERMOD. Modeled concentrations were then compared to measured airborne PM-Pb concentrations that were collected over the same study periods. The time period of modeling and on-site activity data collection was significantly longer than any other study reported in the literature

The quantitative performance measures collectively demonstrate good agreement between model predictions and measurements at RVS and SMO, but the model is biased high at APA. At RVS, the primary downwind site was largely impacted by taxiing and takeoffs; at SMO, it was largely impacted by taxiing and runup. Thus, across these two studies, the three major ground-based activities that contribute to emissions and to PM-Pb hot spots were evaluated and suggest the inventory methodology developed for this project is sound. While model predictions and measurements showed poorer agreement at APA, if the error is ascribed to the emissions inventory then the methodology is conservatively high, which is preferred over being low.

Runup areas, taxiways, and takeoffs were found to be the dominant contributors to Pb hotspot formation. Pb hotspots typically formed when all three of these activities occurred within short distances of each other, typically near the runway ends. The compact spaces between these activities near the runway ends allow the emissions from the source groups to mix and form hotspots. This highlights the importance of the spatial distribution of airport activities for modeling Pb concentrations. It also highlights that airports with compact size might have more issues with high concentrations, even though their total activity levels may be lower than other, larger airports. Separating the locations where these three activities occur at an airport will likely reduce the magnitude of Pb concentration hotspots. Additionally, reducing the amount of time spent idling in the runup areas would reduce their impact on hotspot formation

The highest modeled 12-hour $PM_{2.5}$-Pb concentration was 48 ng/m^3 at APA, and the observed 12-hour concentration was a TSP-Pb value of 72 ng/m^3 at SMO. These are less than the three-month average NAAQS of 150 ng/m^3. However, the PM data collection and modeling focused on size ranges and averaging times that do not follow federal reference method Pb sampling methods. Therefore, these values are not directly comparable to the NAAQS. However, the data collection and modeling methodology presented in this paper could be adapted to match the methods required to assess airport Pb impacts relative to the NAAQS by extending the daily modeling period from 12 to 24 hours and calculating three month averages.

While there are now several studies monitoring Pb at airports, modeling is necessary to get a complete vision of airport Pb impacts. As shown in this paper, concentration gradients near runup areas and runway ends are very steep and monitored concentrations can either miss the highest concentrations or misrepresent exposures to those living or working around airports. Additionally, since the highest concentrations are found in areas with multiple sources (runways,

runup areas, etc.), modeling provides the ability to determine which of these sources have the most influence.

This methodology of data collection, emissions inventory development, and modeling can serve as a useful tool for airports and environmental agencies. While the application of the methodology to every airport is not feasible, it can be applied to individual airports where the magnitude and spatial extent of Pb impacts are of interest. The data collection strategy should be applicable to all general aviation airports; however, as shown at APA, modeling can be difficult at more complex airports.

4.6 Acknowledgements

This study was funded by the Airport Cooperative Research Program. The authors would like to thank Jeff Condray of the Tulsa Airport Authority, Steve Mushrush and the airport operations staff at RVS, Robert Olislagers and the airport operations staff at APA, and Stelios Makrides and the airport operations staff at SMO. Timothy Noack assisted with the data processing.

4.7 References

U.S. EPA. 2013a. Integrated Science Assessment for Lead. EPA600-R-10-075F

U.S. EPA. 2013b. Program Update on Airport Lead Monitoring (4 pp, EPA-420-F-13-032, June 2013) http://www.epa.gov/otaq/regs/nonroad/aviation/420f13032.pdf

U.S. EPA. 2015. Program Overview on Airport Lead Monitoring (4 pp, EPA-420-F-15-003, January 2015) http://www.epa.gov/otaq/documents/aviation/420f15003.pdf

Miranda, M.L; Anthopolos, R.; Hastings, D. A Geospatial Analysis of the Effects of Aviation Gasoline on Childhood Blood Lead Levels. Environ. Health Perspect. Vol. 119, No. 10, 2011, pp. 1513-1516.

ICF International and T&B Systems. 2010. Development and Evaluation of an Air Quality Modeling Approach for Lead Emissions from Piston-Engine Aircraft Operating on Leaded Aviation Gasoline. U.S. Environmental Protection Agency. EPA-420-R-10-007.

Carr, E., M. Lee, K. Marin, C. Holder, M. Hoyer, M. Pedde, R. Cook, and J. Touma. Development and Evaluation of an Air Quality Modeling Approach to Assess Near-field Impacts of Lead Emissions from Piston-engine Aircraft Operating on Leaded Aviation Gasoline. Atmospheric Environment. Vol. 45, No. 32, 2011, pp 5795-5804.

Feinberg, S. and Turner, J. Dispersion Modeling of Lead Emissions from Piston Engine Aircraft at General Aviation Facilities. Transportation Research Record: Journal of the Transportation Research Board, No. 2325, Transportation Research Board of the national Academies, Washington, D.C., 2013, pp. 34-42.

Heiken, J., Lyons, J., Valdez, M., Matthews, N., Sanford, P., Turner, J and Feinberg, N. "Quantifying Aircraft Lead Emissions at Airports." Transportation Research Board. Web-Only Document 21. October 2014. http://onlinepubs.trb.org/Onlinepubs/acrp/acrp_webdoc_021.pdf

Federal Aviation Administration. FAA Registry: Aircraft Inquiry. http://registry.faa.gov/aircraftinquiry/

Chang, J. C., & Hanna, S. R. Air Quality Model Performance Evaluation. Meteorology and Atmospheric Physics, Vol. 87, 2004, pp. 167-196.

4.8 Supplemental Material

4.8.1 Airport Diagrams and Data Collection Locations for the Three Field Campaigns

Figure 4-6, Figure 4-7, and Figure 4-8 show the airport diagrams and maps of data collection locations at RVS, APA, and SMO, respectively.

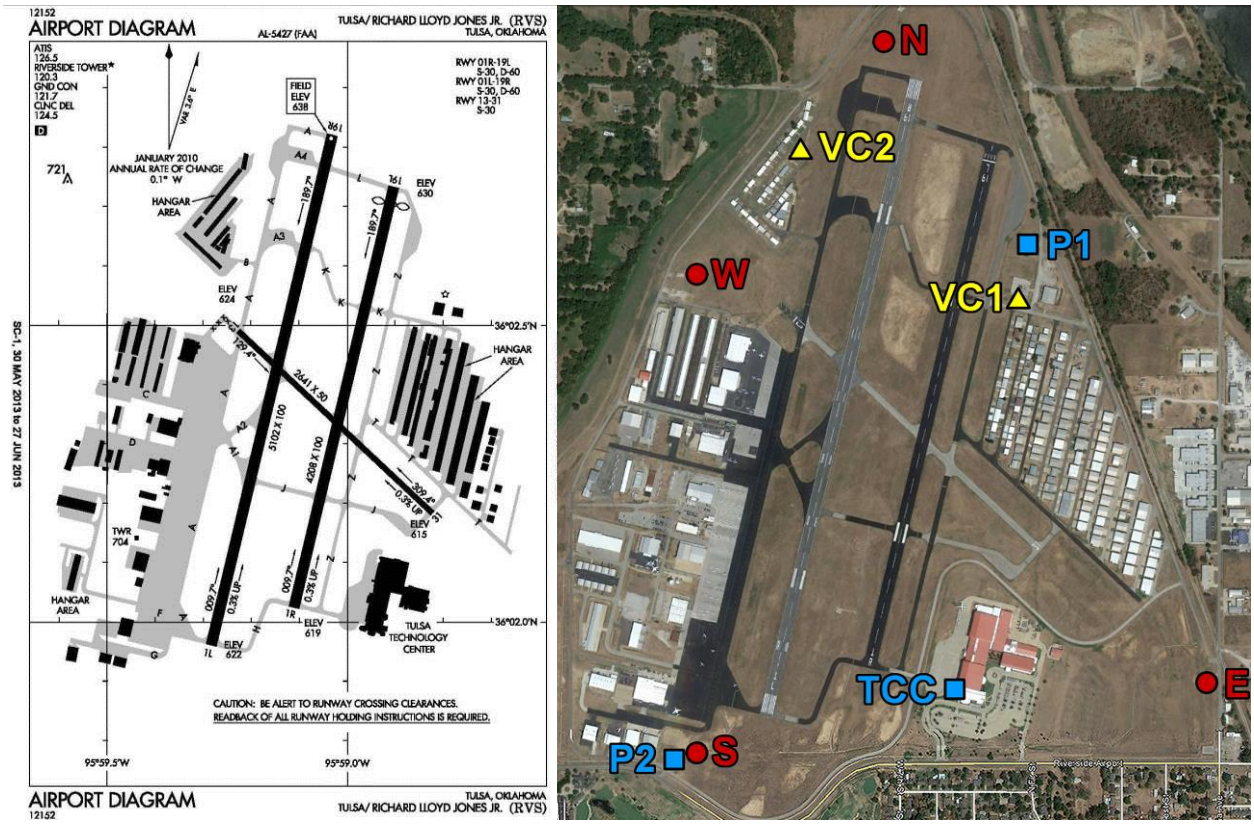

Note: PM sampling was conducted at the North (N), East (E), South (S), and West (W) sites; video cameras were deployed at the VC1 and VC2 sites; and other activity data were manually collected at the P1, P2, and TCC sites.

Figure 4-6 Airport diagram and PM sampling and activity data collection locations deployed at RVS.

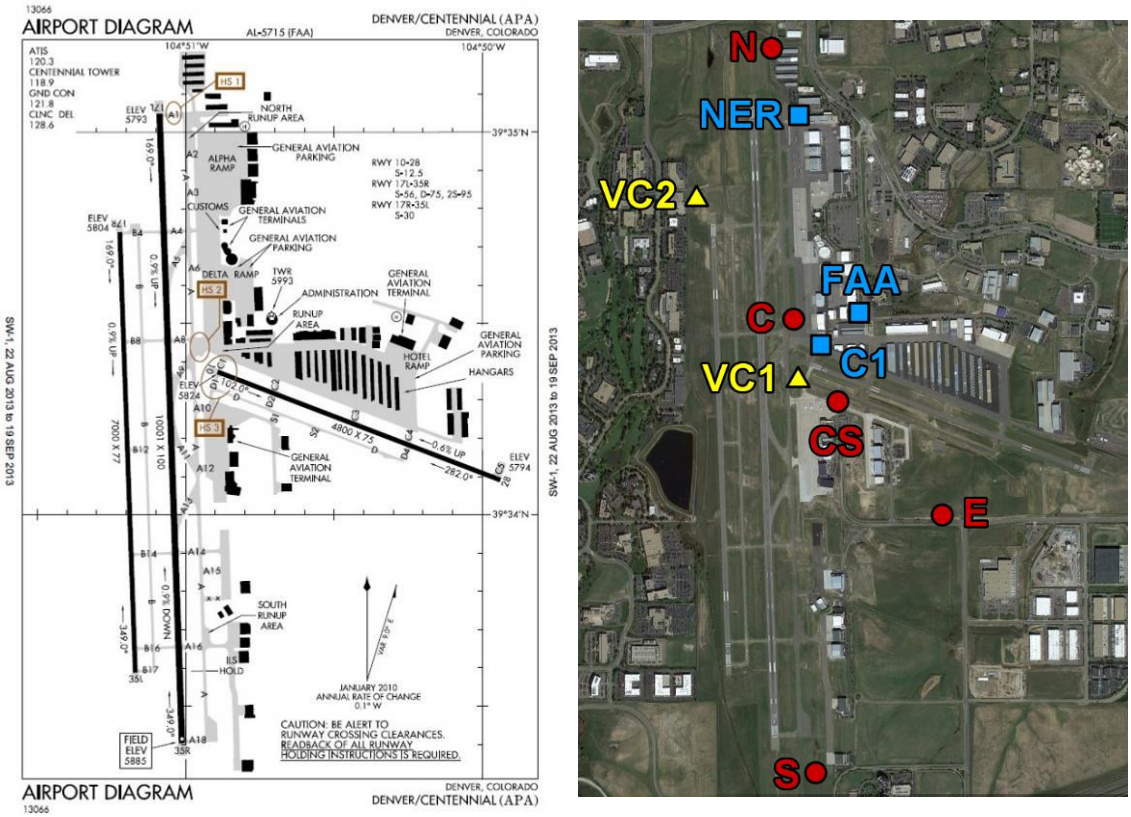

Note: PM sampling was conducted at the North (N), East (E), South (S), Center (C), and Center Secondary (CS) sites; video cameras were deployed at the VC1 and VC2 sites; and other activity data was manually collected at the C1, NER and FAA sites.

Figure 4-7 Airport diagram and PM sampling and activity data collection locations deployed at APA.

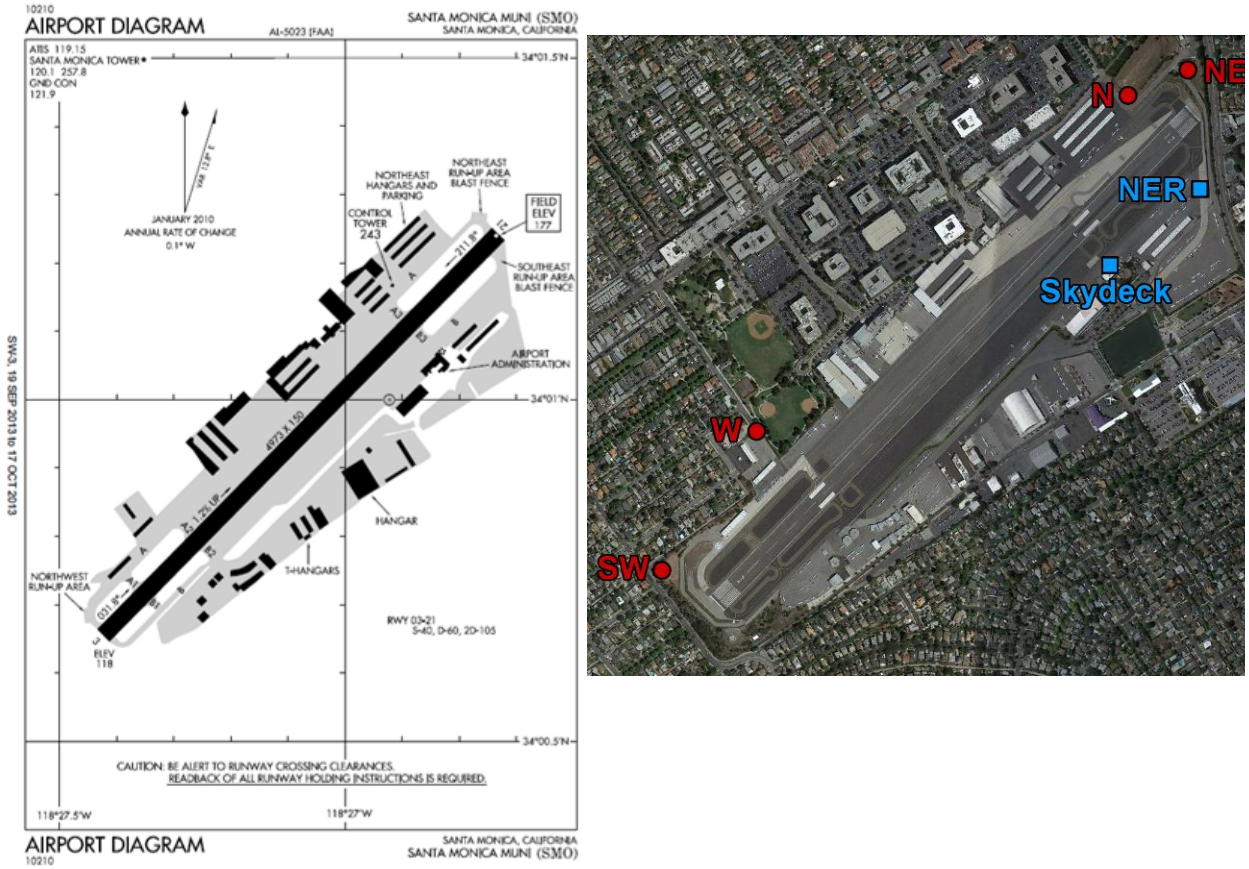

Note: PM sampling was conducted at the North (N), Northeast (NE), West (W), and Southwest (SW) sites; video cameras were deployed at the North site; and other activity data was manually collected at the Skydeck and NER sites.

Figure 4-8 Airport diagram and PM sampling and activity data collection locations deployed at SMO.

4.8.2 Site Specific Data from APA

Figure 4-9 shows average hourly distribution of total operations for all aircraft at APA (not just piston-engine aircraft) as determined from the video camera data. Touch-and-go activities accounted for 25-50% of the total operations depending on the hour with higher proportions of such operations in the mornings. Total operations peaked around 11 AM and the lowest levels were towards the end of the 7 AM to 7 PM MDT sampling periods. About half (51%) of the operations were on runway 17R/35L, which is normally used only by piston-engine

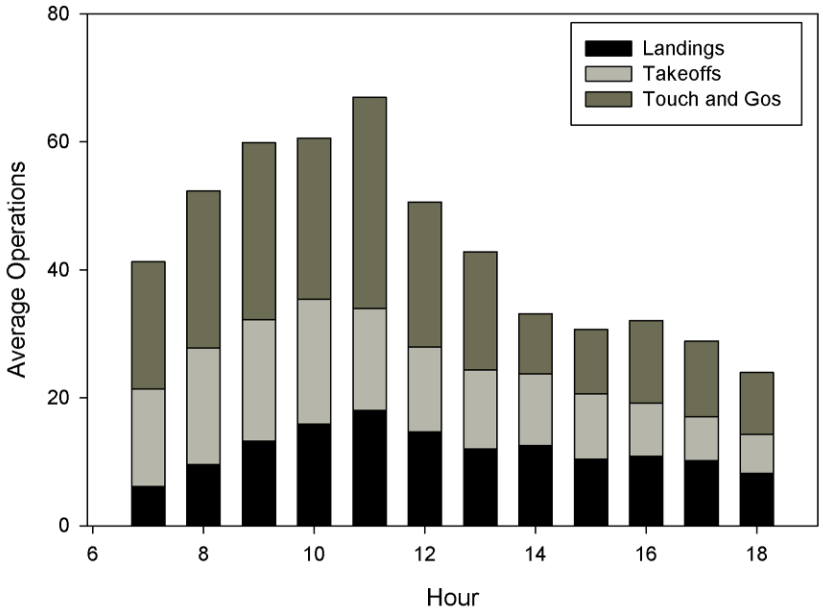

Figure 4-9 Fixed wing aircraft average hourly operations at APA.

aircraft and has high touch-and-go activity. Forty percent (40%) of operations were on runway 17L/35R, which has all of the jet activity and some of the piston-engine activity. Only 9% of operations were on runway 10/28, which is used exclusively by piston-engine aircraft. For the north/south-oriented runways, 60% of operations originated at the north end (17L/17R) and 40% originated at the south end (25L/35R). For the east/west-oriented runway, 97% of operations originated at the west end (runway 10) and 3% originated at the east end (runway 28).

Time-in-mode data were manually collected at APA. Piston-engine aircraft runup activities were observed for 15 hours and included 53 runup operations, with magneto test duration recorded for 42 of these operations. Missing magneto test data primarily resulted from confounding sources of noise. Tail numbers were recorded for 89% of the runup operations. Table 4-4 and Figure 4-10 summarize the runup results. Mean times-in-mode were 97 seconds for the magneto test and 327 seconds for the total time in the runup area. There was large variation in these times, with standard deviations of about 60% and 100% of the means for total runup and magneto testing, respectively. Figure 4-10a shows box plots of the total runup and

Table 4-4 Time-in-mode data for runup operations at APA

	Total Run-Up	Magneto Testing
Number of Aircraft	53	42
Mean ± Std Dev (sec)[1]	327 ± 189	97 ± 102
Median (sec)	287	71

[1] Means are reported with 1σ standard deviation values.

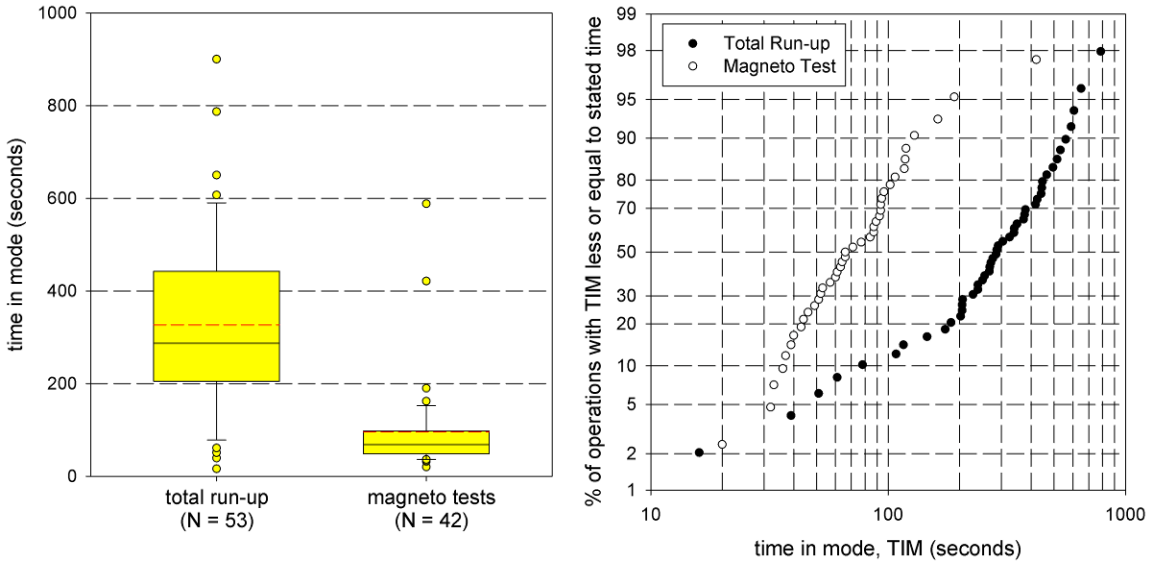

(a) (b)

Notes: (a) box plots (interior solid line is the median, interior dashed line is the arithmetic mean; box boundaries are 25th and 75th percentiles, whiskers are 10th and 90th percentiles, and circles are all records below the 10th percentile and above the 90th percentile); and (b) cumulative distributions as a log-probability plot.

Figure 4-10 Time-in-mode data for total time in the runup area and duration of magneto testing at APA.

magneto test TIM data; Figure 4-10b shows cumulative distributions for the TIM data. The magneto test data are relatively well approximated by a lognormal distribution as evidenced by the nearly linear trend for the log-probability plot. The total runup time data are not well represented by normal or lognormal distributions. Compared to RVS, the mean total runup time

and mean magneto test time were longer at APA. Both runup time and magneto test time also showed higher variability at APA compared to RVS.

4.8.3 Site Specific Data from SMO

At SMO video cameras were continuously operated at the North (primary downwind) site during each 12-hour sampling event to record LTOs. One camera was set up to determine the number of LTOs, while a second camera was set up to enhance runup time characterization. In contrast to RVS and APA, where the runways covered large footprints, the activities at SMO are more concentrated and the fractions of jets, turboprops, and piston-engine aircraft could be determined from the video camera data. Given the positioning of the video camera, however, it was sometimes difficult to distinguish touch-and-go operations from normal landings; therefore, touch-and-go operations are underrepresented and normal landings are overrepresented in this data set. The TIM data collected at SMO may be able to close this data gap. Figure 4-11 shows average hourly piston-engine operations for the entire study period (in contrast, Figure 4-1 for

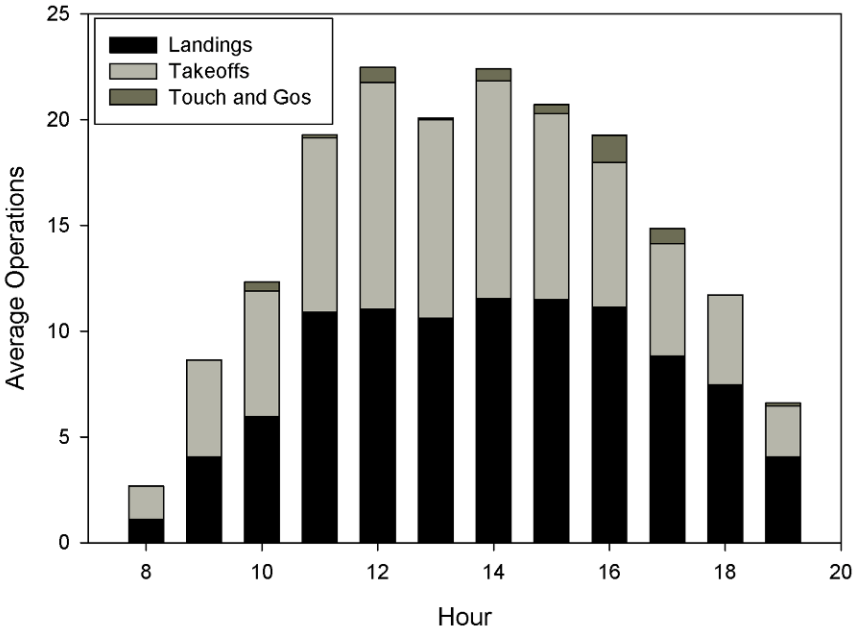

Figure 4-11 Piston-engine aircraft average hourly operations at SMO.

RVS and Figure 4-9 for APA include all fixed-wing aircraft). Touch-and-go activities are counted as two operations each. From 11 AM to 4 PM, the total hourly operations were relatively high and consistent from hour to hour.

Piston-engine aircraft runup activities were observed for 15 hours and included 41 runup operations, with magneto test duration recorded for 36 of these operations. Missing magneto test data primarily resulted from confounding sources of noise. Tail numbers were recorded for 95% of the runup operations. Twenty-three planes bypassed the runup area and did not perform runups that were observed. Table 4-5 and Figure 4-12 summarize the runup results. Mean TIM was 61 seconds for the magneto test and 328 seconds for the total time in the runup area. There was a large variation in these times, with standard deviations of about 70% and 80% of the means for total runup and magneto testing, respectively. Figure 4-12a shows box plots of the total runup and magneto test TIM data, and Figure 4-12b shows cumulative distributions for the TIM data.

Both total runup time and magneto test data are relatively well approximated by a lognormal distribution as evidenced by the nearly linear trend for the log-probability plot. Mean

Table 4-5 Time-in-mode data collected for Runup operations including magneto testing at SMO

	Total Run-Up	Magneto Testing
Number of Aircraft	41	36
Mean ± Std Dev (sec)[a]	328 ± 215	61 ± 52
Median (sec)	244	42

Notes: Means are reported with 1σ standard deviation values

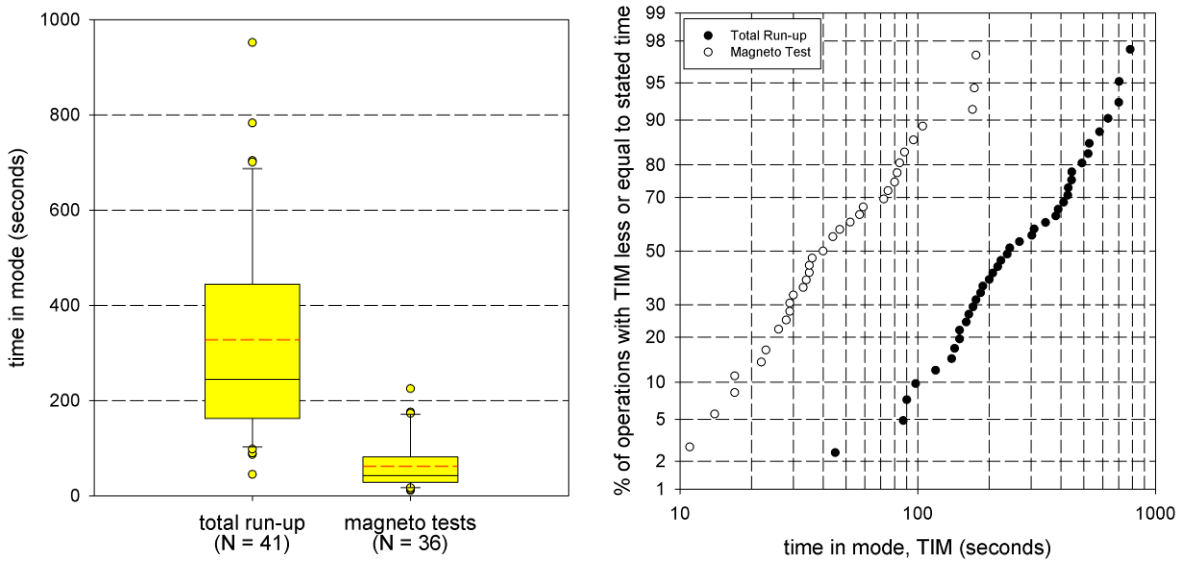

(a) (b)

Figure 4-12 Time-in-mode data for total time in the runup area and duration of magneto testing at SMO.

total runup times at SMO and APA were similar, with shorter total runup times at RVS. The highest variability in total runup time was observed at SMO. Mean magneto test times at SMO were shorter than at RVS and APA. The magneto test times at SMA and RVS had similar variability, with higher variability observed at APA.

Mean magneto test time was less than previously observed by Carr et al. (2011), but the time reported by Carr et al. was within one standard deviation of the observed mean for this study. Most other times-in-mode observed in this study also compared favorably (within approximately 30% of each other) with observations by Carr et al. The approach and landing time observed in this study were significantly greater than that reported by Carr et al. This could potentially be explained by different assumptions for altitude at the start of approach.

4.8.4 Contributions of Discrete Activities to Pb Hotspot Formation at APA and SMO

Table 4-6 shows the source group contributions to airportwide total PM-Pb emissions and to modeled concentrations at the Central monitor at APA. Helicopters were not modeled at APA because of very low activity and lack of spatial activity information. Runup and taxiways were the highest modeled contributors to PM-Pb at the Central monitor, even though they were each only 12% of the total estimated emissions. In contrast to RVS, takeoffs from the nearby runways were not significant contributors to the period-average concentration at the primary downwind monitor. There was large day-to-day variation in the source group contributions to modeled concentrations at the Central monitor. For example, runup contributions ranged from 15% to 96% of total modeled impacts at the monitor. The large range of relative source contributions results from the day-to-day variations in meteorology. Potential overestimation of runup

Table 4-6 PM-Pb emissions and modeled contributions at the Central Monitor, APA

Source Group	Percentage of Total Emissions	Period-Average Contribution at Central Monitor (%)	Range of Contributions at Central Monitor (%)	Range of Contributions at Central Monitor (ng/m^3)
Runup	12%	56%	15% - 96%	1.1 – 57.9
Taxiways	12%	33%	4% - 75%	1.8 – 23.7
Takeoff	7%	1%	0% - 4%	0.0 – 0.5
Climbout	21%	2%	0% - 8%	0.0 – 1.6
Approach	12%	1%	0% - 2%	0.0 – 0.3
Landing	1%	1%	0% - 3%	0.0 – 0.8
Touch and Go	29%	3%	0% - 12%	0.0 – 1.9
Hangars	6%	4%	0% - 23%	0.0 – 2.6

emissions near the central monitor may contribute to the model's overestimation of Pb concentrations.

Days with the largest differences between modeled and measured concentrations generally corresponded to above-average modeled contributions from runup sources. This suggests runup contributions may be overestimated at the Central monitor. The overestimation could result from multiple factors, including the runup emission inventory or the spatio-temporal allocation of these emissions in the modeling.

Similar to RVS, runup areas and taxiways generally had the largest modeled contributions to ground-level concentrations on the airport footprint, especially in areas with higher concentrations. Figure 4-13 shows the modeled total lead concentration at APA (panel a, same as Figure 4-3b) and the individual Pb contributions from taxiways , runup areas, and takeoffs. Taxiways (panel b) had moderate PM-Pb impacts over large portions of the airfield with highest impacts near the ends of runways and at highly trafficked intersections. Runup areas (panel c) have a more limited spatial extent of impacts above measured background PM-Pb concentrations on the airport footprint, but have the highest maximum impacts of all of the source groups. Both taxiways and runup have high impacts near the intersection of Taxiways A and C, resulting in the modeled hotspot at the center of the airport footprint. Contributions from takeoffs (panel d) were constrained to the runway ends.

Modeled airportwide total emissions contributions of the different source groups to modeled concentrations at the Northeast site at SMO are shown in Table 4-7. Runup, taxiways, and takeoffs collectively contributed about 90% of the modeled impacts at the Northeast monitorwhile accounting for only about 35% of the total emissions. Due to the compact size of

the airport, approach and climbout emissions had a larger impact at the Northeast monitor than at the downwind sites at RVS and APA. Relative source contributions at the Northeast sampling locations were much more consistent at SMO than at RVS and APA because of the wind

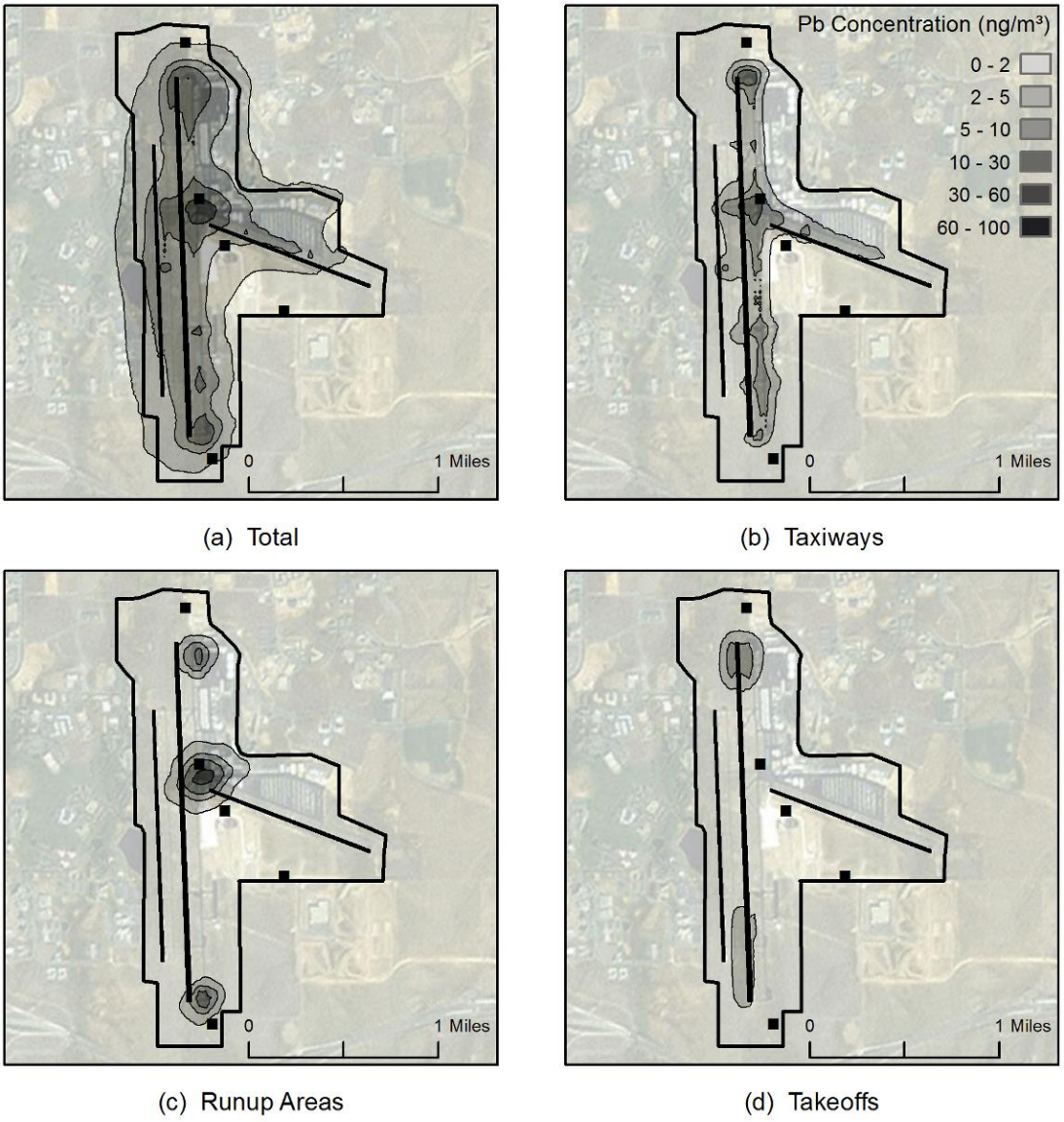

Note: Airport property boundaries are designated by a thick black line; dark interior lines indicate runways.

Figure 4-13 Modeled total and source group specific PM-Pb concentrations at APA.

Table 4-7 PM-Pb emissions and modeled contributions at the Northeast Monitor, SMO

Source Group	Percentage of Total Emissions	Period-Average Contribution at Northeast Monitor (%)	Range of Contributions at Northeast Monitor (%)	Range of Contributions at Northeast Monitor (ng/m^3)
Runup	13%	47%	37% - 52%	1.8 – 17.5
Taxiways	15%	23%	21% - 27%	1.1 – 9.0
Takeoff	6%	18%	15% - 21%	0.8 – 7.1
Climbout	29%	4%	3% - 7%	0.3 – 1.3
Approach	27%	5%	3% - 9%	0.4 – 2.3
Landing	2%	1%	0% - 3%	0.0 – 0.7
Touch and Go	1%	0%	0% - 1%	0.0 – 0.3
Hangars	6%	2%	1% - 3%	0.2 – 0.8
Helicopters	1%	0%	0% - 4%	0.0 – 0.5

consistency at SMO. There was wide variation in the absolute contributions from runups, takeoffs, and taxiways, implying that the SMO field study is appropriate for evaluating the emission inventory. However, the consistent relative contributions make it difficult to distinguish any particular source group as the source of model underestimation. Modeled source group contributions and measured airport operations data did not provide additional insights into the two days with poor model-to-monitor comparisons.

Again, runup, taxiways, and takeoffs had the largest relative contributions to high modeled PM-Pb areas. Figure 4-14 shows the modeled period-average PM-Pb concentration

(panel a, same as Figure 4-3c) and impacts of the taxiways, runup areas, and takeoffs at SMO. Similar to the total modeled PM-Pb impacts, the relative contributions of the taxiways and runup areas extend northeast of the airport footprint. Runup contributions were highest near the modeled hotspot shown in Figure 4-14, while taxiways had high relative contributions throughout the airport footprint. Takeoffs had a higher relative contribution to the modeled hotspot at SMO than at RVS or APA because of the compact nature of the SMO airport layout. However, takeoff impacts were still generally constrained to areas around the runway ends.

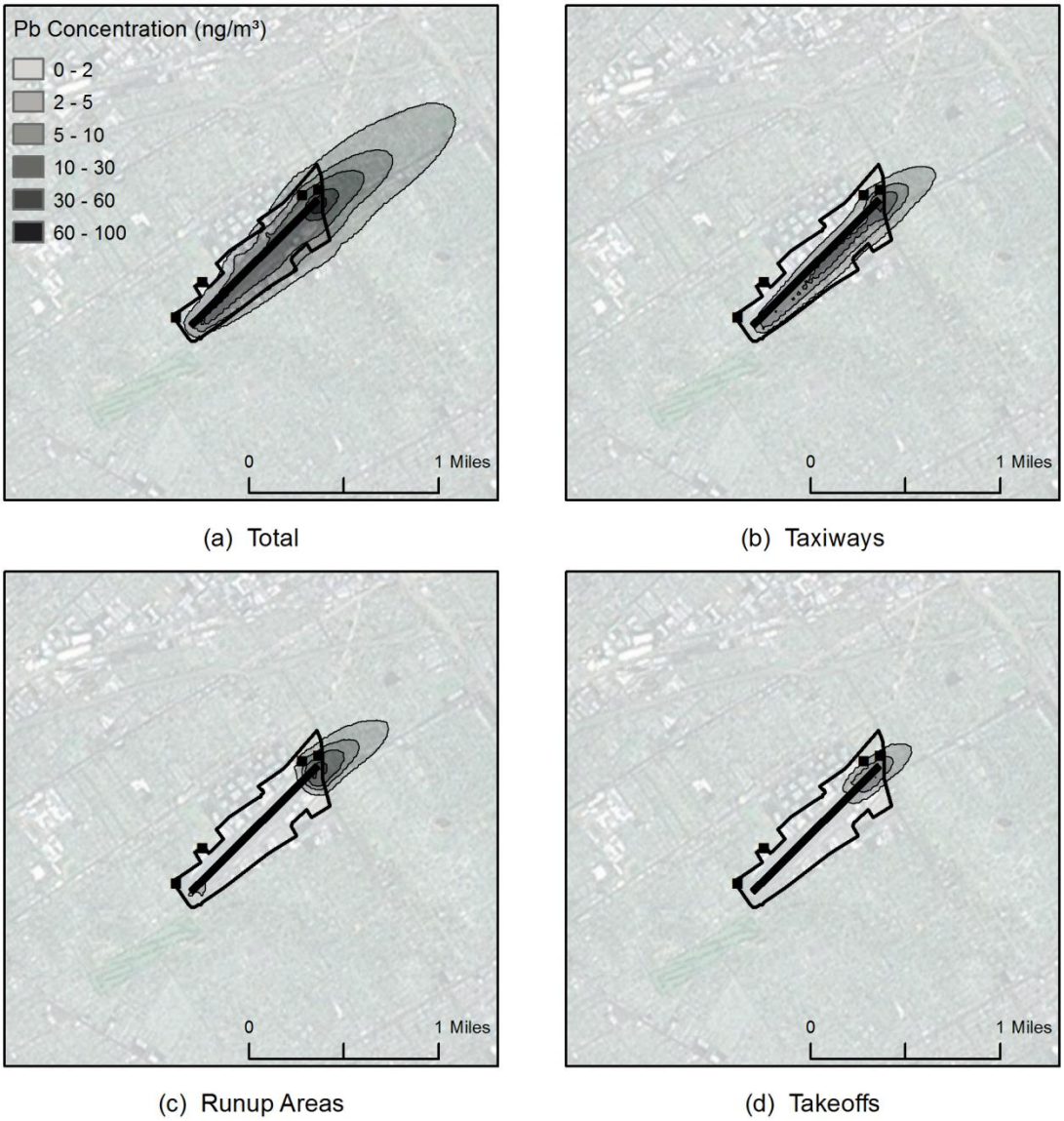

Note: Airport property boundaries are designated by a thick black line; dark interior lines indicate runways.

Figure 4-14 Modeled total and source group specific PM-Pb concentrations at SMO.

Chapter 5: Mitigation of Lead Impacts at Airports

The contents of this chapter appear in an unpublished report for the Airport Cooperative Research Program of the Transportation Research Board, Project Number 02-57.

5.1 Introduction

Chapters 2 through 4 assess the measured and modeled lead (Pb) impacts at general aviation airports. Given that no level of Pb is considered safe ("Lead" 2015) the next step is to attempt to mitigate, to the extent practicable, impacts from airport Pb emissions. The modeling described and implemented in Chapter 4 provides the necessary framework for evaluating potential airport Pb mitigation strategies. The emission inventory automatically updates hourly estimates when parameters such as fuel flow rate or avgas Pb content is changed, and Pb source characteristics can be easily adjusted in AERMOD. This chapter describes the use of the modeling framework described in Chapter 4 to evaluate two mitigation strategies: moving runup areas to reduce maximum airport Pb hotspot concentrations; and replacing the use of avgas with motor vehicle gasoline (MOGAS) in planes that have been certified for its use.

Runup areas are where piston-engine aircraft perform engine and other performance testing prior to takeoff. This operation includes significant idling in addition to magneto tests, where engines are tested through high power cycles to ensure proper performance. Runup areas were identified in Chapter 4 and a previous study (Carr et al. 2011) as significant contributors to airport Pb hotspots. This is in part because runup areas are typically close to major taxiways and runway ends and Pb hotspots tend to result when emissions from takeoffs, idling and taxiing on taxiways, and runup converge. Runup areas are more easily moved at an airport; therefore, this work focuses in part on the potential reductions in hotspot maxima when moving runup areas away from busy taxiways and runway ends.

Replacing avgas with MOGAS in some airplanes has also been identified as a potential strategy for reducing airport Pb impacts. This is because an airport's Pb emissions are linearly proportional to the average Pb content in the fuel burned at the airport. The Federal Aviation Administration (FAA) is currently supporting development and implementation of an unleaded replacement for avgas; however, the development, testing, and adoption of this fuel will take several years (FAA 2014). This timeline is drawn out in part because of the more stringent requirements for the physical properties of aviation fuel, such as octane content and volatility, compared to motor vehicle fuel ("Leaded Aviation Fuel and the Environment" 2013). However, after significant testing, the FAA issued supplemental type certificates (STCs) for a large number of airframes and engines, certifying their use with MOGAS ("Approved Engines and Airframes." 2015, "Approved Engine Models for Autofuel Use." 2006). These lists of aircraft and engines can be compared with the aircraft inventories from the on-site data collection described in Chapter 4 to determine the Pb emissions that can be reduced by using MOGAS.

To place potential reduction of Pb emissions and impacts into perspective, it was desired to evaluate an airport with relatively high Pb concentrations. Thus, Palo Alto Airport (PAO) in Palo Alto, CA was chosen for further on-site activity data collection and modeling. United States Environmental Protection Agency (EPA) – mandated measurements for the full year period ending December 2013 had maximum three-month average Pb concentrations greater than half the Pb National Ambient Air Quality Standard (NAAQS) of 150 ng/m^3 and, therefore, the EPA has required continual Pb monitoring at the airport (U.S. EPA 2015). On-site activity data collection at PAO occurred over 11 days from July 24 to August 3, 2015. The data collection strategy at PAO was different because of time restrictions, as well as restrictions against any digital recording of aircraft activity. In addition to providing data to evaluate mitigation

strategies, the study of PAO serves as another test of the data collection and modeling framework established in Chapter 4.

In Chapter 4, modeled results from RVS and SMO were found to agree well with on-site measured concentrations. Therefore, these two airports were chosen to evaluate the mitigation strategies of interest in this study. APA was not chosen because of the bias in the modeled values compared to the measured concentrations as well as the overall complexity of the airport. Together, the modeling of RVS, SMO and PAO were used to evaluate the two mitigation strategies.

5.2 Methods

5.2.1 On-site Data Collection

At RVS and SMO, video cameras were used to record aircraft activity by runway during the 12-hour period of highest aircraft activity. These hours were paired with on-site airborne Pb sampling. Videos from these airports were played back to document landing and takeoff operations (LTOs) as well as touch and go operations (TGOs) by runway at 10-minute and one-hour time periods. These observations were then used to develop an hourly time-of-day distribution of total aircraft activity as well as determine the fraction of total activity resulting from LTOs and TGOs. At SMO, the fraction of piston engine aircraft activity was determined directly from the video camera data. At RVS, aircraft in the video images were often too small to be conclusively identified as either piston-engine or jet and therefore the fleet characterization data from still photography was used to determine the fraction of piston-engine aircraft. Further details were described in Chapter 4.

At PAO, video cameras were not permitted by the access agreement executed between the City of Palo Alto and Washington University. Therefore, operations were recorded by visual

observation. Over 90 hours of operations data were collected, with each operation recorded by date and time, activity type, runway, and aircraft type. Data was collected between 7 AM and 9 PM PDT, which are the hours that the FAA air traffic tower is open for operation. Hourly observations were used to generate an hourly distribution of operations by activity type. Further details on the observed LTOs and other activity data are presented in the supplemental material.

LTOs were photographed for 30 hours at both RVS and SMO. The data collection schedule was generated using a quasi-random process to populate a 2D matrix with dimensions of time of day and day of week (Weekdays / Saturdays / Sundays). The matrix was weighted towards data collection during hours with higher activity and to ensure adequate data collection on weekends. Photographs were reviewed to develop a time-stamped inventory of LTO activities by tail ID. At PAO, digital photography was not allowed so aircraft type was determined by visually recording the tail ID. The aircraft fleet data collection was paired with the landing and takeoff operations so that the fleet for each type of operation was separately determined.

For all three airports, aircraft tail IDs were processed using the FAA registry (*http://registry.faa.gov/aircraftinquiry/)* to determine the aircraft models and engine types. The database also includes important information such as engine horsepower. For each airport, tail IDs were not included the final database.

Runup operations were manually observed for 15-19 hours at each airport. Data collection was scheduled to capture a range of conditions (time of day, day of week) and included the time aircraft spent in a runup area (by visual observation), the duration of the magneto test (by audible changes in engine noise during runup), and the aircraft tail ID. Some planes bypassed the runup area prior to takeoff and such instances were recorded. In some cases,

the magneto test duration could not be determined because of confounding sources of noise. Tail ID numbers were removed from the final database.

Additional piston-engine aircraft activities such as taxiing, takeoffs, and landings were manually observed at each airport. Data collection was scheduled to capture a range of conditions (time of day, day of week). Observation points were chosen to maximize viewing of the entire airport footprint. Activities were tracked by aircraft and recorded by runway or taxiway. For example, a taxi-back would consist of the following data: landing time (time on runway between wheels down and turning onto taxiway); time taxiing and idling on each taxiway; and takeoff time (time on runway between starting rollout and wheels-up). Approach and climb-out times could not be adequately captured because of the difficulty in establishing aloft locations for the start of approach and end of climb-out. Instead, wheels-up and wheels-down locations on the runways were recorded to inform the development of time-in-mode (TIM) estimates for climb-out and approach and to spatially allocate runway emissions. TIM for touch-and-go operations was recorded as the time between wheels down for the landing portion and wheels-up for the takeoff portion.

At RVS and SMO, aviation gasoline (avgas) samples were collected from either fixed based operators (FBOs) selling avgas at the airport, or from planes based at the airport. Four samples were collected at RVS and two were collected at SMO. Mean avgas Pb concentrations at RVS and SMO were 1.3 and 1.9 g/gal, respectively, with standard deviations of 0.03 and 0.1 g/gal. Avgas samples were not collected at PAO; however, analysis from the previous data collection showed that fuel delivery certificates provided accurate avgas Pb concentrations. Therefore, avgas Pb concentrations from 2015 fuel delivery certificates provided by FBOs at

PAO were used to determine Pb content. The mean avgas Pb content at PAO was 1.7 g/gal with a standard deviation of 0.04 g/gal.

5.2.2 Modeling of Pb Emissions

The activity data collected at each airport was used to develop an emissions inventory, estimating the emissions per average operation and using the FAA's Air Traffic Activity System (ATADS) daily traffic counts to calculate the daily emissions. More detail on the development and use of the emission inventory at RVS and SMO are presented in Chapter 4. Briefly, emissions were estimated for the year 2013. Total daily aircraft activity was taken from ATADS and scaled using the observed aircraft activity during one month of on-site data collection at both RVS and SMO. Emissions were spatially and temporally allocated using the activity patterns observed during the on-site data collection. At each airport, weekend and weekday temporal activity patterns were statistically indistinguishable so the same hourly activity patterns were used for all days. Fuel Pb content, times-in-mode, fuel burn rate and the spatial distribution of emissions were also taken from observations presented in Chapter 4 and are based on airport-specific aircraft activity inventories. Dispersion modeling was conducted at hourly resolution for the year 2013 using EPA's AERMOD modeling system.

Emissions at PAO were modeled using the same general methodology as RVS and SMO, presented in Chapter 4. Figure 5-1 shows the PAO airport diagram and aerial map of the airport footprint. The EPA-mandated Pb monitoring was performed at PAO in 2013 by the Bay Area Air Quality Management District, and the location of the on-site monitoring location is marked on the aerial map. In contrast to RVS and SMO, the measured concentrations for validation of model performance were not collected at the same time as the on-site data collection. In order to generate daily operations by activity type (landing, takeoff, TGO, etc) for 2013 the amount of

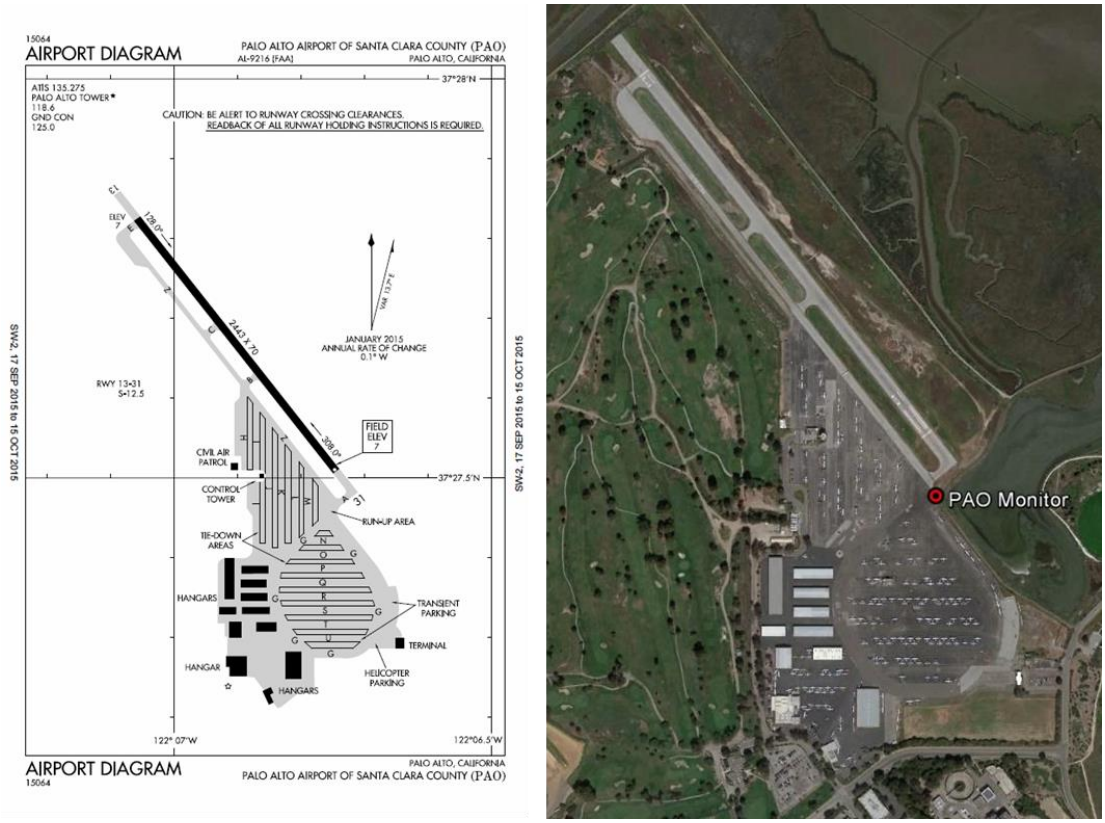

Figure 5-1. Airport diagram and EPA Monitor Location at PAO.

total daily ATADS reported operations for the time period of the on-site data collection was compared with the on-site activity counts to generate a scaling factor for each type. The number of operations by type in the 2013 emissions inventory was then determined by multiplying the 2013 daily operations by the type specific scaling factor. Rotorcraft emissions were not modeled at PAO because of their relatively low fraction of total airport activity and difficulty to accurately allocate emissions. Because of very persistent winds from the northwest, and in order to produce a more conservative (higher) estimate of long-term Pb hotspot concentrations at the airport, all landing and takeoff activity was allocated to runway 31. ASOS meteorology is not collected at PAO so wind data from Moffett field in Mountain View, CA was used for modeling. These measurements are 8 km southeast of PAO and are also close to San Francisco Bay.

The impacts of moving the run-up areas were evaluated by proposing new potential runup areas for each of the three airports. Figure 5-2 shows the centroid of each of the most-used runup areas (labeled NE-, NW-, and SW-Orig) at RVS and the two alternate locations modeled for each of these areas (labeled Z1 and Z2). These new centroids are approximately 100 meters (Z1) and 200 meters (Z2) farther away from the runway ends, but remain along the current taxiways. Figure 5-3 shows the locations of the primary runup area at SMO (NE Orig) as well as two alternative areas approximately 80 meters (NE Z1) and 160 meters (NE Z2) to the southwest of the current runup area. Similar to RVS, the alternative runup areas were shifted along the taxiways more towards the middle of the airport, moving emissions away from the takeoff area. The primary runup area location at PAO (SE Orig), as well as alternative runup area

Figure 5-2 Map of RVS with original and modeled runup locations.

Figure 5-3 Map of SMO with original and modeled runup locations.

locations approximately 50 meters (SE Z1) and 100 meters (SE Z2) to the southwest, is shown in Figure 5-4. In contrast to RVS and SMO, the modeled runup areas were moved away from the runway ends and into the aircraft tie-down areas, instead of parallel to the runway. This prevents additional congestion and two way traffic on the taxiways and taxilanes that would occur if the runup area were moved to the northwest along the runway. At each of the airports in this study, new runup areas were kept the same size and shape as the original areas.

In addition to moving the runup areas, the effects of using MOGAS in aircraft that are certified to use it were also evaluated. Based on the lists of approved aircraft ("Approved Engines and Airframes." 2015, "Approved Engine Models for Autofuel Use." 2006), the inventories for each of the three airports were modified by setting Pb emissions from those aircraft certified to use MOGAS to zero. Again, modeling was performed using AERMOD with the average emissions per LTO and TGO adjusted based on their respective fleets.

Figure 5-4 Map of PAO with original and modeled runup locations.

5.3 Results and Discussion

5.3.1 Model Performance

Modeled impacts of Pb emissions at RVS and SMO were shown to have good agreement with on-site Pb measurements taken during the study. Figure 5-5 shows the measured and modeled 12-hour Pb concentrations at RVS (a) and SMO (b) during the data collection periods at those airports (these figures also appear in Chapter 4 as Figure 4-4a and Figure 4-4c, respectively). The good agreement visually demonstrated by these figures is also supported by performance statistics presented in Chapter 4.

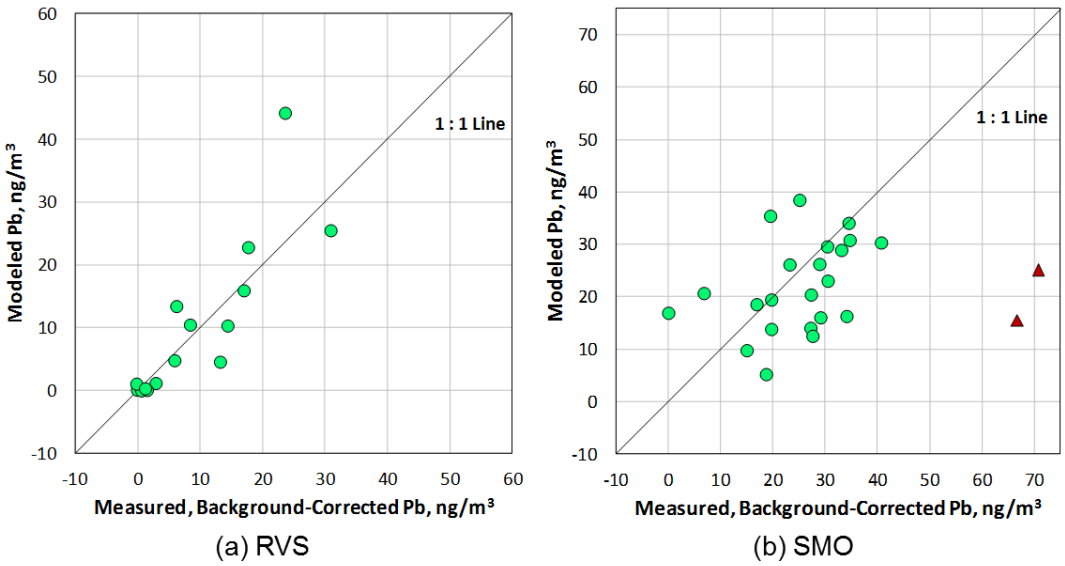

Figure 5-5 Measured and modeled 12-hour Pb concentrations at RVS (a) and SMO (b).

Figure 5-6 shows the measured and modeled 2013 daily Pb concentrations at PAO. The measured concentrations are not background corrected; however, the background Pb levels at the other airports studied were low compared to Pb at the high impact sites, and only small

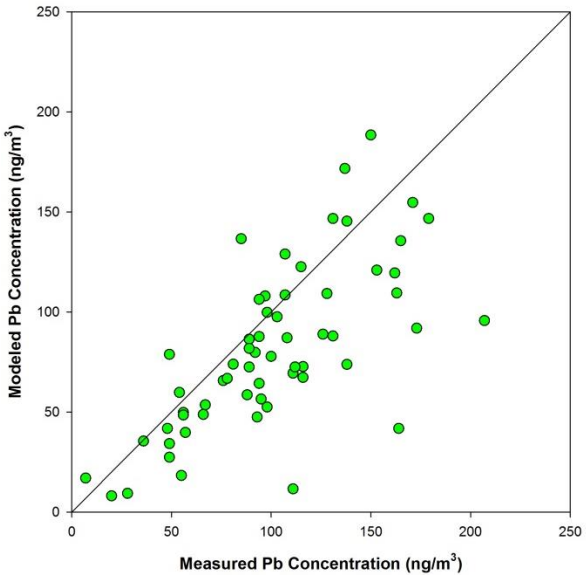

Figure 5-6 Measured and modeled daily Pb concentrations at PAO, calendar year 2013. Measurements data are from compliance monitoring at PAO conducted by the Bay Area Air Quality Management District.

adjustments would be expected. The modeled results again agree well with measured concentrations. Table 5-1 shows several performance statistics comparing the modeled values with the measured concentrations (the metrics are defined in Chapter 4). Based on the ratio of means, modeled results were 20% low compared to measured values at PAO. The fraction of modeled values within a factor of two of the measured values (FAC2) was 88%, higher than both RVS and SMO. The normalized mean square error (NMSE) was less than 0.2 and approximately 70% of that error was from the contribution of random error. Overall, the model to monitor agreement was very good, especially considering there was no day-specific on-site activity data as was available for RVS and SMO, requiring the scaling of ATADS data. The fact that winds used for modeling were from Moffett Field and not PAO, as well as using 2015 avgas Pb content data to estimate 2013 avgas levels could contribute to the differences observed between the modeled and monitored concentrations. Background correction would also move the data toward the 1:1 line but likely only to a small degree.

Figure 5-7 shows the 3-month average modeled concentrations at RVS (a), SMO (b) and PAO (c). The three-month average concentrations are consistent with NAAQS averaging times. Since only the year 2013 was modeled, the 3-month periods of November-January and December-February were calculated using January and February 2013 modeled concentrations. Concentrations are highest during the winter months at all three airports because of relatively weaker dispersion characteristics. These concentrations serve as a base case for evaluating the mitigation strategies.

Table 5-1 Performance Measures for Comparing PM-Pb Model Predictions to Measurements

Performance Measure	PAO, Year 2013
Number of Samples	60
Mean $PM_{2.5}$-Pb, ng/m^3	
– Measured	101
– Model Predicted	81
FAC2	0.88
Fractional Bias, FB	0.22
Ratio of Arithmetic Means	0.80
Normalized Mean Square Error, NMSE	0.18
– NSME systematic error contribution	0.05
– NSME random error contribution	0.13

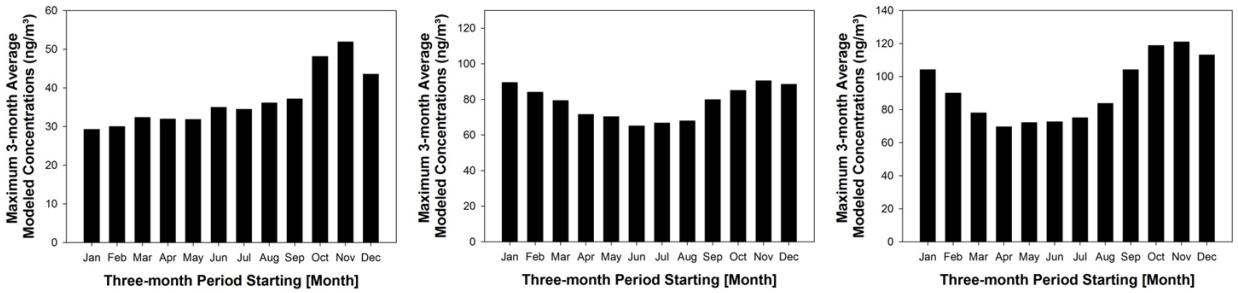

Figure 5-7 Year 2013 three-month average modeled concentrations at (a) RVS, (b) SMO, and (c) PAO. Note since only 2013 was modeled, the 3-month periods of November to January and December to February, were calculated using January and February 2013 modeled concentrations.

5.3.2 Modeled Impacts from Moving Runup Areas

Impacts for the year 2013 were modeled using the EPA's AERMOD modeling system. To be consistent with the Pb NAAQS, three month rolling averages were calculated from the hourly modeling results. At RVS the highest three-month average occurred for the period

November to January and Figure 5-8 shows these three-month average concentration fields for the: (a) base case scenario of using the original runup areas; (b) Z1 runup areas; and (c) Z2 runup areas. The highest concentrations modeled at RVS for these scenarios are dominated by maintenance-related engine testing emissions in the southwest portion of the airport. These emissions were observed a limited number of times that coincided with runup data collection during the on-site data collection period. They were not observed during other activity collection periods and are likely not representative over a full year. Thus, the modeling was repeated with these emissions set to zero.

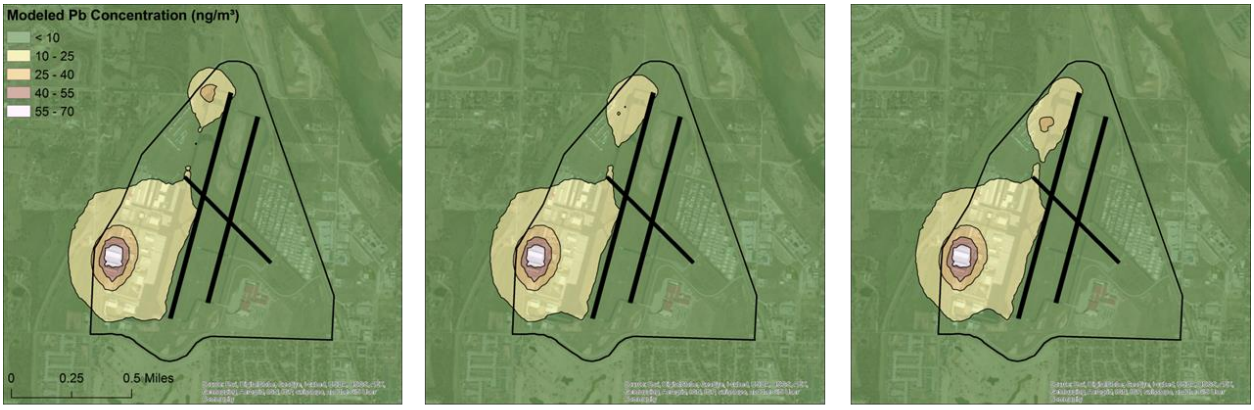

(a) (b) (c)

Figure 5-8 Modeled three-month average concentrations from November-January at RVS using the: (a) original runup areas; (b) Z1 runup areas; and (c) Z2 runup areas. The large hotspot in the southwest corner of the footprint is from engine testing emissions.

Figure 5-9 shows these three-month average concentration fields at RVS with the engine testing emissions removed for the: (a) base case scenario of using the original runup areas; (b) Z1 runup areas; and (c) Z2 runup areas. (Note the contour color scales for Figures 5-8 and 5-9 are different.) The NW runup area had the highest concentrations after engine testing emissions were zeroed out and the highest modeled concentration in this area was 52 ng/m^3 for the base

(a) (b) (c)

Figure 5-9 Modeled three-month average concentrations from November-January at RVS with engine testing emissions removed using the: (a) original runup areas; (b) Z1 runup areas; and (c) Z2 runup areas. Engine testing emissions were excluded from this analysis.

case scenario Figure 5-9a). Concentration fields were also modeled for the counterfactual of all runup area emissions. removed – the best case scenario – and in this case the maximum concentration near the NW runup area was 22 ng/m^3. When runup emissions were moved to the Z1 runup areas, the maximum near the NW runup area was 36 ng/m^3, which is 53% of the maximum possible reduction that would be achieved by completely removing runup emissions. When the runup emissions were moved to the Z2 areas, the maximum around the NW runup area was 48 ng/m^3 which is only 13% of the maximum possible reduction. One possible explanation for this concentration rebound could be that moving to the Z2 areas moves the NW runup area closer to a zone with higher density of taxiways and taxiway emissions. Moving the runup areas inward along the runways also increased the total area with modeled concentrations over 10 ng/m^3; however, given the reduction in maximum modeled impacts, these results suggest that there could be substantial benefit to moving the runup areas to the Z1 locations if the base case hotspot concentrations – which are about 1/3 of the Pb NAAQS of 150 ng/m^3 - were of concern. Concentrations are much higher along the western runway because it is the primary runway used

for conventional takeoffs and landings. The eastern runway is generally used for flight training with planes performing touch-and-gos and taxibacks which do not include runups. More than 90% of takeoffs with associated runups were attributed to the western runway.

The highest base-case three-month rolling average hotspot concentration at SMO was observed for November- January with a Pb concentration of 90 ng/m^3, 60% of the Pb NAAQS. Figure 5-10 shows the concentration field for this three-month average for the: (a) base case scenario of using the original runup area; (b) Z1 runup area; and (c) Z2 runup area. When runup emissions were completely removed, the maximum modeled concentration fell to 58 ng/m^3. Moving runup areas 80 meters to the southwest of the original runup area decreased the three-month average maximum concentration to 68 ng/m^3, which is 69% of the maximum possible reduction by removing runup emissions. Moving the runup emissions to Z2 further reduced the maximum three-month average concentration to 65 ng/m^3, or 78% of the maximum possible reduction. The effect of moving the runup areas incrementally farther away from their original positions diminished quickly because the relative impact of runup emissions is reduced, compared to other airport sources, with increasing distance. In addition to reducing the

(a) (b) (c)

Figure 5-10 Modeled three-month average concentrations from November-January at SMO using the: (a) original runup areas; (b) Z1 runup areas; and (c) Z2 runup areas.

maximum modeled concentration, moving the runup area away from the airport fenceline also reduced the size of the area outside the airport footprint exposed to higher airport impacts.

At PAO the highest modeled three-month rolling average hotspot was observed for November-January with a Pb concentration value of 121 ng/m^3 which is 80% of the Pb NAAQS. Figure 5-11 shows the concentration field for this three-month average for the: (a) base case scenario of using the original runup area; (b) Z1 runup area; and (c) Z2 runup area. Contributions to the base case Pb maximum concentration were 55% from taxiways, 26% from takeoffs, and only 8% from runups. Thus, moving the runup area has only modest effect on the base case hotspot maximum concentration. The counterfactual of no runup emissions was also illustrates this feature, resulting in maximum modeled concentration of 113 ng/m^3 which is only 8 ng/m^3 less than the base case maximum concentration. When the runup emissions were moved 50 meters to the southwest of the original runup area, the three-month average maximum concentration decreased to 114 ng/m^3, which is 88% of the maximum possible reduction by removing runup emissions. Moving the runup emissions to Z2, 100 meters away from the original location, further reduced the maximum three-month average concentration to 113 ng/m^3,

(a) (b) (c)

Figure 5-11 Modeled three-month average concentrations from November-January at SMO using the: (a) original runup areas; (b) Z1 runup areas; and (c) Z2 runup areas.

or 100% of the maximum possible reduction. It is important to note that moving the runup areas also moves the location of some taxiing and idling emissions, so there are additional, but small, reductions in impacts from taxiing at the location with maximum modeled concentration.

5.3.3 Modeled Impacts from Using MOGAS

At RVS approximately 45% of the activity-weighted piston-engine landing and takeoff fleet had aircraft models and engines certified to use MOGAS. Much of this was because of flight schools with certified aircraft performing multiple operations per day. When accounting for aircraft that can use MOGAS, the maximum 3-month average at RVS decreased by 35% from 52 ng/m^3 to 34 ng/m^3. The total reduction was less than the fraction of aircraft because the aircraft certified to use MOGAS tended to have lower overall fuel burn rates. Figure 5-12 shows the 3-month average modeled concentrations around the RVS airport for the November-January averaging period (the period with the highest modeled 3-month average concentration) for the base-case scenario (a) and the scenario using MOGAS (b). For this analysis, the aforementioned

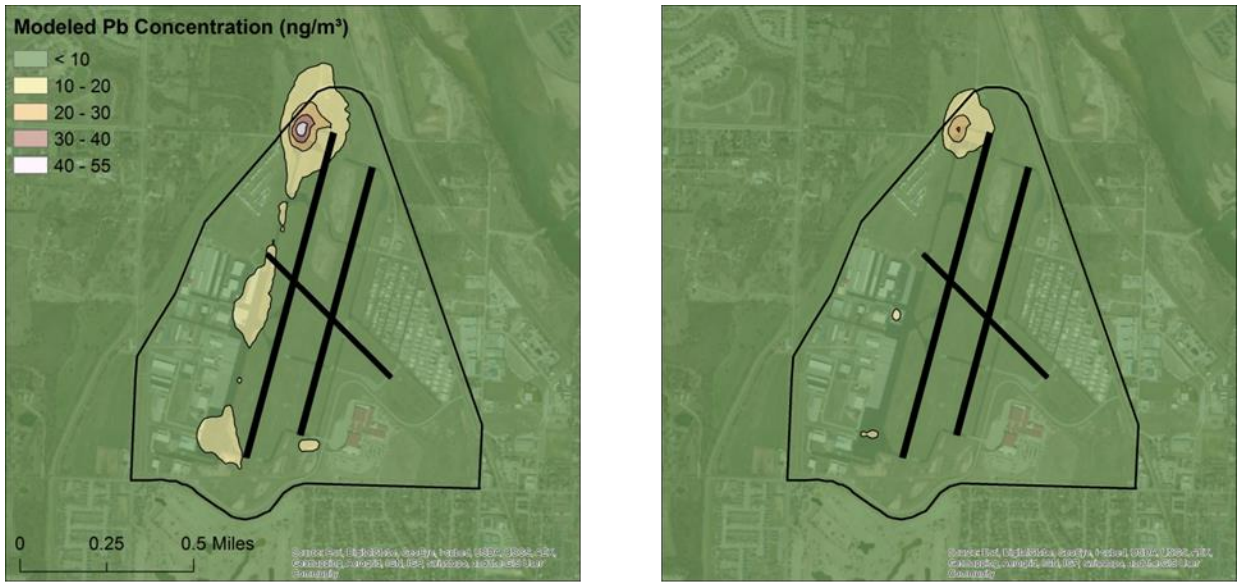

(a) (b)

Figure 5-12 Modeled three-month average concentrations from November-January at RVS using the base case (a) and MOGAS (b) scenarios.

maintenance engine testing emissions were set to zero. In addition to reducing the maximum hotspot concentration, the replacement of avgas with MOGAS also significantly reduced the total area with modeled concentrations greater than 10 ng/m^3.

Approximately 30% of the activity-weighted piston-engine landing and takeoff fleet at SMO had aircraft models and engines certified to use MOGAS. Figure 5-13 shows the 3-month average modeled concentrations at and around the SMO airport for the November-January averaging period (the period with the highest modeled 3-month average concentration) for the base-case scenario (a) and the scenario using MOGAS (b). The maximum 3-month average fell from 90 ng/m^3 to 73 ng/m^3, a 20% reduction, when removing Pb emissions of aircraft that can use MOGAS. Again, the total reduction was less than the fraction of aircraft because the aircraft certified to use MOGAS tended to have lower overall fuel burn rates. Furthermore, the replacement of avgas with MOGAS also significantly reduced the total area with modeled concentrations greater than 10 ng/m^3.

Figure 5-13 Modeled three-month average concentrations from November-January at SMO using the base case (a) and MOGAS (b) scenarios

At PAO about 35% of the activity-weighted piston-engine landing and takeoff fleet had aircraft models and engines certified to use MOGAS. When accounting for aircraft that can use MOGAS, the maximum 3-month average fell from 121 ng/m^3 to 84 ng/m^3, a 30% reduction. Again, the total reduction was less than the fraction of aircraft because the aircraft certified to use MOGAS tended to have lower overall fuel burn rates. Figure 5-14 shows the 3-month average modeled concentrations around the RVS airport for the November-January averaging period (the period with the highest modeled 3-month average concentration) for the base-case scenario (a) and the scenario using MOGAS (b). In addition to reducing the maximum hotspot concentration, the replacement of avgas with MOGAS also significantly reduced the total area with modeled concentrations greater than 10 ng/m^3, as well as impacts that extend beyond the airport boundary.

Figure 5-14 Modeled three-month average concentrations from November-January at PAO using the base case (a) and MOGAS (b) scenarios.

5.4 Conclusions

Hourly Pb concentrations for the full year 2013 were modeled using AERMOD and the emission inventory development described in Chapter 4. Model performance was previously evaluated for RVS and SMO, with models agreeing well with on-site airborne Pb measurements. Data collection was performed at an additional airport, PAO, and full year 2013 Pb concentrations were modeled using the methodology outlined in Chapter 4. Modeled concentrations agreed very well with on-site measured concentrations, which is especially encouraging because activity data collection did not coincide with the Pb measurement time period.

The models set up for each of the airports were used to evaluate potential impacts from moving aircraft runup areas. Figure 5-15 shows the maximum 3-month average concentrations at RVS (a), SMO (b) and PAO (c) for the base case, Z1 and Z2 scenarios. Concentrations for all three scenarios are highest during the winter months at both airports with the period November

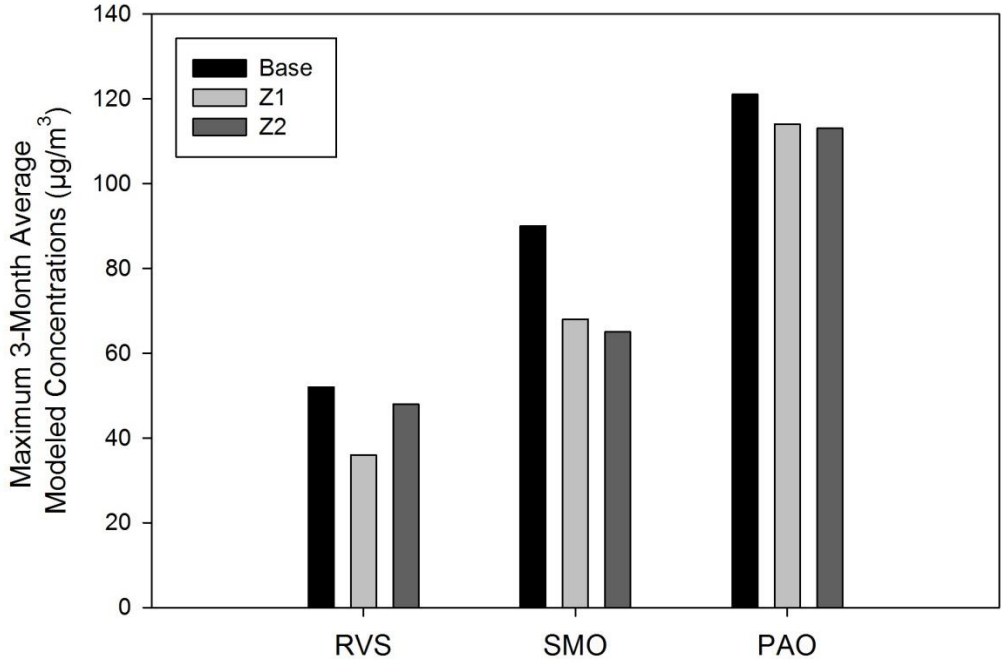

Figure 5-15 Maximum 3-month average concentrations at each airport for different runup area locations.

to January having the highest modeled concentration for all three airports. The effectiveness of moving the runup areas varies by airport. RVS and SMO could potentially see reduction of about 30% in the maximum hotspot concentration, while PAO would only see a reduction of about 8%. Therefore, moving runup areas as a means to reduce Pb hotspot concentrations must be evaluated on an airport-by-airport basis.

It is also important to consider other airport activity when evaluating moving runup areas. As seen in the RVS modeling, moving the runup areas farther away from the runway ends eventually resulted in bringing maximum hotspot concentrations closer to original levels because runup emissions mix with emissions from other busy taxiways. It is also important to note that runup areas are located close to runways in part to reduce noise near airport hangars. The noise impacts of moving the runup areas should also be an important consideration.

At each airport evaluated in the study, replacing avgas in aircraft certified for MOGAS use resulted in significant reductions in modeled maximum Pb concentrations (20% - 35%). Since using MOGAS will reduce Pb emission in all phases of aircraft operation, the entire airport footprint will have reduced Pb concentrations as a result of its use. This is also very useful in reducing impacts that extend outside of airport footprints. Therefore, most general aviation airports should experience significant reduction in Pb concentrations when replacing Avgas with MOGAS when possible. However, some airports may have other characteristics requiring the use of avgas, such as being at high elevation. The cost of adding another fuel storage and distribution system also must be considered.

Since no level of Pb is considered safe, any reduction in Pb concentrations should be considered a benefit. There are other approaches that could also reduce Pb concentrations including modifying pilot and airport traffic behavior in order to reduce airport congestion and

time spent idling. The modeling in this work shows that both moving runup areas and using MOGAS instead of avgas when practicable can potentially result in significant Pb concentration reductions. The economic implications of making these changes are also an important consideration. The results of this study will be used to inform and complement an economic assessment that will be used to determine the feasibility of these mitigation strategies.

5.5 References

"Approved Engines & Airframes." 2015. Accessed October 27, 2015. http://www.autofuelstc.com/approved_engines_airfames.phtml.

"Approved Engine Models for Autofuel Use." 2006. Accessed October 27, 2015. https://www.eaa.org/en/eaa/aviation-communities-and-interests/pilot-resources/auto-fuel-stc/approved-engine-models.

Carr, E., M. Lee, K. Marin, C. Holder, M. Hoyer, M. Peddle, R. Cook and J. Touma. (2011). "Development and evaluation of an air quality modeling approach to assess near-field impacts of lead emissions from piston-engine aircraft operating on leaded aviation gasoline." Atmospheric Environment **45**(32): 5795-5804.

FAA. *Press Release – FAA Selects Fuels for Testing to Get the Lead out of General Aviation Fuel. 8 Sept. 2014. Web. 26 Oct. 2015*

"Lead Poisoning and Health" 2015. Accessed October 9, 2015. http://www.who.int/mediacentre/factsheets/fs379/en/

"Leaded Aviation Fuel and the Environment" (Fact Sheet), the Federal Aviation Administration, June 2013.

U.S. EPA. 2015. *Program Overview: Airport Lead Monitoring* (4 pp, EPA-420-F-13-003, January 2015) http://www.epa.gov/otaq/regs/nonroad/aviation/420f13032.pdf

5.6 Supplementary Material

5.6.1 Aircraft Activity Data Collection at PAO

Detailed aircraft activity data were collected to inform the development of a spatially and temporally resolved emissions inventory. These data have been processed and compiled into databases (e.g., MS Excel spreadsheets). The key data collection elements are summarized below.

- Landing and Takeoff Operations (LTOs) – LTOs were manually observed by the data collection team for a total of 98 hours at PAO. Data collection was scheduled to capture a range of conditions (time of day, day of week). . LTO data were collected for all fixed-wing aircraft. Each observed LTO operation was categorized as a landing, regular takeoff, taxiback takeoff, or touch and go.
- Aircraft Fleet Inventory – Aircraft frame and engine characteristics were collected concurrently with the LTO data collection. The aircraft tail ID was observed for each operation and the FAA Registry (*http://registry.faa.gov/aircraftinquiry/*) was used to identify the aircraft and engine model for each observed tail ID. Aircraft and engine model were paired with the activity type from the LTO data collection to establish different fleet characterizations for discrete and continuous operations. Data were collected for all aircraft, not just piston-engine aircraft, to provide information about the distribution of activities between piston-engine airplanes and turboprops. Because of its small size, there are not jet aircraft used at PAO. Some aircraft were observed multiple times over the entire period of data collection. Given the objective to inventory the fleet from an operations perspective, each observation was an independent entry into the

database. Each database record includes: the observation time stamp; aircraft type, manufacturer, model, year, and number of engines; engine type, manufacturer, model, and horsepower; and number of times the aircraft was identified in the one-hour observation period and in the overall data set. Tail ID numbers were removed from the final database.

- Time in Mode for Runup – Runup operations were manually observed for 19 hours at PAO; however, 6 hours of data collection were lost because of corrupt data files, resulting in 13 hours of useable data. Data collection was scheduled to capture a range of conditions (time of day, day of week) and included the time aircraft spent in a runup area (visual observation), the duration of the magneto test (audible changes in engine noise during runup), and the aircraft tail ID. Some planes bypassed the runup area prior to takeoff and such instances were recorded. In some cases, the magneto test duration could not be determined because of confounding sources of noise. Each record in the database includes the data collection hour, total runup time, magneto test time, and the aircraft attributes listed above for the aircraft fleet inventory.

- Time in Mode for Other Activities – Additional piston-engine aircraft activities such as taxiing, takeoffs, and landings were manually observed for 17 hours at PAO. Data collection was scheduled to capture a range of conditions (time of day, day of week). The observation point was chosen to maximize viewing of the entire airport footprint. Activities were tracked by aircraft and recorded by runway or taxiway. For example, a taxi-back would consist of the following data: landing time (time on runway between wheels down and turning onto taxiway); time taxiing and idling on each taxiway; and takeoff time (time on runway between starting rollout and wheels-up). Approach and

climb-out times could not be adequately captured because of the difficulty in establishing aloft locations for the start of approach and end of climb-out. Instead, wheels-up and wheels-down locations on the runways were recorded to inform the development of TIM estimates for climb-out and approach and to spatially allocate runway emissions. TIM for touch-and-go operations was recorded as the time between wheels down for the landing portion and wheels-up for the takeoff portion. Each record in the database includes a plane identifier (arbitrary), activity (e.g., landing, takeoff, taxiing, idling), and location (e.g., taxiway ID).

Activity data processing was conducted in coordination with the Sierra Research staff. LTO, fleet and TIM data were processed by the WUSTL field operators (Neil Feinberg and Chris Peng) with QA/QC performed by the WUSTL lead investigator (Jay Turner).

Aircraft activity data collection at PAO is summarized in Table 5-2. Figure 5-16 shows the hourly distribution of total operations for piston-engine aircraft as determined from the on-site observations. Touch-and-go activities are counted as two operations each and are distinguished from normal takeoffs and landings. Over the study period there were, on average, 19 operations per hour. Total operations peaked between 10 AM and 12 PM and again at 3 PM. The lowest levels of activity were in the early morning and late evening.

Observed tail numbers were matched to aircraft and engine specifications in the FAA registry. The resulting fleet inventory database includes a record for each operation but no tail numbers. Over the 98 hours of observation, 341 unique aircraft were identified. Fourteen aircraft (4%) accounted for one-third of the operations and 25 aircraft (7%) accounted for half of

Table 5-2 PAO aircraft activity data collection

Date	Activity Data Collection		
	ID	TIM	Runup
7/24/2015	7	0	0
7/25/2015	9	0	0
7/26/2015	9	1	0
7/27/2015	9	0	1
7/28/2015	13	2	0
7/29/2015	8	0	1
7/30/2015	9	0	0
7/31/2015	8	2	0
8/1/2015	8	0	2
8/2/2015	10	0	0
8/3/2015	8	0	0

ID = LTO type and aircraft identification; TIM = time-in-mode data collection; and Runup = run up area activity data collection including TIM for magneto testing.

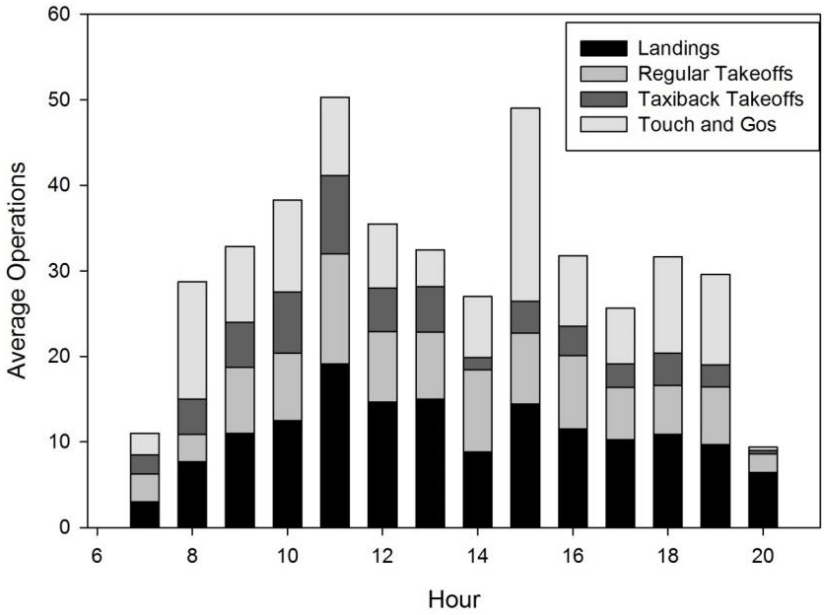

Note: Based on 98 hours of observations.

Figure 5-16 Hourly average operations at PAO.

the operations. Table 5-3 summarizes the distribution of LTOs by aircraft type; 95% of the operations were single-engine piston aircraft.

Table 5-3 Distribution of aircraft types identified by Tail ID at PAO

Plane Type	Count	% of Total
Piston		
Single Engine	2625	95%
Multi Engine	87	3%
Turboprop	54	2%

Table 5-4 and Figure 5-17 summarize the runup results. Mean TIM values were 47 seconds for the magneto test and 276 seconds for the total time in the runup area. There was large variation in these times, with standard deviations of about 70% and 60% of the means for total runup and magneto testing, respectively. Total runup and magneto test TIM data are shown as box plots in Figure 5-17(a) and cumulative distributions in Figure 5-17(b). Both total runup time and magneto test duration data are approximated relatively well by a lognormal distribution as evidenced by the nearly linear trend for the log-probability plot. This means that a few aircraft have much longer TIM than would be expected from the standard deviations about the mean times.

TIM data were also manually collected for piston-engine aircraft taxiing, idling, landings, and takeoffs. Seventeen hours of operations were viewed from the airport tarmac. Table 5-5 shows summary statistics for landing, takeoff, and touch-and-go times, as well as average locations for wheels-up and wheels-down. Runway 31 was used almost exclusively, and all times and distances reflect activity only on this runway. TIM for touch-and-go operations

Table 5-4 Time-in-mode data collected for runup perations at PAO

	Total Run-Up	Magneto Testing
Number of Aircraft	69	64
Mean ± Std Dev (sec)	276 ± 189	47 ± 27
Median (sec)	221	40

Notes: Based on 13 hours of data collection. Means are reported with 1σ standard deviation values.

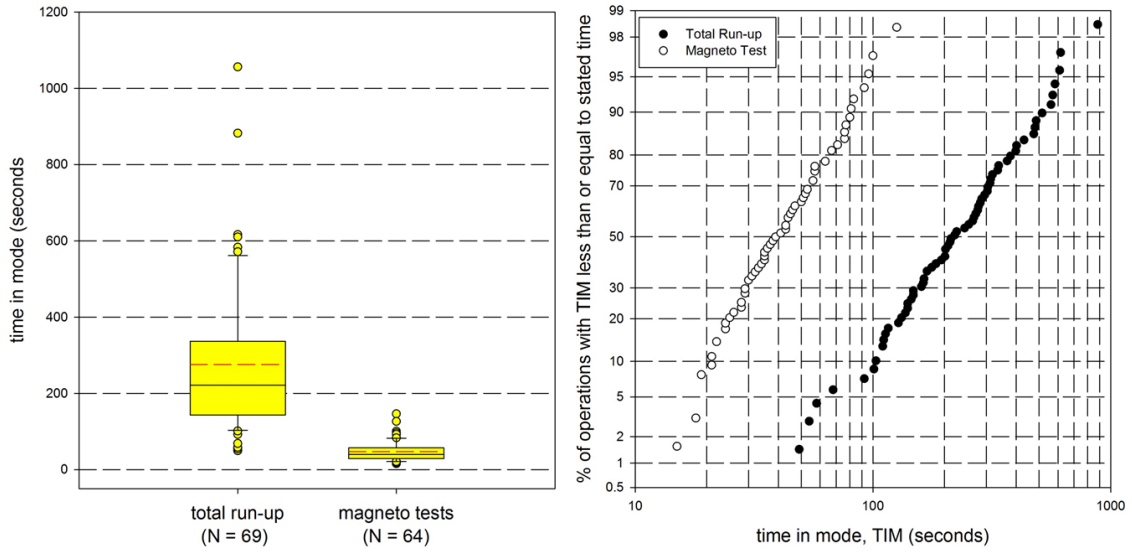

(a) (b)

Notes: (a) box plots (interior solid line is the median, interior dashed line is the arithmetic mean; box boundaries are 25th and 75th percentiles, whiskers are 10th and 90th percentiles, and circles are all records below the 10th percentile and above the 90th percentile); and (b) cumulative distributions as a log-probability plot.

Figure 5-17 Time-in-Mode data for total time in the run-up area and duration of magneto testing at PAO test presented as box plots (a) and cumulative distributions as a log probability plot (b). For the box plots the interior solid line is the median, interior dashed line is the arithmetic mean; box boundaries are 25th and 75th percentiles, whiskers are 10th and 90th percentiles, and circles are all records below the 10th percentile and above the 90th percentile.

Table 5-5 Summary of Time-in-Mode and Location of Aircraft Landing and Takeoff Operations at PAO

Activity/Location	Mean Time (s)	Std. Dev (s)	Mean Wheels-Up (ft.)	Mean Wheels-Down (ft.)
Landing	21	9	-	558
Takeoff	17	29	774	-
Touch-and-Go	20	38	1531	556

Notes: Based on 17 hours of data collection. TIM means are reported with 1σ standard deviation values. "-" indicates no data.

represent the time between wheels-down on landing and the subsequent wheels-up on takeoff. Wheels-up and wheels-down locations are measured as the distance from the start of the runway. There is less variation in TIM for landing and takeoff activities than for runup activities. Activities were logged by aircraft so trip-based times can be constructed. Similar TIM data collection and processing has been performed for other aircraft activities, such as taxiing and idling, and the data are included in the database.

Chapter 6: Summary, Implications and Recommendations

6.1 Summary

This dissertation has significantly advanced the state-of-knowledge concerning piston-engine aircraft Pb emissions and impacts within and near general aviation airports. An initial approach used the FAA's Emission and Dispersion Modeling System (EDMS), with workarounds, to model Pb concentrations at Centennial Airport. Modeling was conducted using daily total aircraft operations with engineering assumptions for the remaining parameters needed to estimate emissions and to spatially and temporally allocate these emissions. EDMS does not include runup operations and emissions by default, so they were modeled as a volume source with the emission rate used as an adjustable parameter to fit the modeling results to daily-average concentrations measured at a single location on-site. The day-to-day agreement was poor but this approach did adequately capture the *distribution* of observed concentrations which is a metric commonly used to evaluate dispersion modeling performance especially in the absence of detailed information to temporally allocate emissions. Subsequent work, however, demonstrated this approach to be inferior. Several assumptions, including but not limited to the spatial allocation of aircraft activities, were determined to be biased based on the on-site activity data that were later collected. These biases were aggregated into the adjustable parameter and to a significant extent resulted in getting the right answer for the wrong reasons.

A comprehensive study with the objective of a better understanding of Pb emissions and concentrations was conducted at three airports across the United States. On-site activity data and Pb concentrations were measured at RVS, APA and SMO. Each of these airports has their own distinguishing features in terms of airport layout and meteorology. Samples collected at each

airport were analyzed for Pb by ICP-MS. A subset of samples was also analyzed by XRF. At each of the three airports, elevated Pb concentrations were measured when sampling was conducted directly downwind of airport operations. Pb and Br were be highly correlated at the high-impact sampling sites. This is consistent with Pb originating from the tetraethyllead avgas additive. Conversely, poor correlation was observed at low impact sites. Also, poor correlation was observed between Pb and crustal elements (silicon and calcium), suggesting little contribution from resuspended soil. Pb isotopic compositions were also analyzed by ICP-MS. The Pb isotopic compositions for PM samples collected at sites with expected high impact from aircraft emissions are distinct from those for samples collected at sites with expected low impacts. Furthermore, Pb isotopic compositions for the high-impact sites are consistent with avgas samples collected at the airports, while the isotopic compositions for the low-impact sites are generally consistent with resuspended soil samples collected at the airports.

The site-specific activity data collected at these airports were used to develop an emission inventory and modeling framework to determine Pb impacts at general aviation airports. Activity data collection included aircraft fleet characterization, hourly activity counts and time-in-mode data for ground-based airport activities. These activity data were used to develop a spatially and temporally resolved emissions inventory, and Pb concentrations were modeled using AERMOD. Modeled concentrations were compared to the measured samples and evaluated for accuracy. Quantitative performance metrics determined the modeling results to be acceptable at all three airports, and excellent at RVS and SMO. Modeled results were biased significantly high at APA, compared to measured concentrations. Runup areas, taxiways, and takeoffs were the dominant contributors to Pb hotspot formation. Pb hotspots typically formed when all three of these activities occurred within short distances of each other, usually near the runway ends. The

compactness of these activities near the runway ends leads to mixing of emissions from the source groups and the formation of hotspots. This highlights the importance of the spatial allocation of airport activities for modeling Pb concentrations. It also highlights that airports with compact size might have more issues with high concentrations, even though their total activity levels and emissions may be lower than other, larger airports.

The activity data collection, emission inventory, and modeling framework developed at RVS, APA, and SMO was applied to another airport, PAO. This airport was chosen because on-site Pb measurements required by the EPA found Pb concentrations greater than half the NAAQS. Modeled concentrations at PAO were in excellent agreement with measured concentrations, especially considering only two weeks of activity data collection was used to build the model. The modeling framework was then used to evaluate two potential mitigation strategies - moving runup areas and using motor vehicle gasoline (MOGAS) in aircraft that have been certified to use it. The effectiveness of moving the runup areas varied by airport. RVS and SMO would experience a reduction of peak hotspot concentrations by about 30%, while PAO would see a smaller reduction of less than 10%. Moving runup areas must be evaluated on an airport-by-airport basis. Replacing avgas in aircraft certified for MOGAS use resulted in significant reductions in modeled maximum Pb concentrations (20% - 35%). Using MOGAS instead of avgas also reduced Pb concentrations across the entire airport footprints. This strategy is also very useful in reducing impacts that extend to and across airport boundaries.

6.2 Implications and Recommendations

1. *Use of FAA Tools*. EDMS serves as an accessible tool for most instances of air quality modeling of airport operations. However, it is generally designed to be used at commercial airports and for pollutants associated with jet emissions. It does not include settings for Pb and

thus required user modification to develop the Pb emission estimates. Additionally, it does not include runup operations as part of aircraft activity. As shown in this work, runup emissions can be a critical contributor to Pb hotspots. It should be noted that in mid-2015, the FAA released to the public a new tool called the Aviation Environmental Design Tool (AEDT). AEDT combines EDMS with existing noise modeling tools. It also now allows for the creation of runup events. However, there is still no option for performing Pb modeling within the tool's default framework.

Despite the aforementioned constraints on using EDMS to model Pb at general aviation airports, compounded by the lack of detailed aircraft activity data available for the initial study, it was able to capture the *distribution* of daily-average Pb concentrations at a single on-site monitoring location when using the runup emission rate as an adjustable parameter. However, subsequent work, including but not limited to the on-site data collection, revealed several errors in the assumptions used to estimate emissions and to spatially allocate the emissions. The good model-to-monitor agreement at a single site on the airport footprint was, to a large extent, obtained for the wrong reasons. Insights gained while conducting the modeling with EDMS suggest that it would be possible to use EDMS/AEDT, ideally with modifications to the program but if not then with workarounds, to generate meaningful Pb concentration fields within and near general aviation airports if on-site activity data are collected to inform the modeling. Given that the use of EDMS/AEDT would greatly simplify the air quality modeling effort compared to using the native AERMOD model, it would be instructive to conduct modeling with EDMS/AEDT for RVS, SMO, and perhaps PAO, using the on-site activity data and other airport information presented in this dissertation. The results should be critically evaluated to determine

whether this is a feasible approach for estimating Pb concentration fields at general aviation airports.

2. *Airport Pb Measurement and Characterization.* The measurements presented in this dissertation represent the most comprehensive evaluation of Pb at airports to date. Br concentrations measured by XRF correlated well with Pb measurements, strengthening the connection between measured Pb and avgas additives. Examining Br in concert with Pb could serve as a useful tool for determining if measured Pb is associated with avgas, potentially even outside airport boundaries. However, Br is volatile and its ratio to Pb could vary considerably based on particle residence time, sampling condition, and post-sampling storage and transport. If Br is to be examined together with Pb, care should be taken to reduce possible volatile losses of Br, including quick sample retrieval and cold storage of samples, as was done in this study.

Pb isotope ratios were also found to strengthen the connection between measured Pb concentrations and airport emissions. Samples with expected high impacts from aircraft activities had isotope ratios more similar to the Pb in the tetraethyllead avgas additive than to local soil, even with potential aircraft exhaust Pb deposition to the soil. Pb isotope ratios measured at each of the three airports in this study generally fall along a two source mixing line with avgas Pb and soil Pb constituting the end members of the mixing line. This study did not utilize a high resolution ICP-MS so the isotope ratio variability was too high to perform quantitative source apportionment based on distance from the mixing line end members. However, sample analysis using a high resolution ICP-MS should provide high quality isotope ratios that could be used for quantitative apportionment of Pb to avgas combustion. This could be another tool for evaluating the contribution of aviation to Pb concentrations near general aviation airports.

The measurements conducted in this study required modeling to place the full impact of aviation Pb emissions into context. This is in most part because of the steep concentration gradients at Pb hotspots. At PAO, modeled concentrations reduced to just one-third of the highest concentration as close as 100 meters away. Concentration gradients have been studied, in part, at McClellan-Palomar Airport. However, a fine scale (within few hundred meters of maximum expected concentration areas) evaluation of these steep gradients by collecting multiple measurements within an expected Pb hotspot would provide a more complete understanding of Pb at airports. It could also help to either validate, or suggest potential improvements to, modeling of Pb emissions.

3. *Collecting and Using On-site Activity Data.* On-site activity data collection was a critical part of the work performed for this dissertation. It was necessary for both the development of a Pb emission inventory for airports and also provided details needed to perform the spatial and temporal allocation of emissions required for air quality modeling. The data collection and model development also highlighted which types of data were most important to collect in order to better understand airport Pb impacts. Key data collection requirements identified in this work include avgas Pb content, aircraft frame and engine characterization, hourly distribution of airport operations, fraction of continuous operations (touch and gos, taxibacks), time spent idling and taxiing on specific taxiway segments, time spent landing and taking off, and time spent idling and performing magneto tests in runup areas. It should be noted that at PAO, all of this data was collected over an 11 day period by only two people, and these data were enough to develop a model that generated Pb concentrations in good agreement with concentrations measured for a separate period with only daily total aircraft operations and hourly winds data available for the day-specific modeling.

4. *Modeling Airport Pb Emissions.* This dissertation includes modeling of Pb concentrations at four different airports. Modeling at three of the four airports showed excellent comparison with measured Pb concentrations, and the results for the other airport were acceptable based on conventional model performance metrics. The model results at PAO were particularly encouraging because the data used to set up the model was collected over a relatively short period of time, and the model was set up for a different time period than the activity data collection. Concentration gradients within the hotspots have not been directly measured and thus modeling is currently the basis for estimating the spatial extent of hotspots. Single monitoring locations can miss the highest concentrations and, given the sharp gradients, can grossly misrepresent exposures to those living or working around airports. Additionally, since the highest concentrations are found in areas with multiple sources (runways, runup areas, etc.) modeling provides the ability to determine which of these sources have the most influence.

This modeling framework can serve as a useful tool for airports and environmental agencies. While the application of the methodology to every airport is not feasible, it can be applied to individual airports where the magnitude and spatial extent of Pb impacts are of interest. It could also be used when an airport is a part of a health study that may include Pb effects. While this study did not model any concentrations that were greater than the NAAQS for Pb, the results did show Pb impacts elevated above background levels that extended beyond airport boundaries and into public space. No amount of Pb is considered safe, and modeling can provide an estimation of Pb concentrations that could be correlated to health effects and blood-Pb levels.

The framework would also be useful for siting regulatory monitors. Currently, EPA monitors are often located within steep hotspot gradients and/or in areas not accessible to the

public. For instance, the monitor at APA requires both a gate card and an escort to access. The combination of these two issues has the potential to misrepresent public exposures, as a monitor even tens of meters away from public space could sample concentrations that are significantly higher than those in the public area. Modeling using this methodology could be used to inform the appropriate siting of monitors that are in both public space and areas of elevated Pb concentration.

5. *Evaluating Mitigation Strategies.* The modeling framework described in this dissertation allowed for the evaluation of two potential Pb mitigation strategies. Those strategies were moving runup areas away from runway ends in order to reduce maximum hotspot concentration and using MOGAS instead of avgas in certified aircraft. The effectiveness of moving runup areas varied by airport. This suggests that in the future, the strategy of moving runup areas should be evaluated on a case-by-case basis. At RVS and SMO, moving the runup areas away from the runway ends resulted in significant reduction in maximum hotspot concentrations. At PAO, moving runup areas had only an incremental effect. While moving runup areas does have the potential to reduce the magnitude of hotspots, it does not reduce total Pb emissions. Additionally, moving the runup areas also increases the total area with elevated Pb concentrations and in some cases could potentially impact more people.

All three airports saw significant benefits in modeled Pb concentrations when replacing leaded avgas with unleaded MOGAS. The use of MOGAS also has the additional benefits of reducing Pb emissions for all aircraft activity modes and locations within an airport. This helps to reduce total potential exposure to Pb both within and outside of airport boundaries. Most airports should see significant benefits of using MOGAS when available. Some airports may have operational constraints on the use of MOGAS, for instance if they are at high elevation and

require the lower volatility of avgas compared to MOGAS. An economic analysis of these mitigation strategies is needed to determine their viability. While there is now an effort to develop unleaded avgas, its final development and implementation will take several years. Therefore, the information presented in this thesis should remain relevant to airport operations for the foreseeable future. More broadly, this dissertation demonstrates a systematic approach to refining the assessment of air quality impacts from facilities with complex and generally ill-characterized operations.

Appendix A: Identification of Emission Source Regions Using Nonparametric Trajectory Analysis

A.1 Introduction

Air quality impacts and meteorology are inherently linked. Coupling emissions with meteorology is the fundamental principle behind dispersion modeling. Similarly, coupling measured concentrations at receptors and meteorology can result in the identification of possible emission source locations. The simplest wind-based receptor model is a "pollution rose" which is a polar plot with a series of barbs that represent the average concentration at the receptor for winds from a given sector. A major limitation of the pollution rose is the subjectiveness in choosing the range of each wind direction sector (e.g. 10°, 15°, 20°…). Nonparametric wind regression (NWR) was developed about ten years ago as a tool that addresses some of the inherent limitations of the pollution rose (Henry et al. 2002). One-dimensional NWR estimates the expected concentration from a given wind direction, θ, by calculating a weighted average of measured concentrations, C_i, paired with measured wind directions, W_i, around θ. The general equation to calculate the expected concentration, $\bar{C}$, is given as follows:

$$\bar{C}(\theta) = \frac{\sum_{i=1}^{n} K\big((\theta - W_i)/\Delta\theta\big) C_i}{\sum_{i=1}^{n} K\big((\theta - W_i)/\Delta\theta\big)},$$

where $K(x)$ is the smoothing kernel used to perform the weighted averaging and $\Delta\theta$ is the wind direction window, centered at θ, that is used for averaging (i.e. the smoothing parameter). The most common smoothing kernel used for NWR is the Gaussian kernel, which is given as:

$$K(x) = (2\pi)^{-1/2} exp(-0.5x^2)$$

As explained by Henry et al. (2002), confidence intervals on the expected concentrations can also be calculated and used to determine the validity of the peaks in the expected concentration curves. NWR is generally used with wind data in intervals of up to an hour and concentration data in intervals of up to a day.

NWR was originally used to determine emission source locations of cyclohexane in the Houston, Texas area (Henry et al. 2002). Using hourly cyclohexane concentration data measured at two sites, two distinct large cyclohexane sources were identified by NWR. Since the analysis was performed at multiple sites, the largest peak for each site was used to triangulate on the largest known source in the area. The results of the triangulation process identified a location that was less than 500 meters away from the actual source location. While data from multiple sites are needed to determine the source location, NWR on data from a single site provides information about the bearings of sources. NWR is now one of the more conventional approaches to identifying source locations (Pancras et al. 2011, Donnely et al. 2010). For example, the Turner Group has performed NWR on several datasets including ambient PM mass and species data for Cleveland, Detroit and St. Louis.

As an example of NWR, consider the following example from the Detroit, MI, compliance monitoring network. Sulfur Dioxide (SO_2) data from the compliance monitor at Southwest High School (hereafter called the Detroit monitor) violates the 1-hour SO_2 NAAQS. A group of stakeholders organized through the Southeast Michigan Council of Governments (SEMCOG) worked in collaboration with the State of Michigan to define the nonattainment area boundaries (subject to EPA review and approval) and develop a control strategy. Hourly average SO_2 concentrations were available for three Detroit Metro sites – two in Michigan and one in Windsor, Canada. Hourly surface winds data were available for the two Michigan sites. Dr.

Varun Yadav in the Turner Group performed 1-D NWR on the data from these three sites. The resulting profiles were deconvoluted into a series of Gaussian peaks and emission source zone windows were extrapolated from each peak using the peak width at half height. These wedges were used to triangulate on the likely region of important SO_2 emission sources. Figure A-1 shows the three monitoring sites, the wedges from NWR analyses used for triangulation, and the resulting identified source zone (green polygon).

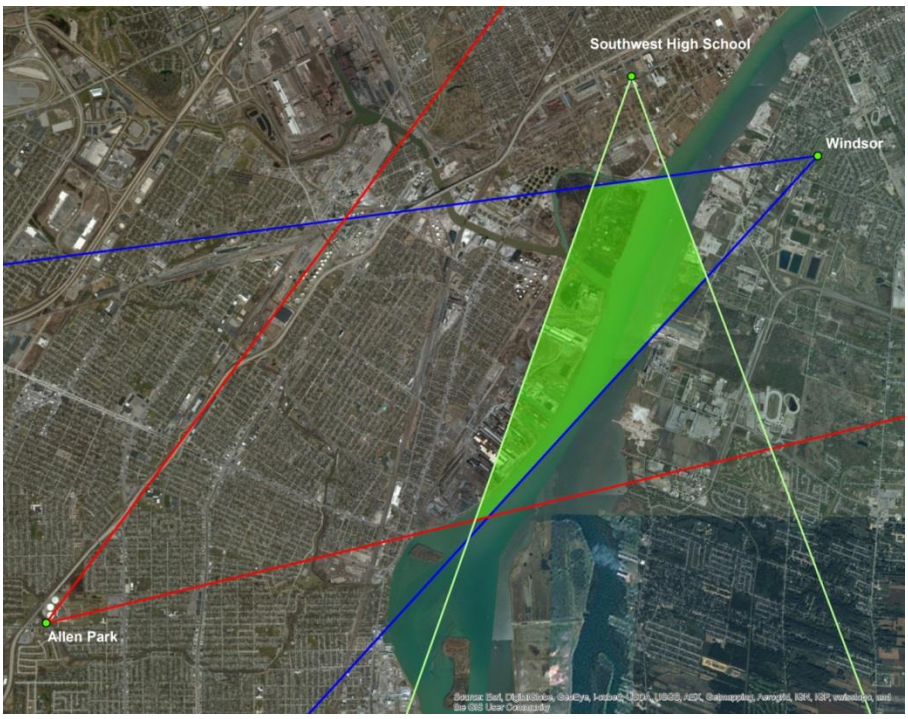

Figure A-1 Triangulation of NWR results for SO_2 monitors in the Detroit area. Analysis performed by Dr. Varun Yadav using hourly data.

A recently developed model that could purportedly be used to determine the location of air pollutant emission sources is Nonparametric Trajectory Analysis (NTA) (Henry et al. 2011). NTA exploits high time resolution (5-minutes or less) concentration and meteorological data to connect the observed concentration at a receptor to the points along the path the air parcel takes before arriving at the receptor (i.e. the upwind trajectory). While such high time resolution data

were typically not available in the past, it is becoming more routinely collected (e.g. SO_2 measured at NCore sites) and data quality is improving (e.g. the use of "trace level" gas monitors). The results of NTA are concentration values in an area around the monitoring site that represent the expected concentration at the monitoring site when the wind passes over the shown location.

NTA was originally used to identify the location of local sources of multiple pollutants in an area around a major highway near Las Vegas, Nevada between December 2008 and December 2009 (Henry et al. 2011). Five minute concentrations of black carbon, sulfur dioxide and other pollutants were measured at three downwind monitoring stations and a single upwind station to assess the impacts of the highway. The study estimated black carbon values up to twice the background levels at sites downwind of the highway. The estimated values were close to other previously measured highway impacts.

NTA has been shown to produce reliable results for estimating impacts of local air pollution sources. However, it has been used to analyze a very limited number of scenarios and under specific circumstances. This study evaluates how well NTA performs for other scenarios including identifying SO_2 sources in Detroit, MI in response to the 2010 revisions to the SO_2 NAAQS that revoked the annual and 24-hour standards and introduced a one-hour standard. NTA was also performed on sulfur species (SO_2 and hydrogen sulfide (H_2S)) in Roxana, IL from measurements collected near a petroleum refinery. NTA was also used to examine black carbon (BC) in Atlanta, GA, an area with significant traffic activity and emissions. Finally, NTA was used to examine nitrogen oxides (NO_x) measured at an industrial zone in Birmingham, AL.

A.2 Methods

A.2.1 NTA Methodology

NTA first calculates back trajectories based on high time resolution surface winds data. The points on the trajectories are given by (x_{ij}, y_{ij}) representing the i^{th} point on the j^{th} trajectory. The expected value of the concentration at the monitoring site is calculated by a weighted sum of the measured concentrations, C_j, for all back-trajectory points that are located within a certain distance, h, of the modeled location (X,Y). Figure A-2, originally from Henry et al. (2011), illustrates the back trajectories and the points that contribute to the expected concentration of the given grid point.

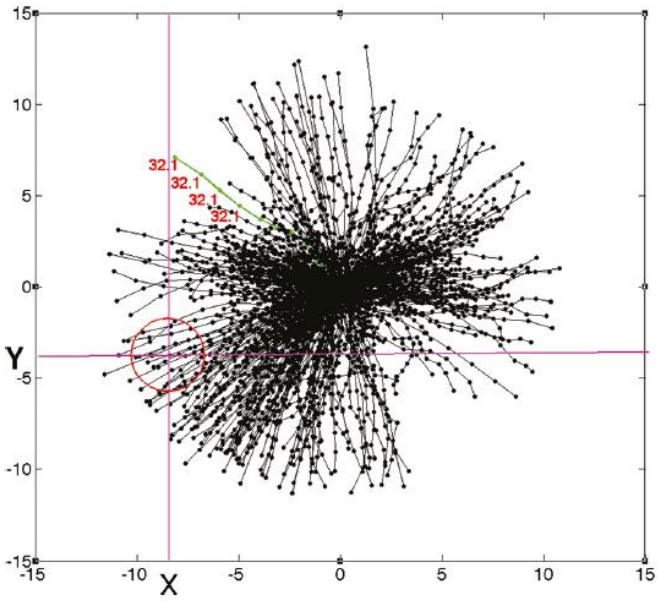

Figure A-2 Sample back-trajectories calculated by Henry et al (2011). Trajectory points within the red circle are used to calculate the expected concentration at the receptor of an air parcel that passes through the point in the center of the circle.

The expected value of the concentration at the receptor when the air passes through the circle around a specific point (X,Y) is given by (Henry et al. 2011):

$$\bar{C}(X,Y) = \frac{\sum_{i=1}^{m}\sum_{j=1}^{n} C_j W_{ij}}{\sum_{i=1}^{m}\sum_{j=1}^{n} W_{ij}}$$

where W_{ij} is the weighting function given by:

$$W_{ij} = K\left(\frac{X - x_{ij}}{h}\right) K\left(\frac{Y - y_{ij}}{h}\right)$$

and K is the Epanechnikov smoothing kernel

$$K(x) = 0.75(1 - x^2) \;\; for \; |x| \leq 1$$

$$K(x) = 0 \quad otherwise$$

The Epanechnikov kernel is used instead of the Gaussian kernel because wind speed a bounded parameter.

A.2.2 SO_2 in Detroit, MI

Starting in 2012, 5-minute as well as 1-hour SO_2 concentrations have been reported for the three SO_2 monitors in the Detroit metropolitan area: Detroit, MI; Allen Park, MI; and Windsor, ON. Additionally, 5-minute meteorology is available for Allen Park and Detroit. The high time resolution concentrations and wind data allowed NTA to be performed at each of these three sites. Expected concentrations at the monitoring site were estimated for a surrounding 20 km by 20 km grid with 200 m grid spacing for each sampling site using data from January through June 2012. In addition to individual site analysis, the results from each site were combined to perform a triangulation analysis similar to that performed by NWR (Figure A-1). NTA results were then compared with the previous NWR analysis to determine the improvement in analysis results when using NTA compared to NWR.

A.2.3 SO_2 and H_2S in Roxana, IL

SO_2 and H_2S concentrations were measured by Dr. Li Du of Washington University at the fenceline of a petroleum refinery in Roxana, IL. Both concentration and wind data were collected at 5-minute time resolution. There are significant sulfur-bearing operations at petroleum refineries; therefore, NTA was performed on the concentration data to determine if it could identify specific source locations. Data from mid-2013 to the end of 2014 were used for this analysis. Expected concentrations were calculated using a 6 km by 6 km grid centered on the monitoring location with 100 m grid spacing.

A.2.4 BC in Atlanta, GA and NO_x in Birmingham, AL

The Southeastern Aerosol Research and Characterization (SEARCH) network includes multiple sites that collect 5-minute resolution pollutant and meteorology data. Two of these sites were examined in detail using NTA. The first site was the Jefferson Street station in Atlanta, GA which is located near several large freeways and should be impacted by traffic emissions including BC. Data from 2011 to 2013 were examined using NTA to identify potential contributors to BC at the monitoring site. Another station examined in detail was located in Birmingham, AL. The site is located near multiple industrial facilities, including steelmaking operations.

A.3 Results and Discussion

A.3.1 SO_2 in Detroit, MI

Concentration and wind data from January to June 2012 were used to perform NTA on SO_2 concentrations measured in Detroit, MI; Allen Park, MI, and Windsor, ON. Figure A-3 shows the normalized contour plots from the NTA modeling of data collected at Detroit (a),

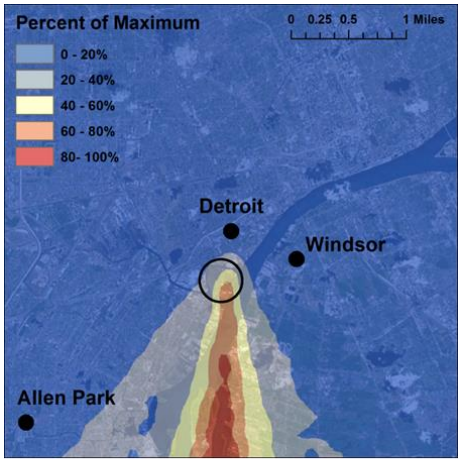

(a)

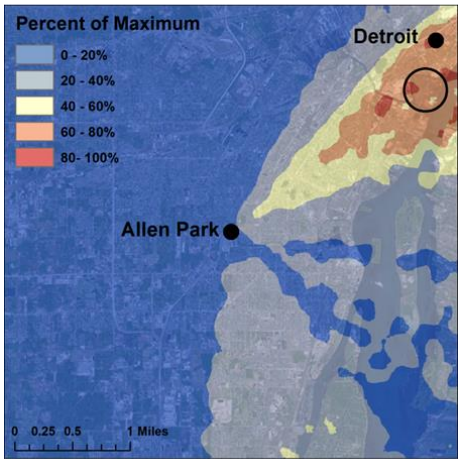

(b)

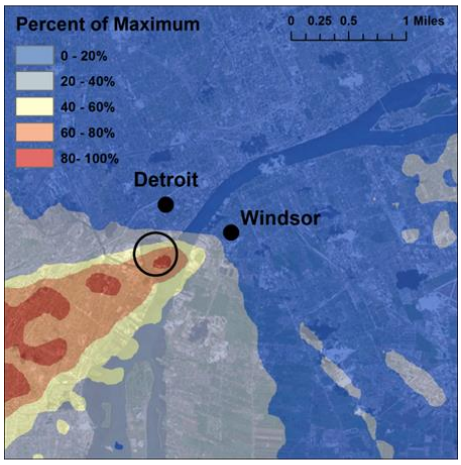

(c)

Figure A-3 NTA Results from the Detroit (a), Allen Park (b), and Windsor (c) monitors.

Allen Park (b) and Windsor (c). The figures show results using meteorology collected at the Detroit monitor for Detroit and Windsor, and the Allen Park monitor for Allen Park. The color at a given location indicates the expected concentration at the receptor when the wind passes through that point, normalized to the maximum concentration over the modeled domain. The black circle in each picture encompasses Zug Island which is a highly industrialized area that has a steel mill, coking operation, and various other emission sources. Each contour plot shows a streak (or cone) of high expected concentration at the monitoring site rather than a completely bounded region. It is encouraging that for both Detroit (Fig A-3a) and Windsor (Fig A-3c) the high concentration zone starts at Zug Island. However, in both cases the streaks extend upwind from Zug Island and likely result from high concentration impacts occurring at high winds speeds that also tend to have persistent wind direction. For the Allen Park plot (Fig A-3b), high concentration contours start well before Zug Island and in this case the site might be too far away from the high emission zone to yield meaningful results. The structure of these plots is very different from the results in the example by Henry et al. (2011) used to demonstrate NTA. An attempt to eliminate the streaking, using the reported standard deviation of the wind direction, shown in these results was made by using Monte Carlo analysis to introduce variance in the wind data. However, this only increased the width of the high expected concentration zone, instead of closing out the back end of these streaks.

The individual NTA results for each of the three sites were combined by multiplying their normalized values. The resulting contour is presented in Figure A-4. This figure also includes the green polygon identified as the source region in the previous NWR analysis (Figure A-1). Compared to NWR, the NTA analysis better constrained the emissions source zone to Zug Island, even when using only two sites – Detroit and Windsor (not shown). This result is

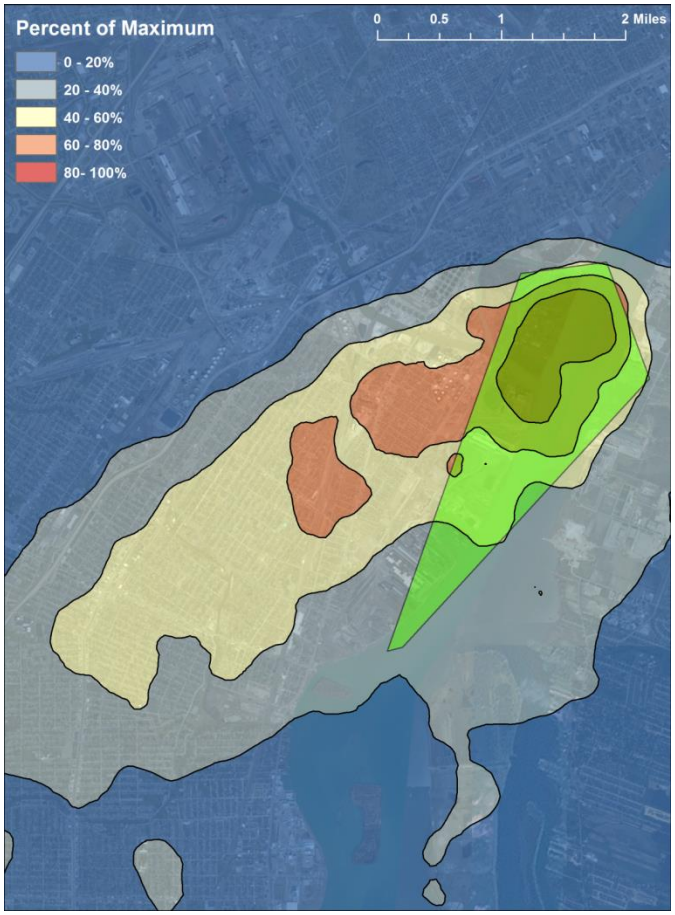

Figure A-4 Triangulation results from NTA. The green polygon represents NWR triangulation results.

consistent with a microinventory conducted by the Michigan Department of Environmental Quality.

A.3.2 SO_2 and H_2S in Roxana, IL

SO_2 and H_2S concentrations in Roxana, IL were analyzed using NTA. Figure A-5 shows the normalized contour plots from the NTA modeling of SO_2. Like in Detroit, the results show cones of high expected concentration zones, instead of more localized areas. However, these cones do start to occur at locations of known sulfur processes. The main refining operations are

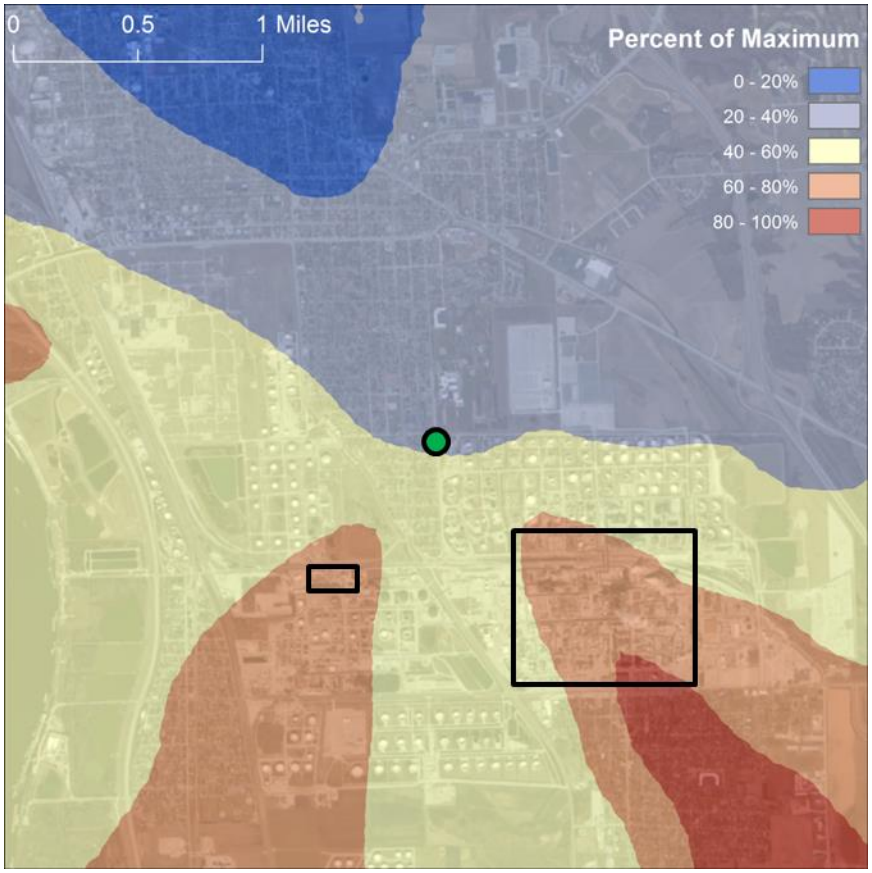

Figure A-5 Normalized SO_2 NTA results from Roxana, IL.

marked on the figure by the large black rectangle to the southeast of the monitoring site (the green dot). A sulfur recover unit, which uses the Claus process, is located to the southwest of the monitoring site and indicated by the small black rectangle.

Figure A-6 shows the normalized contour plots from the NTA modeling of H_2S in Roxana, IL. Again, there is a cone of high expected concentration to the southwest of the monitoring site. The highest expected concentration area starts near the sulfur recovery unit to the southwest of the monitor. There is also a zone of high expected concentration to the northwest of the monitor site. While there is no known source of H_2S in that area, this signal may be a response to docking and cargo loading and unloading locations along the Mississippi River.

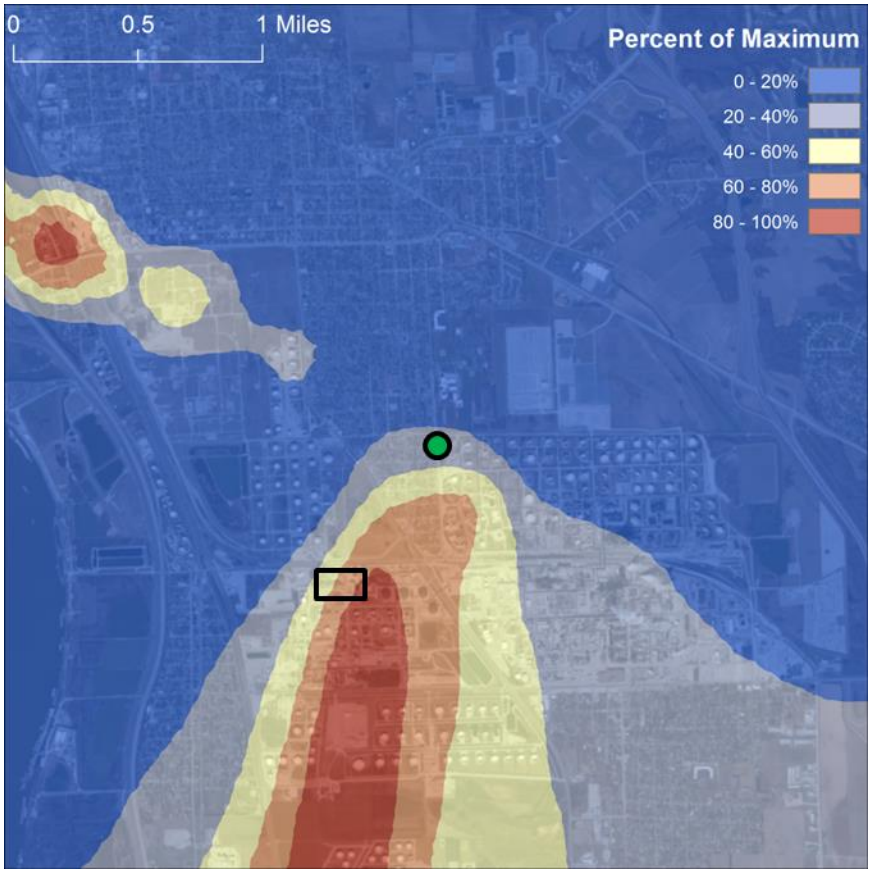

Figure A-6 Normalized H_2S NTA results from Roxana, IL.

While the analyses of SO_2 and H_2S did not highlight known sources specifically, it is encouraging that the cones of high concentration do seem to begin near known sources, similar to what was observed from NTA analysis in Detroit and Windsor.

A.3.3 BC in Atlanta, GA and NO_x in Birmingham, AL

Five-minute black carbon data from Atlanta, GA and NO_x data from Birmingham, AL from the SEARCH network were examined using NTA. BC and NO_x are different from SO_2, as their sources tend to be more widely spatially distributed and can be influenced by both mobile (traffic) and point sources. Figure A-7 shows the results from NTA analysis of BC in Atlanta, GA using data from the Jefferson Street (JST) monitor, indicated by the black triangle. The map

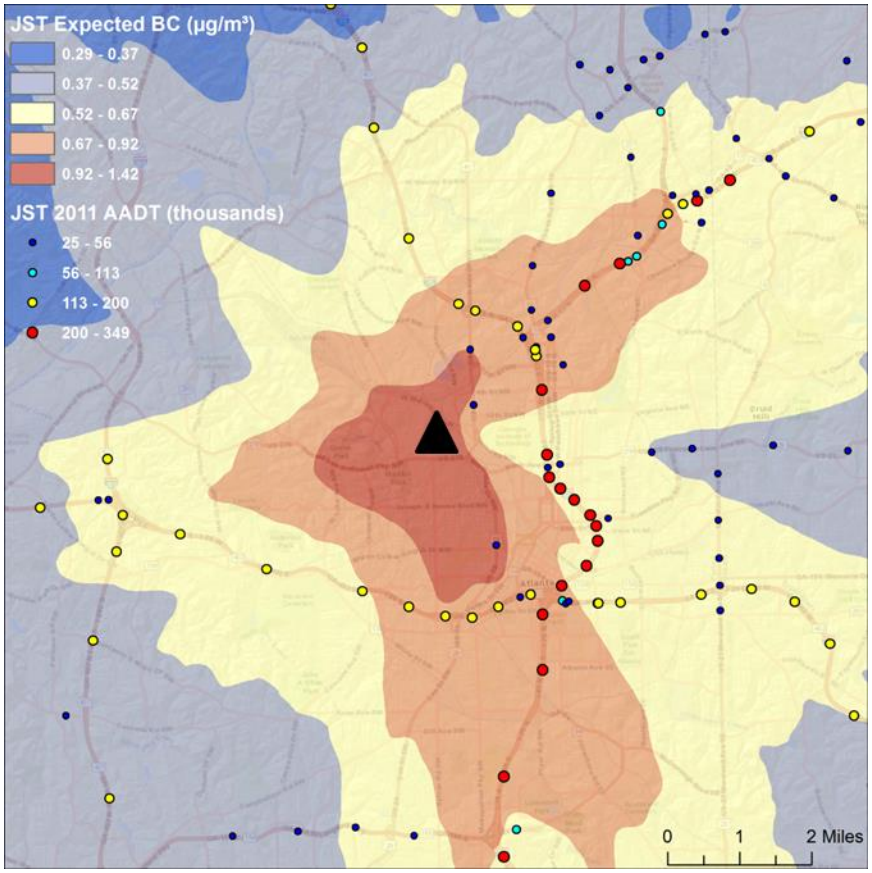

Figure A-7 BC NTA results from Atlanta, GA.

also shows annual average daily traffic (AADT) counts measured on highways around the Atlanta area. In contrast to results from Detroit and Roxana, NTA exhibits high expected concentrations around the monitoring site. Instead of having cones of high concentration, the results appear as lobes that extend outward from the monitoring site and likely indicate potential emission source bearings. These results are indicative of high concentrations when wind speeds are low. The NTA results highlight major roadways and especially interchanges to the northeast and southeast, and to a much lesser extent to the west, as significant contributors to BC measured at the monitoring site. In particular, roadways that are oriented toward the monitoring site (most clearly seen to the northeast) appear to impact the monitoring site. This arises from a corridor effect – the accumulation of emissions as the wind travels down the roadway and toward the

monitoring site. Carbon monoxide and NO_x in Atlanta were also analyzed by NTA and produced similar results.

Figure A-8 shows the results from NTA modeling of NO_x in Birmingham, AL. The Birmingham (BHM) monitoring location is indicated by the black triangle. The figure also shows nitrogen dioxide (NO_2) point source emissions (blue circles) from the 2011 National Emissions Inventory (NEI). Larger markers indicate higher estimated NO_2 emissions. Like BC in Atlanta, the NTA modeling resulted in lobes of high expected concentration extending outward from the monitoring site. The lobe to the northeast corresponds to the area that results in the highest concentrations at the monitor. Within this lobe are two large coking operations and a natural gas compressor station. There is another significant lobe to the southwest. Within this area are a pipe

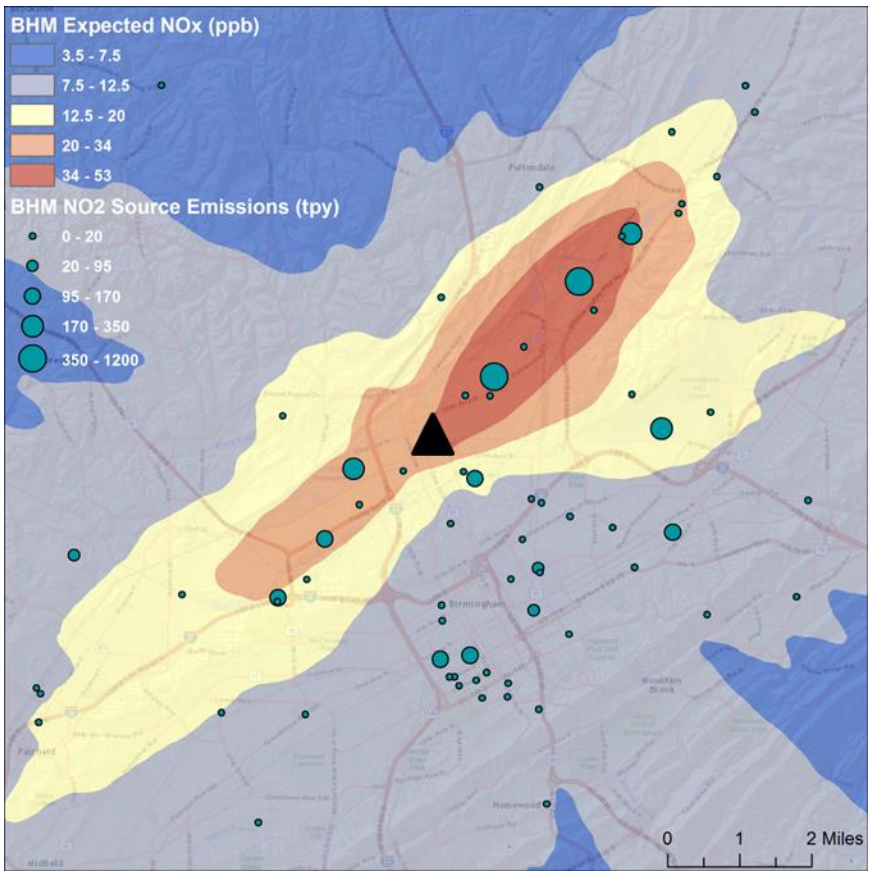

Figure A-8 NO_x NTA results from Birmingham, AL.

company and a railyard. Both lobes also cover areas with large roadways. Carbon monoxide was also examined by NTA in Birmingham and was found to have similar results as NO_x.

Birmingham is a particularly interesting case because it represents a monitor that is impacted by both distributed sources like traffic and significant point sources. In Detroit and Roxana, point sources resulted in cones of high expected concentrations. However, when combined with distributed emission sources, these cones are no longer present. This indicates that the monitoring site is significantly impacted by nearby sources at low wind speeds but also farther away point sources during more advective conditions.

A.4 Conclusions

Using 5-minute wind and concentration data, NTA has been used to examine different pollutants at four locations across the United States. NTA was used to examine pollutants dominated by point source emissions (SO_2 in Roxana and Detroit), mobile sources (BC in Atlanta), and a combination of point and mobile sources (NO_x in Birmingham). In each case, NTA results provided useful results, identifying potential source locations that were consistent with known emitters. In the cases with point source dominated emissions, NTA modeling resulted in cones of high expected concentration that tended to start near known sources, and extend beyond those sources. In the case of distributed mobile sources impacting the monitoring site, results showed lobes of high expected concentration centered on the monitoring site, and extending outward toward areas that could be more significant contributors to high measured concentrations (freeways and interchanges). These results are consistent with high concentrations during calm winds. When there were both distributed mobile sources and large point sources, the NTA results showed high expected concentrations near the monitoring site with lobes that

included major point sources. For each scenario, wind data were also analyzed to confirm that high concentration areas in the NTA patterns did not simply correspond to prevailing winds.

In each scenario evaluated in this study, NTA provided at least as much information as would be provided by pollution roses or NWR. The cones and lobes seen in the results provide, at minimum, the wind directions that would result in high expected concentration. NTA results also provided additional spatial information, observed as the start of cones that tended to indicate point sources and the ends of the lobes that were related to distributed and mobile sources. NTA provided significant spatial information in Detroit, where results from multiple monitoring sites combined to resolve a specific region that included a known area of high emissions.

The NTA results in this study demonstrate some of the value of collecting high-time resolution pollutant and wind data. This is especially true when there are multiple monitoring locations in an area. Monitoring agencies should be strongly encouraged to collect and report 5-minute air quality parameters and surface winds data to enable further analyses

A.5 Acknowledgements

The authors would like to thank Dr. Eric Edgerton of Atmospheric Research & Analysis, Inc. for providing data from the SEARCH network and for his assistance in interpreting NTA results.

A.6 References

Donnelly, A.; Misstear, B.; Broderick, B., Application of nonparametric regression methods to study the relationship between NO2 concentrations and local wind direction and speed at background sites. *Science of the Total Environment* **2010,** *409* (6), 1134-1144.

Henry, R. C.; Chang, Y. S.; Spiegelman, C. H., Locating nearby sources of air pollution by nonparametric regression of atmospheric concentrations on wind direction. *Atmospheric Environment* **2002,** *36* (13), 2237-2244.

Henry, R. C.; Vette, A.; Norris, G.; Vedantham, R.; Kimbrough, S.; Shores, R. C., Separating the air quality impact of a major highway and nearby sources by nonparametric trajectory analysis. *Environmental Science and Technology* **2011,** *45* (24), 10471-10476.

Pancras, J. P.; Vedantham, R.; Landis, M. S.; Norris, G. A.; Ondov, J. M., Application of EPA unmix and nonparametric wind regression on high time resolution trace elements and speciated mercury in Tampa, Florida Aerosol. *Environmental Science and Technology* **2011,** *45* (8), 3511-3518.

Curriculum Vita

Stephen Neil Feinberg

Doctor of Philosophy (Ph.D.) in Energy, Environmental and Chemical Engineering, 2015.
Department of Energy, Environment and Chemical Engineering,
Washington University in St. Louis, St. Louis, MO, USA

Bachelor of Science in Energy, Environmental and Chemical Engineering, 2010.
Department of Energy, Environmental and Chemical Engineering,
Washington University in St. Louis, St. Louis, MO, USA

Publications

Feinberg, S. N.; V. Yadav; J.G. Heiken; J.R. Turner, Midwest Rail Study: Modeled Near-field Impacts of Emissions of Fine Particulate Matter from Railyard Activities. *Transportation Research Record* **2011**, 106-114.

Feinberg, S. N.; J.R. Turner, Dispersion Modeling of Lead Emissions from Piston-Engine Aircraft at General Aviation Facilities. *Transportation Research Record* **2013**, 34-42.

Feinberg, S.N.; J.R. Turner, Modeling of Lead Concentrations and Hotspots at General Aviation Airports. Manuscript submitted for publication.

Feinberg, S.N.; J.R. Turner, Measurement and Characterization of Lead Impacts at General Aviation Airports. Manuscript in preparation.

Feinberg, S.N.; J.R. Turner, Identification of Emission Source Regions Using Nonparametric Trajectory Analysis. Manuscript in preparation.

Major Reports

Heiken, J.; J. Lyons; M. Valdez; N. Matthews; P. Sanford; J. Turner; **N. Feinberg**, Quantifying Aircraft Lead Emissions at Airports. Transportation Research Board. Web-Only Document 21. http://onlinepubs.trb.org/Onlinepubs/acrp/acrp_webdoc_021.pdf

Turner, J.R.; V. Yadav; **S.N. Feinberg**, Data Analysis and Dispersion Modeling for the Midwest Rail Study (Phase 1). Lake Michigan Air Directors Consortium.

Presentations

Feinberg, S.N.; J.G. Heiken, M.P. Valdez, J.M. Lyons, J.R. Turner (2016) Modeling of Lead Concentrations and Hotspots at General Aviation Airports, *95th Annual Meeting of the Transportation Research Board* (1/2016, Washington DC). Accepted for Presentation.

Feinberg, N.; J. Turner, J. Lyons, J. Heiken (2015) Quantifying Aircraft Lead Emissions at Airports, *24th Annual AAAE National Aviation Environmental Management Conference* (4/2015, New Orleans, LA)

Feinberg, S.N.; J. Turner (2014) Lead Impacts from General Aviation Airports: A Weight of Evidence Approach, *American Association for Aerosol Research 33rd Annual Conference* (10/2014, Orlando, FL)

Feinberg, S.N., J.R. Turner (2014) Potential Payoffs from Collected and Reporting Five-Minute Air Quality Data, *2014 National Ambient Air Monitoring Conference* (8/2014, Atlanta, GA)

Feinberg, S.; V. Yadav; J.R. Turner (2013) Weight of Evidence Analysis for Attributing Monitored Sulfur Dioxide Exceedances to Emission Source Zones, *A&WMA 2013 Annual Conference* (6/2013, Chicago, IL)

Feinberg, S.N.; J.R. Turner (2013) Modeling of Lead Emissions from Piston-Engine Aircraft at General Aviation Facilities, *92nd Annual Meeting of the Transportation Research Board* (1/2013, Washington DC).

Rice, J.; S. Brown; P. Roberts; **S. Feinberg**; J. Turner (2012) Characterization of Carbonaceous Matter from the USEPA Coarse PM Pilot Speciation Study**,** *A&WMA Specialty conference: Air Quality Measurement Methods and Technology* (4/2012, Durham, NC).

Feinberg, S.N.; V. Yadav; J.G. Heiken; J.R. Turner (2011) The Midwest Rail Study: Modeled Near-Field Impacts of $PM_{2.5}$ Emissions from Railyard Activities, Paper 11-2794. *90th Annual Meeting of the Transportation Research Board* (1/2011, Washington DC).

Turner, J.; **S. Feinberg**; J. Rice (2011) Carbonaceous Particulate Matter Artifacts Observed in the USEPA Coarse PM Pilot Speciation Study, Paper #693, *104th Annual Conference of the Air & Waste Management Association* (6/2011, Orlando, FL).

Turner, J.R; V. Yadav and **S.N. Feinberg** (2009) The Midwest Rail Study, *USEPA/FHWA/LADCO Midwest Transportation / Air Quality Summit* (10/2009, Grafton, IL)